Deciphering the role of the deubiquitinating enzyme Ataxin-3 in transcriptional regulation and the cellular response to stress

Dissertation

zur Erlangung des Doktorgrades (Dr. rer. nat.)
der
Mathematisch-Naturwissenschaftlichen
Fakultät
der
Rheinischen Friedrich-Wilhelms-Universität Bonn

Vorgelegt von

Jasmin Jatho-Gröger

aus Kiel

Bonn, April 2018

Anfertigung mit Genehmigung der Mathematisch-Naturwissenschaftlichen Fakultät der Rheinischen Friedrich-Wilhelms-Universität Bonn

1. Gutachter: Prof. Dr. Philipp Koch

2. Gutachter: Prof. Dr. Jörg Höhfeld

Tag der Promotion: 12.07.2018

Erscheinungsjahr: 2018

Table of contents

1 Introduction

1.1 Ataxin-3

1.1.1 Structure, expression, localization and posttranslational modifications of ATXN3

The human Machado-Joseph-Disease (*MJD*) or Ataxin-3 (*ATXN3*) gene was first described by Kawaguchi et al. in 1994. It is located in the region 14q24.3-q32.2 on the long arm of chromosome 14 and comprises 48070 base pairs (NG_008198.2 RefSeqGene, pubmed; Takiyama et al., 1994). The gene consists of 11 exons with the start codon in exon 1 and a repeat of the nucleotides cytosine, adenine and guanine (CAG repeat stretch) in exon 10.
So far, 56 different splice variants of *ATXN3* have been identified of which about 20 represent protein-coding mRNAs (Bettencourt et al., 2010; Ichikawa et al., 2001; Kawaguchi et al., 1994). The most frequently expressed isoform in the brain consists of 11 exons which are translated into an ATXN3 protein of 361 amino acids, based on a CAG repeat length of 13 (Harris et al., 2010; Schmidt et al., 1998; Trottier et al., 1998; Ensembl transcript ID ENST00000393287). The CAG repeat, located in exon 10, is translated into a poly glutamine (polyQ) repeat sited at the C-terminus of the corresponding protein.
Structurally, the protein consists of a conserved, globular deubiquitinating N-terminal Josephine domain (JD) with a papain-like fold and a more flexible C-terminal tail containing two ubiquitin-interacting motifs (UIMs) and a polyQ stretch (Albrecht et al., 2004; Burnett et al., 2003; Hofmann et al., 2001; Mao et al., 2005; Masino et al., 2003). One splice variant contains a putative third UIM at the end of the C-terminus (Goto et al., 1997; Fig. 1.1 A).
ATXN3 is a small protein with a molecular weight varying around 42 kDa, depending on the size of the polyQ repeat. The normal form of ATXN3 contains repeats with a range from 12 to ~ 43 whereas the mutated exceeded stretch contains nearly always 60 or more repeats (Fig. 1.1 B; Cancel et al., 1995; Durr et al., 1996; Maciel et al., 1995; Matilla et al., 1995; Matsumura et al., 1996b; Ranum et al., 1995; Sasaki et al., 1995).

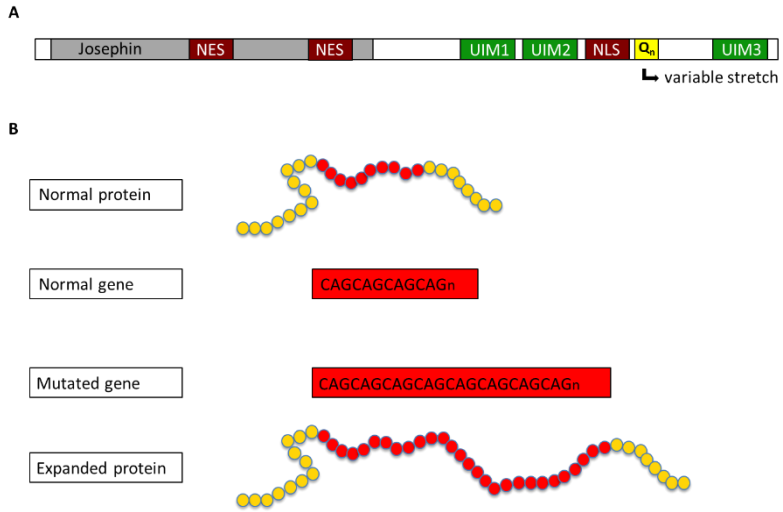

Figure 1.1: Normal and mutated forms of ATXN3

A: *Schematic representation of the protein ATXN3. The protein consists of 361 amino acids with an N-terminal Josephin domain that contains two nuclear export signals (NES). The C-terminal part contains three ubiquitin interacting motifs (UIM 1 to 3), a nuclear localization signal (NLS) and the variable polyQ repeat (Q_n).* ***B:*** *Schematic overview of a normal and mutated ATXN3 gene with different CAG repeat numbers and the corresponding proteins with differences in the length of the polyQ stretch.*

The normal as well as the mutated form of ATXN3 are ubiquitously found throughout the cell and are equally expressed in different neuronal subpopulations within the brain, e.g. purkinje cells of the cerebellum or in neurons of the ventral pons (Paulson et al., 1997a and b).

In most neurons, ATXN3 has a cytoplasmic, dendritic, and axonal localization (Trottier et al., 1998). But it was also shown that ATXN3 is able to translocate from the cytoplasm to the nucleus and back. (Chai et al., 2002; Paulson et al., 1997; Pozzi et al., 2008; Schmidt et al., 1998; Tait et al., 1998; Todi et al., 2007; Trottier et al., 1998). Different regions might be implicated in regulating ATXN3 cellular localization such as a C-terminal nuclear localization signal (NLS) in the proximity of the polyQ repeat and two nuclear export signals (NES; Albrecht et al., 2004; Antony et al., 2009; Breuer et al., 2010; Macedo-Ribeiro et al., 2009; Fig. 1.1 A).

Furthermore, ATXN3 comprises different phosphorylation sites, which might also be involved in influencing the nuclear localization as it was shown for the casein kinase 2 (CK2) mediated phosphorylation of serines 236, 340 and 352 (Mueller et al., 2009). Reina et al. (2010) showed that heat shock-mediated proteotoxic stress leads to the translocation of ATXN3 into the nucleus after phosphorylation of serine 111. In addition to the nuclear localization, it was further shown that phosphorylation of ATXN3 is also important for the protein stability (Mueller et al., 2009).

1.1.2 Physiological roles of ATXN3

As mentioned before, ATXN3 is composed of a globular N-terminal Josephin domain (JD) followed by a flexible C-terminal tail (Masino et al., 2003). Both parts are involved in a number of different physiological functions within the cell. The JD is known to have an isopeptidase activity suggesting ATXN3 to be involved in the ubiquitin-proteasomal pathway (Burnett and Pittman, 2003). Thereby the JD in combination with the C-terminal UIMs can either rescue proteins from degradation or initiate breakdown due to deubiquitinating events (Burnett and Pittman, 2003; Winborn et al., 2008). Additionally to its involvement in protein degradation, ATXN3 has been shown to regulate transcriptional processes by interacting with several transcription factors and histones and is able to influences gene expression (Evert et al., 2006; Li et al., 2002). Furthermore, ATXN3 was shown to be involved in aggresome formation (Burnett and Pittman, 2005), microtubule stabilization (Rodrigues et al., 2010) and myogenesis (do Carmo Costa et al., 2010).
The different physiological functions of ATXN3 will be described in more detail in the next sections.

1.1.2.1 ATXN3 is a deubiquitnating enzyme (DUB)

ATXN3 is a deubiquitinating papain-like cysteine protease in the ubiquitin proteasome system (UPP), representing the main cellular mechanism for the turnover of short-lived or damaged proteins (Albrecht et al., 2004; Doss-Pepe et al., 2003; Scheel et al., 2003). The catalytic site of ATXN3 consists of a triad with cystein 14, histidin 119 and asparagine 134 in the Josephin domain (JD), which is, in contrast to other cysteine proteases, constitutively active and does not need cation-induced conformational changes for its activation (Albrecht et al., 2004).
In order for damaged proteins to be prepared for degradation by proteasomes, ubiquitins (Ub) have to be covalently attached individually or as a poly-ubiquitin chain to one or several lysine residues of target proteins. DUBs can trim polyUb chains down to 4/5 moieties for optimal recognition by proteasomes or completely remove Ub chains to rescue substrates from degradation (Reyes-Turcu et al., 2009; Reyes-Turcu and Wilkinson, 2009). Those mechanisms of editing and removal of poly-ubiquitin chains as well as recycling of ubiquitin are critical for cellular homeostasis.
Inhibiting the deubiquitinating activity of ATXN3 results in an increase of polyubiquitinated proteins, which supports the idea of ATXN3 being involved in the interactions with polyubiquitinated proteins targeted for proteasomal degradation (Berke et al., 2005; Schmitt

et al., 2007).

Binding of ubiquitin chains by ATXN3 occurs at two adjacent but distinct ubiquitin binding sites within the JD and the two or three C-terminal UIMs (Burnett *et al.*, 2003; Chai *et al.*, 2004; Nicastro *et al.*, 2009). ATXN3 preferentially binds the poly-ubiquitin linkages lysine 63 and with less affinity, the poly-ubiquitin linkages lysine 48. And it displays even higher activity toward mixed 48- and 63-linkage polyubiquitin (Winborn et al., 2008). Thereby ATXN3 recognizes polyUb chains of four or more ubiquitin monomers (Berke et al., 2005; Burnett et al., 2003).

It was further suggested that ATXN3 functions as a polyUb-editing protease. Instead of a complete disassembly of polyUb chains, a shortening of the chain is preferred in order to yield free Ub and to trim chains down to four residues for optimal proteasomal recognition (Burnett et al., 2003; Burnett and Pittman, 2005; Kuhlbrodt et al., 2011; Nicastro et al., 2010; Winborn et al., 2008).

A cooperative interplay between the UIMs and the two Ub-binding sites of the JD in order to cleave Ub chains was suggested by Nicastro et al. (2010): the UIMs might help to recruit and bind the polyubiquitinated substrates and the two Ub-binding sites may align the position of the isopeptide bonds relatively to the catalytic site in a way that allows for a sequential editing. In contrast, for the regulation of the dub activity itself, the catalytic activity of ATXN3 is UIM independent and can be enhanced via monoubiquitination of ATXN3 without the presence of any co-factors (Todi et al., 2009).

Furthermore, the length of the CAG repeat does not influence the deubiquitinating function of ATXN3 (Masino *et al.*, 2004; Tzvetkov and Breuer, 2007).

In summary, these observations support the conclusion that ATXN3 acts as a deubiquitinating enzyme and contributes to the proteasomal degradation of proteins by the ubiquitin proteasome machinery.

1.1.2.2 Ataxin 3 regulates the retrotranslocation of ERAD substrates and is important for the protein quality control

The efficient clearance of misfolded proteins is essential to ensure cellular homeostasis by preventing the accumulation of toxic protein species. For this, chaperones as well as ubiquitin-proteasome systems (UPS) are essential. Chaperones are involved in folding and refolding processed of proteins and the UPS is mandatory for degradation of misfolded proteins. Several ATXN3 interacting partners have been discovered so far, providing information about the protein's functions in the protein quality control.

ATXN3 binds the p97/valosin-containing protein (VCP) through the C-terminal arginine/lysine-rich motif in proximity to the polyQ repeat (Boedderich et al., 2006;

Hirabayashi et al., 2001; Matsumoto et al., 2004; Mao et al., 2005; Rao et al., 2017; Zhong and Pittman, 2006). VCP/p97 is involved in the regulation of endoplasmic reticulum-associated degradation (ERAD), a cellular process important for the degradation of misfolded endoplasmic reticulum (ER) proteins (Liu et al., 2012; Zhong et al., 2006). Thereby, the ERAD system alleviates cytotoxic stress caused by misfolding of secretory proteins. For this purpose, VCP is implicated in the retrotranslocation of misfolded proteins from the ER into the cytoplasm for proteasomal degradation. ATXN3 forms a complex with VCP/p97 in order to regulate this process (Wang et al., 2006). Although ATXN3 has been associated with the ERAD, there is still a dispute about whether ATXN3 promotes or decreases degradation by this pathway (Liu et al., 2012; Wang et al., 2006; Zhong and Pittman, 2006).

ATXN3 is further known to interact with the human homologues of yeast DNA-binding protein RAD23, hHR23A and hHR23B through the ubiquitin-binding site 2 of the josephin domain (Nicastro et al., 2005; Wang et al., 2000). Similar to p97/VCP, also hHR23A and hHR23B are involved in the delivery of ubiquitinated substrates for proteasomal degradation (Wang et al., 2000).

Ube2w and Ataxin 3 were found to coordinately regulate the ubiquitin ligase C-terminus of Hsc70 interacting protein (CHIP; Scaglione et al., 2011). CHIP is an E3 ubiquitin ligase which bridges the chaperone and UPS system by interacting with chaperones in order to ubiquitinate misfolded proteins, thus targeting them for proteasomal degradation. Ataxin 3 participates in the initiation, regulation and termination of the CHIP ubiquitination cycle (Scaglione et al., 2011).

When the protein quality control via proteasome is not sufficient to degrade or correct misfolded proteins, cells also have a deposition method: they can sequester aggregates by collecting them at the microtubule-organizing center (MTOC). These so-called aggresomes at the perinuclear region are then degraded by lysosomes, promoting the maintenance of cellular homeostasis.

ATXN3 colocalizes with aggresomes and preaggresome particles as well as with proteins, which are involved in the transport of misfolded proteins and in the formation of aggresomes (Burnett and Pittman, 2005). It is proposed that ATXN3 is responsible for the transport and stabilization of misfolded proteins to the MTOC as it is associated with parts of the cytoskeleton and transport proteins such as dynein and histone deacetylase 6 (Burnett & Pittman, 2005; Mazzucchelli et al., 2009; Rodrigues et al., 2010).

Finally, also ubiquitination is implicated in the formation of aggresomes since it was shown that ubiquitination of ATXN3 at Lys-117 improved its ability to promote aggresome formation (Todi et al., 2010). Another study suggested that trimming K63-linked polyubiquitin chains by ATXN3 promotes mutant superoxide dismutase 1 (SOD1) aggresome formation and vice versa, knockdown of ATXN3 decreases mutant SOD1 aggresome formation, thereby

increasing cell death induced by mutant SOD1 (Wang et al., 2012).
Concluded, its interactions with ERAD substrates such as p97/VCP, hHR23A and hHR23B, with CHIP and its implications in the aggresome formation, make the deubiquitinating enzyme ATXN3 an important factor in the regulation of protein quality control and thus an important regulator for maintenance of cellular homeostasis.

1.1.2.3 Ataxin 3 is involved in transcriptional regulation processes

Besides the aforementioned roles in protein quality control mechanisms, ATXN3 has further been shown to play a role in the regulation of transcriptional processes. Since ATXN3 interacts with several transcriptional regulators, the transcriptional regulation via ATXN3 might arise through a variety of mechanisms. Known interaction partners are: TATA box-binding protein (TBP)-associated factor 4 (TAF4; Shimohata et al., 2000), cAMP response element-binding protein (CBP; Chai et al., 2002; Li et al., 2002; McCampbell et al., 2000), p300 (Li et al., 2002), p300/CBP-associated factor (PCAF; Li et al., 2002), the transcription repressors nuclear receptor co-repressor (NCoR1) and histone deacetylase 3 (HDAC3) (Evert et al., 2006a) as well as forkhead box O (FOXO) transcription factor FOXO4 (Evert et al., 2006b).
TAF4 is a transcription initiation factor, which helps coordinating processes for the initiation of transcription by RNA polymerase II. Expanded polyglutamine stretches of ATXN3 were found to interact with TAFII130, thus interfering with CREB-dependent transcription.
CBP, p300 and PCAF are transcriptional coactivators that form complexes with other co-activators and proteins with acetyltransferase activity. By binding these co-activators through its C-terminal region, ATXN3 might repress the transcription. Additionally, part of the N-terminal region of ATXN3 binds histones, which seems to repress acetylation by blocking the access to histone acetylation sites (Li et al., 2002).
In addition to interactions with transcription factors or coactivators, also direct binding of ATXN3 to DNA can likely take place. This might be achieved through a leucine zipper motif located at amino acid 223 to 270 as it was shown for the matrix metalloproteinase-2 (MMP-2) promoter (Evert et al., 2006). In this context it was further revealed that ATXN3 functions as a transcriptional co-repressor (Evert et al., 2006). ATXN3 recruits the nuclear receptor co-repressor (NCoR1) and the histone deacetylase 3 (HDAC3) resulting in complexes, which are able to deacetylate the MMP2 promoter, by binding to DNA motifs in distinct chromatin regions of the promoter leading to the transcriptional repression. Although mutated ATXN3 interacts with HDAC3 and NCoR as well, no deacetylating repressor complexes are formed, as it is the case for normal ATXN3. Consequently, no inhibition of the MMP2 transcription

occurs and transcription can be activated after binding of GATA-2. This mechanism demonstrates that ATXN3 is able to epigenetically regulate the transcription of target genes (Evert et al., 2006). Moreover, ATXN3 can inhibit histone acetylation and repress transcription in vivo via interaction with the polyQ repeat (Li et al., 2002).

The transcription factor FOXO4 is important for the regulation of many cellular pathways including oxidative stress signaling, longevity, insulin signaling, cell cycle progression, and apoptosis (Araujo et al., 2011). It was shown that ATXN3, as a transcriptional co-activator together with FOXO4, is involved in the regulation of the *superoxide dismutase 2 (SOD2)* gene expression. Thereby, ATXN3 directly interacts with FOXO4 and binds *in vivo* the endogenous *SOD2* gene promoter in proximity to the FOXO4 consensus motif. Thus, normal ATXN3 enhances the FOXO4 dependent transcription of *SOD2*, whereas the expanded ATXN3 is associated with a decrease of the *SOD2* expression (Araujo et al., 2011).

In summary, ATXN3 is involved in various processes of transcriptional regulation either as a co-repressor, by direct binding of DNA or due to ubiquitination and deubiquitnation of transcription factors. The various functions of ATXN3 and its thus wide distribution in the cell are summarized in Fig. 1.2.

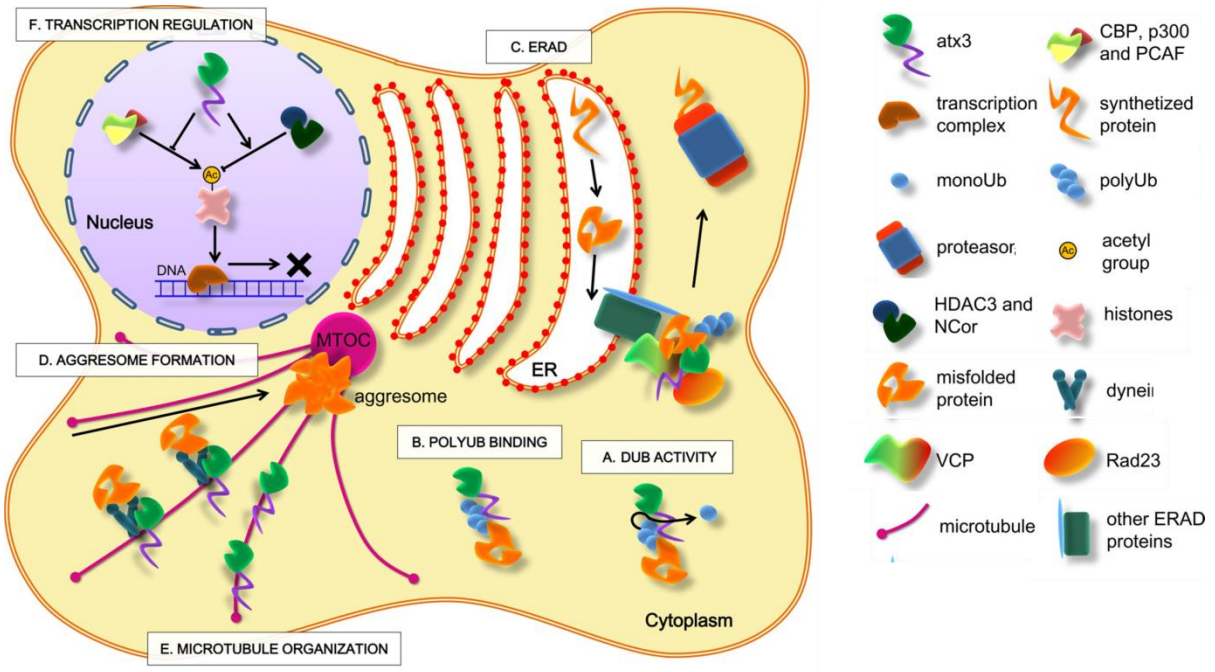

Figure 1.2: The different roles of ATXN3 and its consequently wide distribution in the cell

ATXN3 displays deubiquitinating (DUB) activity (A) and interacts with polyUB chains (B). It participates in protein homeostasis via ERAD (C). Additionally, regulation of protein quality control due to formation of aggresomes (D) and microtubule organization via interactions with MTOC were found (E). And ATXN3 is involved in transcriptional regulation processes such as regulation of histone acetylation (F). Adopted from Matos et al. (2011).

1.1.2.4 Ataxin 3 as a disease protein for Machado-Joseph Disease (MJD)

Besides the various functions of ATXN3, the expanded form of the protein is also involved in the formation of nuclear inclusions (NIs). Those are exclusively present in neurons of brain areas such as the cerebellum, ventral pons, in the substantia nigra, globus pallidus, dorsal medulla and dentate nucleus (Paulson et al., 1997b). The formation of NIs was reproduced in cell and animal models overexpressing mutant ATXN3 (Ikeda et al., 1996; Schmidt et al., 2002). NIs are heavily ubiquitinated, protein aggregates, which are most likely formed due conformational changes of the expanded polyQ stretch in the C-terminus of ATXN3. In addition to polyQ-expanded ATXN3, NIs also sequester several other proteins, including members of the cell quality control systems such as proteasome constituents, transcription factors including TATA-binding protein (TBP), ubiquitin and molecular chaperones, which might be recruited to prevent ATXN3 misfolding and aggregation (Chow et al., 2004; Paulson et al., 1997b; Schmidt et al., 2002; Seidel et al., 2010). The decrease of free availability of these proteins may promote cytotoxicity within the cell through different possible mechanisms: impairment of transcription (Chai et al., 2002; McCampbell et al., 2000), disturbances of the quality control systems of the cells (Muchowski et al., 2000; Paulson et al., 1997b; Schmidt et al., 2002; Warrick et al., 1999), hindrance of axonal transport (Gunawardena et al., 2003) and disturbances caused by recruitment of Ub-binding proteins or other polyQ-containing proteins (Donaldson et al., 2003). All of these altered and dysregulated cellular functions are reflected in the phenotype of patients suffering from Machado-Joseph Disease (MJD), a disease, which is caused by ATXN3.

Machado Joseph Disease (MJD), also known as spinocerebellar ataxia type 3 (SCA3) is an autosomal dominant neurodegenerative disease of late onset and the most frequent form of ataxia in humans (Schöls et al., 1995, 2004). It was first described in two families of emigrants from the Azorean islands based on the clinical phenotype and named after those families (Nakano et al., 1972; Rosenberg et al., 1976). In the 90s genetic testing showed that MJD and the spinocerebellar ataxia of type 3 (SCA3) are based on the same gene defect (Haberhausen et al., 1995). Nowadays it is known that the hereditary disease exists worldwide and affects all ethnicities. Although the official Human Genome Organization (HUGO) name for this disease is MJD, it is also termed SCA3 or MJD/SCA3 in the literature (Paulson H, 2012).

Kawaguchi et al. (1994) discovered that MJD originates from an expansion of CAG repeats in exon 10 of the MJD1 gene, which leads to a C-terminal elongated polyglutamine (polyQ) tract of its gene product ATXN3. This makes MJD a member of a group of in total nine polyQ diseases, including Huntington's disease (HD), dentatorubral-pallidoluysian atrophy (DRPLA), spinal and bulbar muscular atrophy (SBMA) and spinocerebellar ataxia (SCA) types 1, 2, 3 6, 7 and 17 (Gatchel and Zoghbi, 2005; Shao and Diamond, 2007; Zoghbi and

Orr, 2000).

Regarding the CAG tract it was revealed that its length is negatively correlated with disease onset resulting in variations of age of onset between 5 to 70 years (Maciel et al., 1995; Paulson H, 2012; van de Warrenburg et al., 2002) and a positive correlation with the severity of the disease. As mentioned before, the normal form of ATXN3 contains repeats with a range from 12 to ~ 43 whereas the mutated exceeded stretch contains about 60 or more repeats. Furthermore, scarce intermediate expansions with 45 to 59 repeats might either manifest as a mild form of ataxia, as restless leg syndrome or does not lead to any symptoms (Gu et al., 2004; Padiath et al., 2005; Takiyama et al., 1995; Van Alfen et al., 2001).

The ubiquitous expression of ATXN3 results in progressive dysfunction in many regions and pathways, such as the brainstem, pyramidal and extrapyramidal pathways, lower motor neurons, oculomotor system and peripheral nerves (Cancel et al., 1995; Durr et al., 1996; Matusmura et al., 1996; Rub et al., 2004; Sasaki et al., 1995; Takiyama et al., 2004).

Although the core clinical feature in MJD is progressive ataxia due to cerebellar and brainstem dysfunction, there is a wider range of symptoms observed in MJD. This includes vestibular and speech difficulties after onset of the disease and visual and oculomotor problems including nystagmus, slowing of saccades, disconjugate eye movements, spasticity, and ophthalmoplegia with disease progression. In advanced stages of disease, patients are wheelchair-bound and suffer from dysarthria and dysphagia (Paulson H, 2012). The clinical phenotype worsens in cases with homozygous heredity suggesting a gene dosage effect (Carvalho et al., 2008). So far, there is no cure for the disease and survival after disease onset ranges from ~20 to 25 years (Klockgether et al., 1998).

In accordance with the symptoms, signs of neurodegeneration such as brain atrophy and neuronal loss are widespread and variable, most often involving regions of the hindbrain such as deeper structures of the basal ganglia, various brainstem nuclei and the cerebellum (Koeppen et al., 1999; Paulson HL 2007, 2012; Rub et al., 2004).

1.1.2.5 The ‘loss of function’ and ‘gain of function’ hypothesis for Machado-Joseph Disease

As mentioned above, there are some evidences, such as an increase in disease severity and a decrease in the age of onset with a higher repeat number, suggesting that the unstable expansion of the polyQ repeat of ATXN3 is responsible for the emergence of the pathology of MJD. Additionally, several transgenic models expressing polyQ sequences outside the natural gene environment displayed a neurodegenerative phenotype (Ikeda et al., 1996; Paulson et al., 1997b). But so far, the mechanism how polyQ expanded ATXN3 causes the

pathogenesis of MJD, is still a matter of intensive debate.

One important argument for the idea that polyQ containing aggregates are responsible for the pathology of MJD is that they recruit and sequester more Ataxin 3 and numerous other cellular proteins (Chai et al., 2002; Donaldson et al., 2003). In this case, these proteins would be hampered in fulfilling their functions, leading to disturbances of important cellular processes, promoting a potential 'Loss of Function' hypothesis.

The 'Gain of Function' hypothesis on the other hand proposes that the proteolytic cleavage of the expanded polyglutamine stretch in the ATXN3 protein leads to the generation of cytotoxic and aggregation-prone shorter soluble fragments, forming intranuclear inclusions (Berke et al., 2004; Haacke et al., 2006; Takahashi et al., 2008). These aggregates might interfere with the normal activity of the nucleus causing the cell to degenerate and die. This theory was previously investigated in our institute. It was found that glutamate-induced excitation of patient-derived neurons initiates Ca^{2+}-dependent proteolysis of ATXN3 followed by the formation of SDS-insoluble aggregates. This phenotype could be abolished by calpain inhibition, confirming a key role of this protease in ATXN3 aggregation (Koch et al, Nature, 2011). Regarding the two hypotheses, conformational changes of ATXN3, aggregation formation of whole protein or proteolytic cleave products mediate cellular mechanisms and function, which might cause cell death (Fig. 1.3)

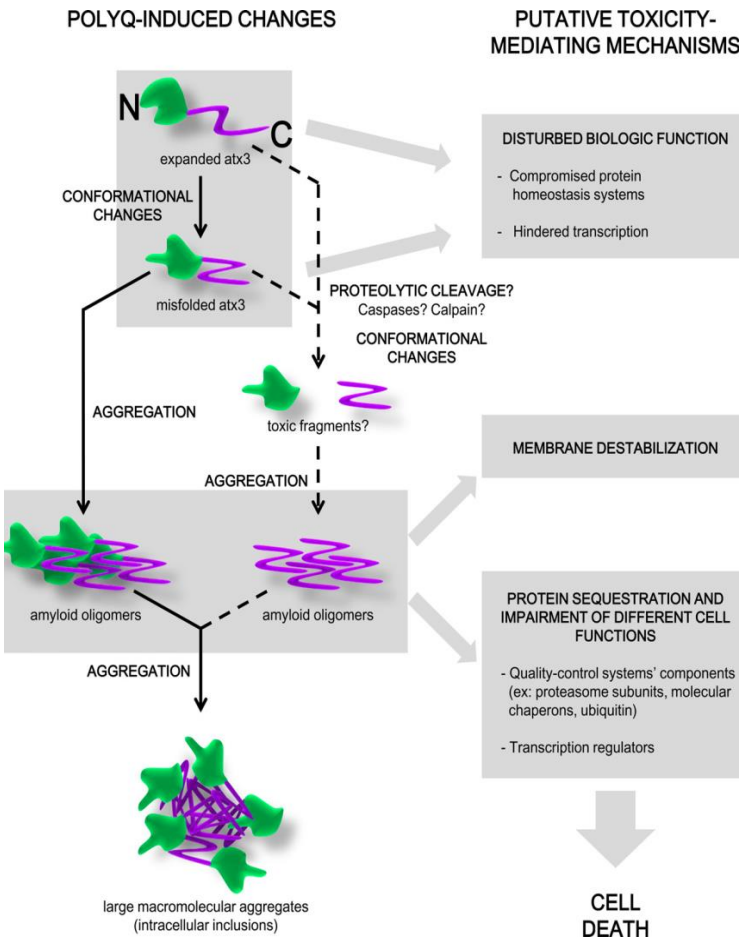

Figure 1.3: Mechanisms of ATXN3 toxicity.

The conformational changes caused by the polyQ stretch may disturb the biologic function of ATXN3, thereby compromising the protein homeostasis system, the cytoskeleton or hindering transcription. Aggregation of whole protein or toxic fragments, products of proteolytic cleavage by calpains, can lead to membrane destabilization and the impairment of protein sequestration mechanisms. Those impairments of cellular functions and homeostasis finally induce cell death. Scheme from Matos et al. (2011).

1.1.2.6 Implications of Ataxin 3 in cellular stress responses

While aggregation due to mutated ATXN3 is responsible for the pathology of MJD, non-expanded ATXN3 was shown to be involved in multiple cellular functions, including transcriptional regulation and helping to maintain protein homeostasis via deubiquitination of target proteins or ubiquitin-editing processes (Berke et al., 2005; Matos et al., 2011; Reyes-Turcu et al., 2009; Reyes-Turcu and Wilkinson, 2009). Additionally, there is also evidence suggesting that the biological function of ATXN3 might further be connected to cellular systems of stress response.

An important indicator for this hypothesis is the fact that ATXN3 shifts to the nucleus in response to proteotoxic stress (Mueller et al., 2009; Reina et al., 2010) and furthermore that some types of cellular stress increase ATXN3 ubiquitination, consequently increasing its activity (Todi et al., 2009). More precisely, ATXN3 activity as a deubiquitinating enzyme, participating in protein homeostasis pathways might be important for cellular stress response, since it is important in dealing with stress-induced misfolded proteins, which might also be responsible for an exacerbation of cellular stress. In *C. elegans*, the orthologs of ATXN3 and p97/VCP (CDC-48) were shown to synergistically mediate both stress responses and longevity, depending on the deubiquitylation activity of ATXN3. Thus, a mechanistic link between protein degradation and longevity through editing of the ubiquitylation status of substrates involved in insulin–IGF-1 signaling was suggested (Kuhlbrodt et al., 2011). While investigating potential roles of ATXN3 in response to cellular stress, it was also shown that ATXN3 as a DUB regulated basal level of hsp70 and modulated hsp70 in response to a subset of cellular stresses (Reina et al., 2012).

It was further demonstrated that ATXN3 might play a role in the stress response not only due to its DUB- and ubiquitin-binding functions, but also due to transcriptional regulation. After application of the oxidative stressor H_2O_2 it was shown that ATXN3 interacts as a redox-sensitive, transcriptional coactivator with the forkhead box O (FOXO) transcription factor FOXO4 and activates the FOXO4-dependent transcription of the antioxidant enzyme *manganese superoxide dismutase (SOD2)* gene. But in comparison to normal ATXN3, mutant ATXN3 displayed a reduced capability to activate the FOXO4-mediated *SOD2* expression and further interfered with binding of FOXO4 to the *SOD2* gene promoter (Araujo et al., 2011).

Another proteotoxic stimulus could be the presence of misfolded and/or aggregated expanded ATXN3 by itself, resulting in cellular stress. Additionally, stress induced transport to the nucleus might trigger even more serious consequences to the cell, since ATXN3 is protected from degradation and enhances toxicity after nuclear localization (Bichelmeier et al., 2007; Breuer et al., 2010). In terms of this theory, it was shown that aging and a possible

dysfunction of ATXN3 caused by the unstable expansion resulted in an inability for ATXN3 to protect against proteotoxic stress, leading to cell toxicity (Reina et al., 2010). Moreover, as a result to thermal stress, expanded ATXN3 shifted to the nucleus in a CK2-dependent manner, triggering and/or enhancing cytotoxic effects (Mueller et al., 2009).
In summary, normal ATXN3 might contribute to the regulation of the cellular response to stress, whereas expanded ATXN3 might display an impaired stress response and might even worsen already toxic effects.

1.2 Genome engineering in human cells

Genome-engineering tools facilitate site-specific genetic changes of the DNA such as deletions, insertions, inversions and replacements. These manipulations are often necessary to understand how genes are functioning within a given cellular context, to investigate gene regulation mechanisms and to model human disease conditions using either *in vitro* cellular models or *in vivo* model organisms.
The discovery of the DNA double helix in 1953 induced the development of the genome engineering field, with various technologies for the manipulation of DNA to be created. Furthermore, since the discovery that cells have an endogenous machinery to repair lethal double-strand DNA breaks (DSBs), researchers focused on approaches to introduce precise breaks in the genomic locus of DNA where changes were to be introduced (Doudna and Charpentier, 2014). For this two different pathways are crucial: homology-directed repair (HDR) and nonhomologous end-joining (NHEJ).
HDR requires an exogenously homologous DNA sequence to guide repair and to insert specific point mutations or desired sequences through recombination of the target locus with the 'donor templates'. When the homologue DNA piece is absent, the cell can use NHEJ instead (Pardo et al., 2009). During this repair process insertion/deletion mutations (indels) of various lengths can be introduced, which can disrupt the translational reading frame of a coding sequence or the binding sites of *trans*-acting factors in promoters or enhancers (Sander and Joung, 2014).
More recently, protein-based systems and site-directed zinc finger nucleases (ZFNs; (Bibikova et al., 2001, 2003; Kim et al., 1996; Porteus et al., 2003) and TAL effector nucleases (TALENs; Boch et al., 2009; Christian et al., 2010; Moscou et al., 2009) were developed. ZFNs and TALENs are artificial fusion proteins containing an engineered DNA binding domain fused to a nonspecific nuclease domain from the restriction enzyme FokI. When targeted to paired adjacent sequences, the FokI domains of these programmable, site-specific nucleases form a dimer that activates the nuclease activity, thus creating a DSB near their binding sites (Wang et al., 2016). Afterwards, the cell uses its repair mechanism for the

induced DSB and will incorporate the mutation.

Although both approaches were used for site-directing genome editing, they also displayed various challenges for the researchers such as difficulties in designing, cloning and validating of those proteins for a specific DNA locus (Doudna and Charpentier 2014; Sander and Joung, 2014; Wang et al., 2016). Thus, the introduction of site-specific modifications in the genome of both, cells and model organisms has been a challenging and error-prone task so far.

1.2.1 Gene editing –CRISPR/Cas9

In contrast to ZFN and TALEN methods, which are based on protein-DNA interactions for targeting, RNA-guided nucleases (RGNs) use simple Watson-Crick base pairing between the engineered RNA and the target DNA site. Thus, the approach is less complex in development since there are no difficult processes of design, synthesis or validation.

CRISPR (clustered regulatory interspaced palindromic repeats) was first described in 1987 by Japanese researchers as a series of short direct repeats interspaced with short sequences in the genome of Escherichia coli and later in a larger number of bacteria and archaea (Ishino et al., 1987; Mojica et al., 2000).

Since 2005 it is known that CRISPR systems are adaptable immune mechanisms that are formed by many bacteria and archae to protect themselves from phages and plasmids by the recognition of foreign DNA (Bolotin et al., 2005; Mojica et al., 2005; Pourcel et al., 2005). Other findings that CRISPR loci are transcribed and that cas (CRISPR-associated) genes encode proteins with putative nuclease and helicase domains lead to the conclusion that CRISPR-Cas is an adaptive defense system that might use antisense RNAs which have been incorporated in the genome, as memory signatures of past invasions (Makarova et al., 2006).

In 2007 experiments with *Streptococcus thermophilus* evidenced the adaptive immunity due to CRISPR. After infection of *Streptococcus thermophilus* with phages, resistant cells emerged possessing new CRISPR spacers identical with the phage genome, which caused the phage resistance phenotype (Barrangou et al., 2007). The requirement for the incorporation of spacers in the genome is an encounter with foreign DNA elements, making this system comparable to the adaptive immunity in higher eukaryotes.

Three stages need to be processed for adaptive immunity: In the first stage DNA fragments of invading plasmids or phages are inserted into the host CRISPR locus as spacers between CRISPR RNA (crRNA) repeats. In the second stage precursor crRNA (pre-crRNA) is transcribed, translated and cleaved by Cas proteins, which generates individual sequence-

specific crRNAs after maturation. Every crRNA is composed of a repeat part and an invader-targeting spacer portion. In the third stage, by using crRNAs as a guide, Cas proteins recognize and cleave foreign nucleic acids at sites complementary to the crRNA spacer sequence.

In 2012, the first study was published demonstrating that the CRISPR/Cas9 mechanism can be repurposed for genomic engineering and further that this system works, compared to previous existing genome engineering techniques, with an intriguing ease and efficiency (Jinek et al., 2012). Those advantages made CRISPR-Cas the most preferred tool for genome editing so far.

Since type II CRISPR systems are the only ones that require just one Cas protein, namely Cas9, for cleavage, it is preferably used for genome engineering. Cas9 is a naturally evolved, RNA-guided nuclease. It recognizes its target DNA through a base-pairing interaction between a single guide RNA (sgRNA) and its targeted DNA strand of about 20 nucleotides. In addition to Cas9, the type II CRISPR systems includes a designed single guide RNA (sgRNA) that acts like crRNAs and two template options for DNA repair; non-homologous end joining or homology directed repair (Fig. 1.4).

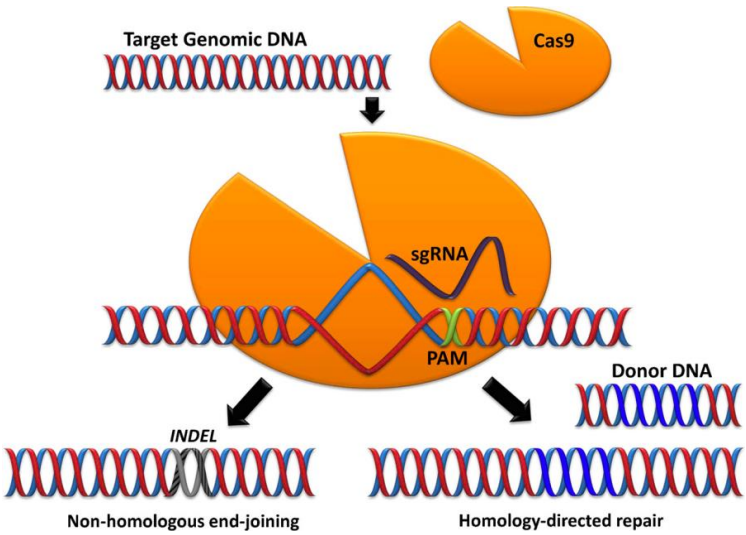

Figure 1.4: CRISPR/Cas9 function
Scheme of CRISPR-Cas9 based genome editing. Targeted genome strand breaks in the DNA can be repaired via the nonhomologous end-joining (NHEJ) repair pathway, which introduces insertion or deletions creating errors, or through the homologous directed repair (HDR) pathway, that can be used to recombine selected markers at specific sites in the genome. *(Scheme: Waddington et al., 2017).*

The Cas9 nuclease contains an RNA binding domain, an alpha helix recognition lobe (REC), a nuclease lobe that include the RuvC and HNH for DNA cleavage, and a protospacer adjacent motif (PAM) interacting site (Hsu et al., 2014; Van der Ooost et al., 2014).

The Cas9/sgRNA complex scans the DNA for a PAM (5'-NGG) site (4,5,6). PAM is a component of the invading plasmid, but not of the host CRISPR locus. The absence of the PAM sequence at the CRISPR locus in the host genome prevents the locus from being

targeted by nucleases and thus prevents it from self-cleavage (Mali et al., 2013). Recognition of a PAM site leads to unwinding of the DNA, and allows the sgRNA to check for complementary DNA adjacent to the PAM site. The PAM site recognition is involved in activating the nuclease domains HNH and RuvC which create a double-stranded break (DSB) in the target DNA, leading to DNA degradation (Hsu et al., 2014; Jinek et al., 2012; Van der Oost et al., 2014). Cas9 releases and searches for another PAM site in case the sgRNA is not complementary (Sternberg et al., 2014).

The DSB generated by Cas9 activates the NHEJ or HDR DNA repair pathways. NHEJ causes random insertions or deletions (indels) at its targeted site, and HDR can create desired mutations or indels through homologous recombination guided by donor DNA.

Single guide RNAs can be expressed along with Cas9 nuclease in the same vector to target specific DNA sites for genome editing, which makes it a fast and easy approach. With this comparably easy to manage technique it is possible to create cell lines and model organisms with any mutation or knockout that is desired.

1.3 Stem cells

Depending on their potency, stem cells have the remarkable potential to develop into all different cell types in the body, which makes them essential for the development of complex organisms. In mammals, stem cells can be classified into two main groups: embryonic stem cells (ES) that are able to develop all three germ layers of an organism and adult or somatic stem cells, which are responsible for the homeostasis and regeneration of tissues or organs such as the liver, hair follicles or the intestinal system (Baddour et al., 2012; Boehnke et al., 2012; Radtke and Clevers, 2005). All stem cells are undifferentiated cells that retain the unique ability to both continuously self-renew and to undergo differentiation into more restricted and specialized progeny at the same time.

Stem cells are further categorized by their potency, the cell's ability to differentiate into other types of cells. The lowest potency is found in unipotent stem cells such as spermatogonial stem cells, which can only form one single lineage. In contrast, multipotent stem cells possess the potential to form multiple closely related and discrete cell types of one tissue (Weissman, 2000). Examples for multipotency are neural stem cells giving rise to neurons and glial cells or hematopoietic stem cells differentiating into myeloid and lymphoid lineages (Clements and Traver, 2013). During embryonic neurogenesis, multipotent neural stem cells initiate a complex pattern of consecutive cycles of symmetrical as well as asymmetrical division to construct the exceptional complexity of the brain (Breunig et al., 2011; Kriegstein and Alvarez-Buylla, 2009; Rakic, 1988; Reynolds & Weiss, 1992). During adulthood,

multipotent stem cells are responsible for organ homeostasis and endogenous repair mechanisms after injury. Moreover, only the hippocampus and the subventricular zone (SVZ) of the human brain have been identified to harbor multipotent neural stem cells, providing a limited potential of self-repair of the brain (Eriksson *et al.*, 1998; Gage, 2000).

Pluripotent stem cells, particularly human embryonic stem (hES) cells arise at the earliest stages of human development and are able to generate all three germ layers giving hES cells the potential to form any cell type of the body *in vitro* (Smith, 2001; Thomson *et al.*, 1998). Therefore, the usage of pluripotent cells became inevitable in regenerative medicine (Lovell-Badge, 2001; Tabar and Studer., 2015) as well as in the field of disease modeling, drug discovery and cell therapy development (Colman & Dreesen, 2009; Han et al., 2011; Shi et al., 2017).

1.3.1 Human pluripotent stem cells

The vast development of human stem cell science started in 1994 after the inner cell mass (ICM) from human blastocysts was isolated and cultured. Shortly afterwards, the derivation of the first hES cell lines were reported by Thomson and coworkers in 1998 (Bongso et al., 1994; Thomson et al., 1998). These discoveries lead to the progression of this discipline and in the development of various methods such as immunosurgery as well as mechanical and laser assisted isolation in order to establish hES cell lines from the ICM of cultured blastocyst and the morula (Ilic and Ogilvie, 2017; Kim et al., 2005; Marteyn et al., 2011; Peura et al., 2008; Strelchenko et al., 2004). At this time, hES were thought to be the future of regenerative medicine, resulting in improvements of culture conditions to meet the requirements for the regulations for medical products and good manufacturing practice (GMP) guidelines by replacing compounds of animal origin with chemical compounds (Unger et al., 2008).

Furthermore, by analyzing the molecular characteristics of hES cells, broad knowledge was achieved to decipher the mechanisms of pluripotency (Chambers et al., 2003; Li, 2005; Niwa et al., 1998; Rodda et al., 2005). These efforts have been rewarded in 2006 when Takahashi and Yamanaka discovered that the retorviral overexpression of the four transcription factors (TF), Oct3/4, Klf4, Sox2 and c-Myc is sufficient to directly reprogram adult somatic cells to the state of induced pluripotent stem cells (iPSC; Nakagawa et al., 2008; Takahashi et al., 2007). Those iPS cells displayed, aside from some reported reporgramming-dependent genomic and epigenetic aberrations, the same characteristics of self-renewal and differentiation potential as hES cells (Gore et al., 2011; Hussein et al., 2011; Lister et al., 2011).

Following the discovery of induced pluripotency, reprogramming technology developed towards safer integration-free methods such as direct protein transduction or mRNA and mature microRNA transfection and Sendai virus. Thereby, also the number of transcription factors was changed within the reprogramming protocols or replaced by chemical compounds (Anokye-Danso et al., 2011; Fusaki et al., 2009; Miyoshi et al., 2011; Nakagawa et al., 2008; Schlaeger et al., 2015; Warren et al., 2010; Zhu et al., 2010). Still, approaches in regenerative medicine and disease modeling the search for protocols for efficient differentiation of pluripotent cells in vitro into authentic somatic cell types such as insulin producing beta cells, cardiac myocard, as well as neural stem cells, neurons and glial cells remain a key task.

Nevertheless, the emergence of iPS cell technology with non-embryonic origin revolutionized the stem cell field as it circumvents ethical and legal issues connected to hES cell research and allows the generation of any cell type from any individual in unlimited quantities.

1.3.2 Differentiation potential of human pluripotent and neural stem cells

Human pluripotent stem cells (hPSCs) represent the most immature cell population, having the potential to differentiate into all three embryonic germ layers (Thomson et al., 1998). During the last decade, the translation of basic knowledge from developmental neurobiology has helped to create protocols for the generation of distinct neural cell types from hPS cells. In the earliest protocols, hPS cells were sequentially exposed to a cocktail of extrinsic factors to straightly direct them into a mature neural cell type such as neurons and glia. Those ‚run-though' protocols comprised some disadvantages such as the generation of incompletely differentiated cultures and batch-to-batch variations due to time-consuming differentiation protocols (Kim et al., 2011). Also, for experimental validations and repetitions, the cell number generated by those protocols was too low, which made the reproducibility of experiments very difficult (Reinhardt et al., 2013). Therefore, protocols were developed to generate intermediate cell populations: transiently emerging neural stem cells (NSCs), which have the capability to both efficiently form mature neural cell types and robustly expand to produce a sufficient cell number. Two examples are rosette-forming neuroepithelial stem cells (Elkabetz et al. 2008; Koch et al. 2009) and primitive pre-rosette neuroepithelial stem cells (Li et al. 2011; Reinhardt et al. 2013), which can be aligned to specific stages of human neurodevelopment and differ in morphology, self-renewal capacity and differentiation potential (Conti and Cattaneo, 2010; Karus et al., 2014).

Rosette-forming neuroepithelial stem (r-NES) cells develop after spontaneous conversion of early neuroepithelium (NE) precursor cells, which depends on SHH and Notch agonists when

kept in culture for a few passages (Elkabetz et al., 2008). These cells express the rosette-markers PLZF and Dach1, form characteristic rosette structures with apical ZO1 expression and show interkinetic nuclear migration, characteristics similar to early neural tube forming cells (Elkabetz et al., 2008; Zhang et al., 2001). Furthermore, it was shown that exposure to the mitogens FGF2 and EGF and B27 supplement mix generates a homogenous and stable rosette-type long-term self-renewing NE stem cell population (lt-NES cell; Koch et al., 2009; Nemati et al., 2010). This cell population can be differentiated into glial or neuronal cells with highly reproducible neuronal differentiation rates and display a stable neurogenic differentiation pattern even after propagation for over 100 passages. Furthermore, lt-NES cells remain susceptible to morphogens such as Sonic hedgehog (SHH), FGF8 and retinoic acid, facilitating the targeted generation of different subtypes such as midbrain dopamine neurons or spinal motor neurons even after long-term cultivation (Falk et al., 2012; Koch et al., 2009). Compared to hESC, these cells exhibit significantly shorter doubling times (38 vs. 51-81 hours) and a higher clonogenicity.

The pre-rosette neuroepithelial stem cells were reported by Reinhardt et al. (2013) and are derived and propagated by using only small molecules (small molecule neural precursor cells; smNPCs). Their maintenance of self-renewal relies on inhibition of BMP/TGFβ signaling and activation of Wnt and SHH, a combination that is distinct from FGF2 and EGF required for lt-NES cells. Furthermore, smNPCs can be efficiently specified into neural tube and neural crest lineages, which gives them a developmental potential upstream of lt-NES cells. It was further demonstrated that culturing smNPCs with FGF2 results in the formation of rosette-like structures, which have been previously associated with the neural plate-stage of embryogenesis. Compared to ltNES cells smNPCs can be cultured at a wide range of cell densities since they can grow clonally, thus facilitating the handling since less splitting steps are required.

1.4 Aim of this study

Transcriptional regulation is an essential cellular mechanism that is dysregulated in many polyQ diseases and contributes to their pathology. Previous studies have shown that ATXN3 is involved in transcriptional regulation processes by binding to specific DNA-motifs and chromatin areas of genes, activation of transcriptional co-regulators and formation of histone deacetylating complexes, resulting in the repression of target genes.

The aim of this study was to decipher how ATXN3 might be involved in the transcriptional regulation and the cellular response to stress. To that end two patient-specific stem cell derived neural stem cell lines were genetically edited by using a CRSIPR/Cas9 KO system, specific for the human ATXN3 gene, in order to generate isogenic cell lines, which only differ in their state of ATXN3. For each patient foster line, three KO cell lines emerged: one total knock-out (KO) of ATXN3 and two hemizygous cell lines expressing the expanded (ATXN3_exp) or non-expanded allele (ATXN3_non-exp), respectively.

This approach enables to search for differentially expressed genes, which might be attributed to the expanded and non-expanded allele or a complete KO of ATXN3 within an isogenic genetic background.

Possible candidate genes, which are differentially expressed between the isogenic cell lines, were to be analyzed regarding their physiological interactions with ATXN3, functional consequences for the generated cell line and an underlying mechanism of this interaction.

2 Materials

2.1 Technical equipment

Appliance	Name	Manufacturer	Registered office
Autoclave	D-150	Systec	Wettenberg, Germany
Balance	BL610	Sartorius	Göttingen, Germany
Balance	LA310S	Sartorius	Göttingen, Germany
Block heater	Thermomixer	Eppendorf	Hamburg, Germany
Centrifuge (cell culture)	Megafuge 1.0R	Sorvall	Hanau, Germany
Centrifuge (table top)	5415D	Eppendorf	Hamburg, Germany
Counting chamber	Fuchs-Rosenthal	Faust	Halle, Germany
Digital camera	C 5050 Zoom	Olympus Optical	Hamburg, Germany
Nucleofector	Nucleofector 2b	Lonza	Basel, Switzerland
Fluorescence lamp	HAL100	Carl Zeiss	Jena, Germany
Fluorescence microscope	Axioskop 2	Carl Zeiss	Jena, Germany
Freezer -80°C	HERAfreeze	Kendro	Hanau, Germany
Gel electrophoresis chamber	Agagel	Biometra	Göttingen, Germany
Imaging system	Chemidoc 2000	Bio-Rad	München, Germany
Imaging system	Geldoc EZ	Bio-Rad	München, Germany
Incubator	HERAcell	Kendro	Hanau, Germany
Inverse light microscope	Axiovert 25	Carl Zeiss	Jena, Germany
LED light source	Colibri 2	Carl Zeiss	Jena, Germany
Liquid nitrogen store	MVE 611	Chart Industries	Burnsville, USA
Microscope	Axiovert 40 CFL	Carl Zeiss	Jena, Germany
Microscope	Axiovert 200M	Carl Zeiss	Jena,Germany
Microscope	Axio Imager Z1	Carl Zeiss	Jena,Germany
Microscope	DMI6000 B	Leica Microsystems	Wetzlar, Germany
Microscope camera	Axiocam MRM	Carl Zeiss	Jena, Germany
Micro-Spectrophotometer	Nanodrop ND-1000	Thermo Fisher Scientific	Wilmington, USA
Micropipettes	Labmate L2-L1000	Labmate	Langenfeld, Germany

Appliance	Name	Manufacturer	Registered office
Multilabel reader	EnVision 2104	Perkin Elmer	Rodgau, Germany
PAGE/Blot equipment	Mini-Protean 3	Bio-Rad	München, Germany
PCR cycler	T3000 Termocycler	Biometra	Göttingen, Germany
pH-meter	CG840	Schott	Mainz, Germany
Pipette-boy	Accu-Jet	Brand	Wertheim, Germany
Platereader	Infinite® 200 PRO	Tecan	Männedorf, Switzerland
Power supply for electrophoresis	Standard Power Pack P25	Biometra	Göttingen, Germany
Real-time qPCR machine	Mastercycler realplex	Eppendorf	Hamburg, Germany
Refrigerators 4°C /-20°C	G 2013 Comfort	Liebherr	Lindau, Germany
Secure horizontal flow hood	HERAsecure	Kendro	Hanau, Germany
Shaker	Bühler KS15	Johanna Otto	Hechingen, Germany
Sterile laminar flow hood	HERAsafe	Kendro	Hanau, Germany
Stereo microscope	STEMI 2000-C	Carl Zeiss	Göttingen, Germany
Table centrifuge	Centrifuge 5415R	Eppendorf	Hamburg, Germany
Thermocycler	T3 Thermocycler	Biometra	Göttingen, Germany
Ultracentrifuge	Sorvall	Discovery 90 SE	Hanau, Germany
Vacuum pump	Vacuubrand	Brand	Wertheim, Germany
Vortexer	Vortex Genie 2	Scientific Industries	New York, USA
Water bath	1008	GFL	Burgwedel, Germany

2.2 Cell culture and molecular biology consumables

Consumables	Manufacturer	Registered Office
6-well culture dishes	Corning	Corning, USA
12-well culture dishes	Corning	Corning, USA
24-well culture dishes	Corning	Corning, USA
96-well culture dishes	Corning	Corning, USA
Cell Strainer 40 µm Nylon	Corning	Corning, USA
Coverslips	Menzel Gläser	Braunschweig, Germany
Cryovials 1 ml	Nunc	Wiesbaden, Germany
Cryovials 1.8 ml	Nunc	Wiesbaden, Germany
Blotting membrane, nitrocellulose	Sigma-Aldrich	Deisenhofen, Germany
PCR strip tubes 0.2 ml	peqLab	Erlangen, Germany
Petri dishes ∅ 10 cm	PAA	Pasching, Austria
Serological pipettes 1 ml	Sarstedt	Nümbrecht, Germany
Serological pipettes 2ml	Sarstedt	Nümbrecht, Germany
Serological pipettes 5ml	Costar, Corning	Corning, USA
Serological pipettes 10ml	Greiner Bio-One	Kremsmünster, Austria
Serological pipettes 25ml	Costar, Corning	Corning, USA
Syringes 50 ml	BD Biosciences	Heidelberg, Germany
Syringe fier 0.2 µm	PALL	Dreieich, Germany
TC dishes ∅ 3.5 cm	FALCON, Corning	Corning, USA
TC dishes ∅ 6 cm	FALCON, Corning	Corning, USA
TC dishes ∅ 10 cm	FALCON, Corning	Corning, USA
Tubes 0.5 ml	Axygen, Corning	Corning, USA
Tubes 1.5 ml	Axygen, CorningBio-One	Corning, USA
Tubes 2 ml	Axygen, CorningBio-One	Corning, USA, Germany
Tubes 15 ml	FALCON, Corning	Corning, USA
Tubes 50 ml	FALCON, Corning	Corning, USA
Whatman® Filter paper	GE Healthcare	Little Chalfont, UK
qPCR plates	4titude	Wotton, UK
qPCR seals	4titude	Wotton, UK

2.3 Chemicals

Chemicals	Manufacturer	Registered office
2-Mercaptoethanol	Invitrogen	Karlsruhe, Germany
30% Bis/Acrylamide	Carl Roth	Karlsruhe, Germany
Agar	Sigma-Aldrich	Deisenhofen, Germany
Agarose	PeqLab	Erlangen, Germany
Ampiciline	Sigma-Aldrich	Deisenhofen, Germany
Ascorbic acid (L-)	Sigma-Aldrich	Deisenhofen, Germany
Ammonium persulfate	Sigma-Aldrich	Deisenhofen, Germany
Azide	Sigma-Aldrich	Deisenhofen, Germany
B-27 supplement	Gibco by Life Technologies	Waltham, USA
Bromphenol blue	Sigma-Aldrich	Deisenhofen, Germany
BSA solution (7.5%)	Sigma-Aldrich	Deisenhofen, Germany
$CaCl_2$	Sigma Aldrich	Deisenhofen, Germany
$CdCl_2$	Sigma-Aldrich	Deisenhofen, Germany
Chloroform	Carl Roth	Karlsruhe, Germany
Chloroquin	Sigma Aldrich	Deisenhofen, Germany
complete, mini, EDTA free	Roche Diagnostics	Mannheim, Germany
Cycloheximide	Sigma Aldrich	Deisenhofen, Germany
DAPI	Sigma Aldrich	Deisenhofen, Germany
DAPT	Axon Medchem	Groningen, The Netherlands
DMEM	Gibco by Life Technologies	Waltham, USA
DMEM/F12 (1:1)	Gibco by Life Technologies	Waltham, USA
DMSO	Sigma Aldrich	Deisenhofen, Germany
DNA ladder (100bp/1kbp)	PeqLab	Erlangen, Germany
dNTPs	PeqLab	Erlangen, Germany
Doxycycline	Sigma Aldrich	Deisenhofen, Germany
EDTA	Sigma Aldrich	Deisenhofen, Germany
EGF	R&D Systems	Minneapolis, USA
Ethanol	Sigma Aldrich	Deisenhofen, Germany
Ethidium bromide	Sigma-Aldrich	Deisenhofen, Germany
FCS	Invitrogen	Karlsruhe, Germany
FGF2	R&D Systems	Minneapolis, USA
G418 solution	Carl Roth	Karlsruhe, Germany
Geltrex	Gibco by Life Technologies	Waltham, USA
Glucose	Sigma-Aldrich	Deisenhofen, Germany

Chemicals	Manufacturer	Registered office
L-Glutamate	Sigma-Aldrich	Deisenhofen, Germany
Glycerol	Sigma-Aldrich	Deisenhofen, Germany
Glycin	Sigma-Aldrich	Deisenhofen, Germany
H_2O_2	Sigma-Aldrich	Deisenhofen, Germany
HCl	Sigma Aldrich	Deisenhofen, Germany
Isopropanol	Sigma Aldrich	Deisenhofen, Germany
Laminin	Thermo Fisher Scientific	Waltham, USA
LB-Medium powder	Carl Roth	Karlsruhe, Germany
L-glutamine (100x)	Gibco by Life Technologies	Karlsruhe, Germany
2-Mercaptoethanol	Invitrogen	Karlsruhe, Germany
Methanol ROTIPURAN	Carl Roth	Karlsruhe, Germany
Mowiol	Carl Roth	Karlsruhe, Germany
Myo-Inositol	Sigma-Aldrich	Deisenhofen, Germany
N2 supplement (100x)	Gibco by Life Technologies	Karlsruhe, Germany
Neurobasal medium	Gibco by Life Technologies	Karlsruhe, Germany
N,N-Dimethylformamide	Sigma-Aldrich	Schnelldorf, Germany
Non-essential amino acids (100x)	Gibco by Life Technologies	Karlsruhe, Germany
DPBS	Gibco by Life Technologies	Waltham, USA
PFA	Sigma Aldrich	Deisenhofen, Germany
Penicillin-Streptomycin	Gibco by Life Technologies	Karlsruhe, Germany
Poly-L-ornithine	Sigma-Aldrich	Deisenhofen, Germany
Puromycin	PAA	Pasching, Austria
p-Coumaric acid	Sigma-Aldrich	Deisenhofen, Germany
Polyvinylalcohol	Sigma-Aldrich	Deisenhofen, Germany
Powdered milk	Carl Roth	Karlsruhe, Germany
Pyocyanin	Sigma-Aldrich	Schnelldorf, Germany
Rotenone-Calbiochem	Merck	Darmstadt, Germany
SDS	Sigma-Aldrich	Deisenhofen, Germany
Sodium pyruvate (100x)	Invitrogen	Karlsruhe, Germany
TEMED	Sigma Aldrich	Deisenhofen, Germany
TriFast peqGOLD	PeqLab	Erlangen, Germany
Tris	Sigma Aldrich	Deisenhofen, Germany
Triton-X-100	Sigma Aldrich	Deisenhofen, Germany
Trypane Blue	Invitrogen	Karlsruhe, Germany
Trypsin inhibitor (TI)	Gibco by Life Technologies	Waltham, USA

Chemicals	Manufacturer	Registered office
Trypsin-EDTA (10x)	Gibco by Life Technologies	Waltham, USA
$ZnCl_2$	Sigma-Aldrich	Deisenhofen, Germany

2.4 Cell culture

2.4.1 Cell culture media

All cell culture reagents were prepared under sterile conditions and stored at 4°C; % = v/v.

MEF (mouse embryonic feeder)	
86%	DMEM-high-glucose
10%	FCS
1x	Sodium pyruvate
1x	L-Glutamine
1x	Non-essential amino acids
1x	Pen / Strep

Neural stem cell (N2) medium	
98%	DMEM/F12
1x	N2 Supplement
1x	Penicillin/Streptomycin
0.4%	D-Glucose solution

Basic small molecule medium	
98,3%	DMEM/F12
0.5x	N2 Supplement
1x	Penicillin/Streptomycin
0.2%	D-Glucose solution

Neural stem cell freezing medium	
70%	KnockOut™ Serum Replacement
20%	Cytocoon™ Buffer II
10%	DMSO

Neuronal generation (NGMC) medium	
96.8%	DMEM/F12
0.5x	N2 Supplement
0.5x	B27 supplement
1x	Non-essential amino acids
1x	Penicillin/Streptomycin
0.2%	D-Glucose

FCS-based freezing medium	
90%	FCS, heat inactivated
10%	DMSO

2.4.2 Cell culture solutions

1xTrypsin/EDTA (TE)	
90%	PBS
10%	Trypsin/EDTA (TE) 10x

Trypsin inhibitor (TI)	
100%	PBS
0.25 mg/ml	Trypsin inhibitor (>700 units/mg) mixed in PBS, sterile-filtered and stored at 4°C

Poly-L-ornithine (PO)	
100%	H_2O
1.5 mg/ml	Poly-L-ornithine (PO) mixed, sterile-filtered and stored at 4°C

Laminin (Ln) coating solution	
100%	H_2O
1 µg/ml	Laminin (Ln) in PBS

Geltrex (GT) LDEV-free coating solution	
98%	DMEM/F12
2%	Geltrex

Cyto buffer for cell freezing	
43,25g	Myo-Inositol (in 800ml distilled water)
200ml	PBS
5g	Polyvinylalcohol
Add Polyvinylalcohol in small portions, stir continuously. The mixture was sterile-filtered and stored at 4°C	

Glucose solution (0,4g/ml)	
100%	Ampuwa H_2O
0.4 g/ml	L-glucose mixed in Ampuwa H_2O , sterile-filtered and stored at 4°C

Balanced salt solution (BSS) for L-glutamate treatment	
25mM	Tris,
120mM	NaCl
15mM	D-glucose
5.4mM	KCl
1.8mM	CaCl2
0.8mM	MgCl2
H2O was added to 500 ml, the pH was adjusted to 7.4, the mixture was sterile-filtered and stored at 4°C	

2x HBS buffer	
8 g	NaCl
0.38 g	KCl
0.1 g	Na_2HPO_4
5 g	Hepes
1 g	Glucose
H_2O was added to 500 ml, the pH was adjusted to 7.05, the mixture was sterile-filtered and stored at -20°C	

2.4.3 Cell culture additives

Reagent	Concentration	Solvent
B27 supplement	50x	supplement mix
bDNF	10 µg/ml	PBS + 0.1% BSA
CHIR99021	10 mM	DMSO
Chloroquin	50 mM	H_2O
DAPT	25 mM	DMSO/Ethanol (1:5)
DNase	10 mg/ml	H_2O
Doxycycline	1 mg/ml	H_2O
EGF	10 µg/ml	PBS
FGF2	10 µg/ml	PBS + 0.1% BSA
G418	50 mg/ml	H_2O
gDNF	10 µg/ml	PBS + 0.1% BSA
L-Ascorbic acid	200 mM	H_2O
N2 supplement	100x	supplement
Purmorphamine (PMA)	5 mM	DMSO
Puromycin	1 mg/ml	H_2O
Y-27632 (Rho-Kinase-Inhibitor)	5 mM	H_2O

2.4.4 Cell lines

Cell line	Source
E. coli DH5a	Invitrogen, Deisenhofen, Germany
HEK-293FT	Leiden, Netherlands, Dr. Alex Van der Eb
iPS cell line MJD 1	Bonn, Germany
iPS cell line MJD 2	Bonn, Germany
iPS cell line MJD 3 control	Bonn, Germany (Koch et al., 2011)

2.5 Molecular biology

.

2.5.1 Reagents

PFA fixation solution (4%)	
40 g	PFA
1000 ml	H_2O
The solution was heated until PFA dissolved completely, pH adjusted to 7.4 and sterile filtered.	

6x DNA loading buffer	
2 ml	EDTA (0.5M; pH 8.5)
6 g	Sucrose
0,2 ml	2% Bromphenol-blue-solution
0,2 ml	2% Xylene-cyanol-solution
0,2 g	Ficoll
3,8 ml	Aqua bidest.
The solution was mixed well, prepared in 1 ml aliquots and stored at 4°C	

Immuno-blocking solution	
89.9%	PBS
10%	FCS
0.1%	Triton X100 (only for intracellular epitopes)

Moviol / DABCO	
12 ml	Tris solution (0.2 M; pH 8.5)
6 ml	H_2O
6 g	Glycerol
2.6 g	Moviol
0.1 g	DABCO

50x Tris-acetate-EDTA-buffer (TAE)	
242 g	Tris
100 ml	EDTA solution (0.5M; pH 8.5)
57.1 ml	Water-free acetic acid (100%)
add	H_2O to 1000ml

SDS-PAGE separation gel buffer	
99.6%	Tris solution (1.5M; pH 8.8)
0.4%	SDS

SDS-PAGE stacking gel buffer	
99.6%	Tris solution (1.5M; pH 6.8)
0.4%	SDS

SDS-PAGE buffer 10x	
30 g	Tris
144 g	Glycin
add H_2O to 1000 ml (pH 8.0)	
For running buffer add 1% SDS to 1x SDS-PAGE buffer For blotting buffer add 20% Methanol to 1x SDS-PAGE bufffer	

Protein loading buffer	
75.75%	Tris solution (0.1 M; pH 6.8)
20%	Glycerol
4%	SDS
0.25%	Bromphenol blue

10x TBS	
80g	NaCl
2g	KCl
30g	TrisBase
add H_2O to 1000 ml, pH 7.4	
For 1x TBST dilute 10x TBS 1:10 with H_2O and add 1% Tween-20	

Lysis buffer	
2.5 ml	Tris HCl (1 M)
5 ml	NaCl (1.5 M)
2.5 ml	EDTA (0.5 M)
Triton™ X-100	100 µl
Add to 50 ml aqua bidest.	

TE4-buffer	
1.58 g	Tris-HCl
0.29 g	EDTA
add H_2O to 1000 ml	
Adjust pH to 8 with solid NaOH	

Enhanced chemiluminescence (ECL) solution	
4.5 ml	H_2O
0.5 ml	Tris HCl (1 M)
50 µl	Luminol
20 µl	p-coumaric acid
1.5 µl	H_2O_2 (30%)

PCR master mix (10 ml)	
1 ml	10x reaction buffer
600 µl	$MgCl_2$ (50 mM)
40 µl each	dNTPs
8.24 ml	Ampuwa H_2O

qPCR master mix (5 ml)	
2000 µl	GoTaq® Flix buffer
1000 µl	$MgCl_2$ (25 mM)
20 µl each	dNTPs
7.5 µl	1000x SYBR-green
1 µl	Fluorescin
400 µl	DMSO
1511.5 µl	Ampuwa H_2O

2.5.2 Enzymes

Enzyme name	Manufacturer	Registered office
Alkaline Phosphatase, Shrimp	Roche Diagnostics	Penzberg, Germany
DNaseI (cell culture)	Roche	Basel, Switzerland
DnaseI (molecular biology)	Invitrogen	Karlsruhe, Germany
GoTaq G2 Flexi DNA polymerase	Promega	Mannheim, Germany
Phusion High Fidelity DNA Polymerase	New England Biolabs	Frankfurt, Germany
T4 DNA Ligase	New England Biolabs	Frankfurt, Germany
Taq DNA Polymerase, recombinant	Invitrogen	Karlsruhe, Germany

2.5.3 Plasmids

Plasmid name	Source or parent DNA seauence
pMD2.G	Gift from Dider Trono, Lausanne, Switzerland
psPAX2	Gift from Dider Trono, Lausanne, Switzerland
pLVX-EtO	Modified from pLVX-Tet-ON-Advanced (Clontech)
pLVXTP	Equivalent to pLVX-Tight-Puro (Clontech)
pChMTFVSV	Gift from Oleg Georgiev, Zürich, Switzerland
pLVXTP-MTF1-VSV	Modified from pLVX-Tet-ON-Advanced (Clontech)
pLVXTP-ATXN3C71	Modified from pLVX-Tet-ON-Advanced (Clontech)

2.5.4 Restriction endonucleases

Enzyme name	Restriction site	Manufacturer	Registered office
NotI	5'…GC^GGCCGC…3' 3'…CGCCGG^CG…5'	New England Biolabs	Frankfurt, Germany
MluI	5'...A^CGCGT...3' 3'...TGCGC^A...5'	New England Biolabs	Frankfurt, Germany

2.5.5 Bacterial solutions

LB agar	
20 g	LB-Medium powder (Roth)
15 g	Agar
H_2O was added to 1 l, the mixture was autoclaved and stored at 4 °C	

LB medium	
40 g	LB-Medium powder (Roth)
H_2O was added to 2 l, the mixture was autoclaved and stored at 4 °C	

2.5.6 Kits

Name	Producer	Office
CellTiter-Glo® Luminescent Cell Viability Assay	Promega	Mannheim, Germany
DNeasy Blood & Tissue Kit	Qiagen	Hilden, Germany
iScript cDNA Synthesis Kit	Bio-Rad	München, Germany
Nucleofector™	Lonza	Basel, Switzerland
peqGOLD Gel Extraction Kit	Peqlab Biotechnologie	Erlangen, Germany
peqGOLD Plasmid Miniprep Kit	Peqlab Biotechnologie	Erlangen, Germany
Pierce™ BCA Protein Assay Kit	Thermo Fisher Scientific	Rockford, USA
PureYield Plasmid Maxiprep System	Promega	Mannheim, Germany
RNeasy Kit	Qiagen	Hilden, Germany
ROS-ID Total ROS/ Superoxide detection kit	Enzo Life Scienes	Lörrach, Germany

2.5.7 Primer

Cloning primer* Name	Primer sequence (5'-3')
MTF-1VSV-NotI_F	ATAATAGC^GGCCGCGCCGCCACCATGGGGGAACACAGTCC
MTF-1VSV-MluI_R	CAGTA^CGCGTGCGAGCTCGCAGGATTTGAG

Sequencing primer Name	Primer sequence (5'-3')
Seq: Atxn3_1_F	GGCTCCAGACAAATAAACATGGA
Seq: Atxn3_1_R	GATCGATCCTGAGCCTCTGA
Seq: Atxn3_3_F	TGAGGAGGATTTGCAGAGGG
Seq: Atxn3_3_R	ACGCATTGTTCCACTTTCCCA

qPCR primer Name	Primer sequence (5'-3')
qPCR:MT1A_F	GCAAAGGGGCATCAGAGAAG
qPCR:MT1A_R	TGGGTCAGGGTTGTATGGAA
qPCR:MT1E_F	ATCCTCTGGGTCTGGGTTCT
qPCR:MT1E_R	GGGAAGAAGGGGAGAGTGAG
qPCR:MT1G_F	GCCCTGCTCCCAAGTACAAA
qPCR:MT1G_R	AGGGGTCAAGATTGTAGCAAA
qPCR:MT2A_F	CCGACTCTAGCCGCCTCTT
qPCR:MT2A_R	CAGCAGCTTTTCTTGCAGGA
qPCR:MTF1_F	AGACTTTCTCTTCAGCCCCT
qPCR:MTF1_R	AACTCTGACACATCCATGGC
qPCR:SOD2_F	TGGGGTTGGCTTGGTTTCAA
qPCR:SOD2_R	AAGGCCTGTTGTTCCTTGCA
qPCR:RPLPO_F	AGCCCAGAACACTGGTCT
qPCR:RPLPO_R	ACTCAGGATTTCAATGGTGCC
qPCR:18S_F	TTCCTTGGACCGGGGCAAG
qPCR:18S_R	GCCGCATCGCCGGTCGG

2.5.8 Antibodies

Primary antibody	Dilution	Source
Atxn3c clone 1H9-2	1:1000	BioLegend
Atxn3 1C2	1:1000	Millipore
Beta-III-tubulin	1:2000	Sigma-Aldrich
B-actin	1:5000	Millipore
DACH1 rb	1:100	ProteinTech
GFAP	1:500	DAKO
MAP2ab	1:250	Sigma-Aldrich
Metallothinein [UC1MT]	1:500	Abcam
Nestin ms	1:600	R&D Systems
NeuN	1:100	Millipore
Pax6 rb	1:500	Developmental studies hybridoma bank (DSHB)
PLZF ms	1:50	Merck

Primary antibody	Dilution	Source
Sox2 ms	1:300	R&D Systems
VSV-G tag	1:1000	Thermo Fisher
ZO-1 rb	1:100	DSHB

Secondary antibody	Dilution	Source
Alexa488 gt-anti-ms	1:1000	Life technologies
Alexa488 gt-anti-rb	1:1000	Life technologies
Alexa555gt-anti-ms	1:1000	Life technologies
Alexa555gt-anti-rb	1:1000	Life technologies
HRP-gt-anti-ms	1:1000	GE Healthcare Life Sciences
HRP-gt-anti-rb	1:1000	Thermo Scientific

ms = mouse; rb = rabbit; gt = goat

2.6 Software

Name	Application	Producer
ApE – A plasmid Editor v2.0.47	Cloning strategies	M. Wayne Davis
AxioVision 40 4.5.0.0	Fluorescence microscopy	Carl Zeiss
ClustalW v1.83	Sequence alignment	EMBL-EBI
EnrichR	Gene analysis	Kuleshov et al., 2016
Excel 2008	Data analysis	Microsoft
Image J 1.42q	Quantifications	NIH
Imagelab 5.0 build 18	Western blot documentation	Bio Rad
GenomeStudio 2011	SNP analysis	Illumina
Microsoft Office 2008	Figures and text processing	Microsoft
Photoshop CS3	Figures processing	Adobe
Primer3 v0.4.0	Primer picking	Rozen and Skaletsky (2000)
Prism 5	Data analysis and statistics	GraphPad
Quantity One 4.6.8	Electrophoresis gel documentation	Bio Rad
Word 2008	Writing documents	Microsoft

3 Methods

3.1 Cultivation of human pluripotent stem cell-derived neural stem cells

Small molecule neural precursor cells (smNPCs) were generated from induced pluripotent stem cells as previously described (Reinhardt et al., 2013) and cultured on GelTrex-coated 6-well (Falcon) cell culture plates. Cell expansion medium consisted of DMEM-F12 (Gibco) with 1:200 N2 supplement (Invitrogen), 1:200 B27 supplement lacking vitamin A (Gibco), with 1% penicillin/streptomycin (Gibco), freshly supplemented with 3 µM CHIR 99021, 0.3 µM Purmorphamine (PMA), and 100 µM ascorbic acid (AA), with a medium change every day. Typically, cells were split 1:4 every 3 or 4 days. For splitting, cells were digested into single cells for about 8 minutes at 37°C by using Trypsin-EDTA (Gibco). The same amount Trypsin-Inhibitor was added to stop the digestion and the mixture was diluted in DMEM (Gibco) for centrifugation at 1200x for four minutes. The cell pellet was resuspended in fresh smNPC expansion medium and plated on GelTrex-coated cell culture dishes.

3.2 Differentiation of neural stem cells into neurons

Small molecule neural precursor cells are multipotent stem cells that constantly retain their capability to generate defined cultures of neurons and glial cells over a certain period of time, making them a useful neural progenitor population. Before final differentiation, medium of smNPCs was exchanged to DMEM/F12, containing EGF and FGF2, for 24 h (Koch et al., 2009). The generated long-term neuroepithelial-like cells (ltNESc) were transferred to geltrex (GT)-coated cell culture dishes and differentiated to neuronal cultures by withdrawing of growth factors from the culture medium upon reaching confluence. Culture medium was exchanged every second day. Neuronal enrichment was achieved by adding 10 µM DAPT (Sigma).

3.3 Generation of isogenic induced pluripotent stem cell-derived neuronal cultures via CRISPR/Cas editing

In order to generate isogenic iPSC-derived neuronal cultures expressing either the KO or the normal ATXN-3 gene, a CRISPR/Cas editing system (Santa Cruz; Figure 3.1) was applied via nucleofection of smNPCs. The CRISPR/Cas system consists of two parts: three CRISPR/Cas9 Knockout (KO) plasmids each encoding the Cas9 nuclease and a target-specific 20 nt guide RNA (sc-417498A1: 5'…ATCCTCAATTGCACATCAG...3'; sc-417498A2: 5'…TCAACAGTCCAGAGTATCAG…3'; sc-417498A3: 5'…ATCCTGAGCCTCTGATACTC…

3') and a homology-directed repair (HDR) plasmid which incorporates, when co-nucleofeted with the CRISPR/ Cas9 KO plasmid, a puromycin resistance gene for selection of cells where Cas9-induced DNA cleavage has occurred. Also a total number of three of the HDR plasmids was used, each containing a HDR template corresponding to the cut sites generated by the corresponding CRISPR/Cas9 KO plasmids providing a specific DNA repair template for a double strand break.

3.3.1 Nucleofection of ATXN3-CRISPR/Cas KO system into SCA3 patient-derived neural stem cells

2.5 x 10^6 cells of two SCA3 patient-derived iPSc-derived smNPCs cell lines were used for the nucleofection with the ATXN3-CRISPR construct, according to the manufacturer's protocol (Lonza). Briefly, cells were washed with PBS, harvested by using Trypsin-EDTA and centrifuged for 4 min. at 1200x. Then, cells were counted and 2.5 x 10^6 cells of the counted cells were centrifuged a second time. The pellet was cleared from any residual medium and resuspended in 100 µl of a Nucleofector® solution. Afterwards, 2 µg of the ATXN3-CRISPR/Cas9 DNA were added to the nucelofector-cell suspension. The mixture was transferred to a cuvette, placed into a holder of the Nucleofector and the recommended program was started. Finally, the nucelofected cell suspension was resuspended in 500 µl of the pre-warmed culture medium and transferred into the medium containing six-well plates.

3.3.2 Cultivation and screening of nucleofected ATXN3 /CRISPR clones

48h after the nucleofection with the ATXN3 /CRISPR construct, smNPCs were selected in culture medium containing 1 µg/µl puromycin for two days. Following the removal of puromycin form the culture medium the surviving cells were cultured for three weeks until resistant colonies emerged. As soon as colonies began to form spherical bulges, they were picked with a 100 µl micropipette by scratching and soaking, and then plated onto 96 well-plates. Within a few days the clones reached confluency and were dissociated with trypsin-EDTA, separated and plated onto a 24-well and expanded. As soon as enough cells of a clone were present to secure the propagation, one well of a six-well was harvested in lysis buffer and a western blot analysis was done for screening purposes.

3.4 SDS –PAGE and western immuno blotting

For SDS-PAGE, cells were harvested and lysed in RIPA buffer (50 mM Tris, 150 mM NaCl, 2% SDS, 25 mM EDTA, 1x Roche cOmplete mini protease inhibitor) for 1h at 4°C. Lysates were clarified by centrifugation (10.000 rcf; 10 min) boiled for 5 minutes at 95°C and loaded onto 12% SDS-PAGE gels containing resolving- and stacking gels. Gels were casted using 30% Acrylamid/Bisacrylamid (37.5:1; Carl Roth), TEMED, 10% APS, 10% SDS and the respective gel buffers. Loaded protein lysates were electrophoresed at 100V in MINI-Protean chambers (Biorad) and transferred onto nitrocellulose membranes by using a Trans-Blot® Turbo™ Transfer System (0.5A, 15V, 1h; Biorad).
Following the blotting, membranes were blocked with 5% milk powder (Carl Roth) in TBST for 1h and incubated with the respective primary antibody (listed) over-night at 4°C. Washed membranes were incubated with an HRP-linked secondary antibody (1 h) and imaged with the ChemiDoc™ XRS+ System. Quantification of signals from sub-saturated blots was done using ImageJ. Protein signal was normalized to the loading control pan-actin.

3.5 SNP analysis and sequencing

Genomic DNA was prepared using the DNeasy Blood & Tissue Kit (Qiagen). Whole-genome single nucleotide polymorphism (SNP) genotyping was performed at the Institute of Human Genetics at the University of Bonn. Genomic DNA at a concentration of 50 ng/µl in TE4 buffer was used for whole-genome amplification. Afterwards, the amplified DNA was fragmented and hybridized to sequence-specific oligomers bound to beads on an Illumina OmniExpressExome v1.2 chip. Data were analyzed using Illumina GenomeStudio V2011.1 (Illumina). Genotypes were produced using the genotyping module of GenomeStudio and copy number variation (CNV) analysis was performed. Furthermore, B-allele frequencies and log R ratios were visualized.

3.6 RNA extraction with Trifast

Cells were lysed with 1ml Trifast directly in culture plates, homogenised and collected in a 1.5ml tube. For the following phase separation, 200µl chlorophorm were added to the probes and tubes were shaked for 30 seconds at RT. Afterwards, the mixture was incubated for 7-15 minutes at RT and centrifuged at 12,000g for 10 minutes. Following centrifugation, three phases were visible within the tube. The top phase, containing RNA, was carefully transferred to a fresh tube without being contaminated with the other phases. For the next step, the RNA precipitation, 500 µl isopropanol were added to the tube, the mixture was

shaked and incubated on ice for up to four hours. After the following centrifugation step (12,000g, 10 min., 4°C), a gel-like RNA-precipitate was visible. The pellet was twice washed with 800 µl of 75 % EtOH-Diethyl pyrocarbonate (DEPC) water and centrifuged as before. The remaining ethanol was air dried for 30-60 min. Last, the pellet was redissolved with 20 µl of DEPC water and shaked at RT for 30 minutes.

3.6.1 RNA purification with DNaseI

For RNA purification DNaseI (Invitrogen) was used to digest single- and double stranded DNA in extracted RNA samples. 2.5 µl of 10x DNaseI reaction buffer and 2.5 µl of DNaseI were added to each RNA sample and incubated for 15 min at RT. Next, in order to inactivate the DNaseI, 2.5 µl EDTA (25mM) were added and the mixture was incubated for 10 min. at 65°C. Following the RNA purification, the RNA concentration was measured using a micro-spectrophotometer (Nanodrop ND-1000).

3.7 L-glutamate treatment of neuronal cultures

Three clones of each group were cultured in 3.5-cm dishes for four weeks in differentiation medium until neuronal cultures were fully mature. Cells were washed two times with 2 ml BSS (balanced salt solution) containing 25 mM Tris, 120 mM NaCl, 15 mM glucose, 5.4 mM KCl, 1.8 mM CaCl2, 0.8 mM $MgCl_2$, pH 7.4 and treated with 100 µM L-glutamate (Sigma, no. G8415) in BSS for 30 min. Afterwards, cells were washed again two times and kept in differentiation medium for another 30 min (recovery phase), followed by two additional wash steps with BSS. Cells were exposed to a second excitatory stimulus by adding 100 µM L-glutamate for 30 minutes. Afterwards, neurons were cultured for 24 h at 37°C. On the next day, cells were harvested in TriFast™ for RNA extraction.

3.8 Gene expression analysis

For gene-expression microarrays, mRNA of neuronal cultures from three clones of each group in biological duplicates (n=6) under normal culture conditions and following exposure of the cultures to 100 µM L-glutamate, were isolated using TriFast™. Samples were analyzed on the HumanHT-12 v4 Expression BeadChip (Illumina). RNA samples were handled following Illumina's laboratory guidelines. Data processing was performed using GenomeStudio V2010.3 Gene Expression Module (V1.8). For data normalization raw-probe and gene-level data were extracted without background subtraction, selecting those probes with a detection *P* value of <0.5 as computed by GenomeStudio and the resulting probe intensity values were quantile-normalized across the data set.

3.9 Quantitative RT-PCR

Total RNA was obtained from cultured cells by using a TriFast-chloroform-exraction and mRNA transcripts were incubated with DnaseI. For the reverse transcription, 1 µg of RNA was used and reversely transcribed into cDNA by using the iScript cDNA Synthesis Kit (BioRAD) in accordance with the manufacturer's protocol. Quantitative RT-PCR reactions were performed in triplicates on a Biorad-iCycler realplex mastercycler using the Promega GoTaq G2 Flexi DNA polymerase and the SYBR-green detection method. PCR products were assessed by dissociation curve analysis (iCycler iQ™ Real-Time PCR Detection System) and data were normalized to RPLPO or 18S mRNA expression levels (RT-PCR primers listed) to ensure comparable expression levels of genes. Analyses were done using the ΔΔCt-value method.
PCR products were separated on a 2% agarose gel in TAE buffer containing 1:10000 ethidium bromide and visualized in a UV-light gel documentation system.

Step	Temperature	Time
Initial denaturation	95 °C	2 minutes
40 cycles:		
Denaturation	95 °C	15 seconds
Annealing	60 °C	15 seconds
Elongation	72°C	20 seconds

3.10 Immunocytochemical analysis

Cells were fixed in 4% PFA for 15 min at room temperature, washed twice with PBS and blocked with 10% FCS and 0.1% Triton-X-100 in PBS for one hour at room temperature. Afterwards, primary antibodies (listed) were applied overnight at 4°C in blocking solution. Cells were washed twice with PBS before secondary antibodies (listed) were applied for 1 h at room temperature.
Cell nuclei were counterstained with DAPI and finally cells were rinsed with PBS, mounted with Moviol and covered with a glass coverslip.

3.11 Assessment of cell viability

Cells from the different isogenic conditions were incubated on 10 cm-dishes under DAPT treatment for four days at 37°C and 5% CO_2 to initiate differentiation of an increased number of neurons. Afterwards, the obtained premature neurons were plated at 40.000 cells per well in 96-well microtiter plates and differentiated into mature neurons for four weeks. Following

differentiation, the compounds Rotenone [5 µM, 25 µM and 50 µM], $CdCl_2$ [10 µM, 25 µM and 50 µM], $ZnCl_2$ [100 µM, 150 µM and 200 µM] and L-glutamate [2 mM, 5 mM, 7.5 mM and 10 mM] were added to wells, respectively and cultures were incubated for additional 48 hours. Cell viability was evaluated by using the CellTiter-Glo Luminescent Cell Viability Assay (Promega). The substrate was prepared using the manufacturer's instructions and 25 µL of the CellTiter-Glo cell lysis reagent was added to each well. For cell lysis and equilibration of signal, 96-well plates were mixed on a compact shaker (Bühler) for 30 min at RT. Subsequently, the contents of the device were transferred to a 96-well clear bottom black plate and luminescence was measured on an EnVision Multilabel Plate Reader (Perkin Elmer). The assay generates a luminescence signal during a luciferase reaction. Since the luciferase reaction requires ATP, the luminescence produced is proportional to the amount of ATP present, an indicator of cellular metabolic activity. The relative cell survival rate [%] was calculated by comparing the rotenone-treated cells with a DMSO control and the Cd-, Zn- and L-glutamate- treated cells with a H_2O control.

3.12 Superoxide and total ROS induction

For measuring total cellular levels of ROS and superoxide, the total ROS/Superoxide detection kit was used. One-week-old neurons were transferred to GT-coated 96 well plates and differentiated for another three weeks. On the day of the experiment, differentiation medium was replaced by DMEM/F12 (without B27) and after four hours, cells were treated with pyocyanin [150, 300 and 500 µM] for 30 min., respectively. Afterwards, the detection kit was used according to the manufacturers instructions (ENZO). Recording of superoxide (Ex=550nm, Em=610nm) and total ROS (Ex=488, Em=520) fluorescence signals was performed using a plate reader (Tecan Group Ltd.).

3.13 Design of lentiviral vectors

As a conditional overexpression system, a modified variant of the Lenti-XTM Tet-On Advanced system (Clonetech) was used (the CMV promoter had been exchanged by an EF1α promoter in the pLVX-Tet-On plasmid to regulate expression of rtTAAdv. protein).
For constant overexpression of MTF-1 with a VSV taq (MTF-1_VSV) and a truncated form of ATXN3 (ATXN3_C71), the pLVX-Tight-Puro vector was used. The cDNA for both genes was amplified by PCR (cloning primers listed). MTF-1 was amplified from the plasmid pChMTF-1_VSV (Gift from Oleg Georgiev, Switzerland). PCR products were separated by agarose gel electrophoresis, extracted by manual excision of the respective band under UV light, isolated

by gel purification (peqGOLD™ Gel Extraction Kit, Peqlab), digested using appropriate restriction enzymes (listed) and ligated (T4 DNA Ligase, NEB) into linearized, dephosphorylated (FastAPTM, Fermentas) pLVX-Tight-Puro vector under control of the inducible TREtight promoter, resulting in pLVXTP-gene vectors (listed).

3.14 Production and concentration of lentiviral particles

For production of lentiviral particles, HEK293-FT cells were grown on a polyornithine- coated 15 cm dish in MEF medium. 70-80% confluent cells were co-transfected with lentiviral plasmids of the second generation by calcium-phosphate precipitation as described previously (Kutner et al, 2009). Briefly, 7 µg of the envelope plasmid pMD2.G and 15 µg of the packaging plasmid psPAX2 together with 30 µg of the transfer vector were mixed, and H2O was added to a final volume of 1400 µl. 178 µl of CaCl2 solution (2,5 M) was added, and the solution was slowly mixed with 1400 µl of 2xHBS buffer (pH=7,05). The suspension was incubated for 40 min at RT and added drop wise to the 293FT cells that were pre-incubated with with chloroquin (25 µM, 5 min, 37°C in MEF). The next day, transfected cells were washed with PBS (37°C) once. The supernatants of day two and three were pooled, filtered through a 0,45 µm filter and concentrated by centrifugation (44000 g; 4°C, 2h). Viral particles were resuspended in virus freezing medium and stored in aliquots at -80°C.

3.15 Lentiviral transgenesis of pluripotent stem cell-derived neural stem cells

To generate an smNP cell line for conditional overexpression of MTF-1_VSV and ATXN3_C71, smNP cells from SCA3 patient-derived iPS cell lines were first transduced with lentiviral particles containing the EF1α regulated rtTAAdv protein. 48 hours after transduction, cells were chemoselected with G418 (100 µg / ml, PAA) for four days. Next, cells were transduced with the respective pLVXTP-gene virus to obtain inducible cell lines for the respective gene. Cell lines were continuously cultured in G418 and puromycin containing culture media (Puromycin: 1 µg / ml, PAA; G418: 100 µg / ml, PAA).

3.16 Cycloheximide chase

Cells were differentiated into neurons for five weeks. On the first day of experiment medium was removed and 200 µg/ml cycloheximide (dissolved in 100% EtOH) in fresh medium was added to the cells. Cells with t=0 were collected immediately and stored in -80° C. Remaining

cells were chased for t=4, 12, 24 and 48 h and lysates were collected at each time point. After all lysates were collected, they were centrifuged at 12.000 rpm at 4° C for 30 min and protein concentrations were measured. 50 µg of protein were loaded on a 12 % gel and western immuno blot was performed as described before (anti-VSV antibody with dilution 1:1000 was used to detect the MTF1_VSV signal and β-actin was used with a dilution 1:10.000 as a control).

3.17 Statistical analysis

Quantitative data of each cell line was generated in biological duplicates and ≥3 technical replicates unless otherwise mentioned. All results show means ±standard deviation (SD). Means and SD were computed using Microsoft Excel 2008 and GraphPad Prism6 software. A student's t-test was performed to determine whether a significant difference between groups exits. A two-way ANOVA was performed to determine whether a significant difference exists between groups when influenced by two independent variables. Multiple pairwise comparisons of means were performed by Tukey's posthoc test (*p <0.05; **p<0.01; ***p <0.001; ****p <0.0001).

4 Results

Modeling protein functions in iPSC-derived in vitro cultures is challenging in regard to high variations in differentiation protocols and genetic variations between cell lines. For instance, when using a stem cell based model system, it has to be considered that in contrast to mouse models, being inbred strains, humans are genetically diverse. DNA sequencing analysis indicates that every time human DNA is passed from one generation to the next it accumulates 100–500 new mutations (Besenbacher et al., 2015; Kondrashov et al., 2002; Xue et al., 2009). Thus, in an ideal case, isogenic cultures are applied where cell lines differ only in the gene of interest. In addition, stable intermediates generated during the lengthy differentiation process represent an attractive alternative cellular source.

One example for such an intermediate cell population are small molecule neural precursor cells (smNPCs), which fulfill two major requirements: reproducibility and comparability between single experiments and different stem cell lines. They represent a robust intermediate stem cell population between pluripotent stem cells and differentiated neuronal cultures that can be generated from either control or patient-derived iPS cell lines (Reinhardt et al., 2013). These cells were applied to address how an expansion and/or loss of the protein Ataxin 3, in accordance with the loss of function hypothesis, might affect gene expression in human isogenic iPSC SCA3 patient-derived neuronal cultures. Due to their stability and clonal growth in culture, smNPCs are also amenable to genetic manipulations. Thus, CRISPR-Cas9-based gene editing could be used to genetically manipulate smNPCs in order to generate isogenic iPSC-derived neural stem cell lines expressing either the non-expanded or the expanded allele of ATXN3. In addition, and as a control, neural stem cells with a complete knockout of the ATXN3 gene were generated.

4.1 CRISPR/Cas9 genomic editing is suitable for the generation of stable stem cell-derived neural stem cell lines

In order to rule out any influences due to the human genetic diversity, isogenic iPSC-derived neural stem cell lines were generated, using CRISPR/Cas9-mediated gene editing. The CRISPR/Cas system consists of two parts: three CRISPR/Cas9 Knockout (KO) plasmids each encoding the Cas9 nuclease and a target-specific 20 nt guide RNA for ATXN3 and a homology-directed repair (HDR) plasmid which incorporates, when co-nucleofeted with the CRISPR/ Cas9 KO plasmid, a puromycin resistance gene for selection of cells where Cas9-induced DNA cleavage has occurred.

Of the HDR plasmids also a total number of three were used, each containing a HDR template corresponding to the cut sites generated by the corresponding CRISPR/Cas9 KO plasmids providing a specific DNA repair template for a double strand break (DSB).

In order to generate ATXN3 KO cell lines, two human patient-derived small molecule neural precursor cell lines were nucleofected with the CRISPR/Cas9 system. After nucleofection three different KO conditions arised: a knockout of ATXN3 in both alleles (bi-allelic knockout) or in only one allele (mono-allelic knockout) of both cell lines, resulting in clones that expressed either the non-expanded (ATXN3_non-exp), the expanded (ATXN3_exp) or no ATXN3 (ATXN3_KO) as it is depicted in Figure 4.1.

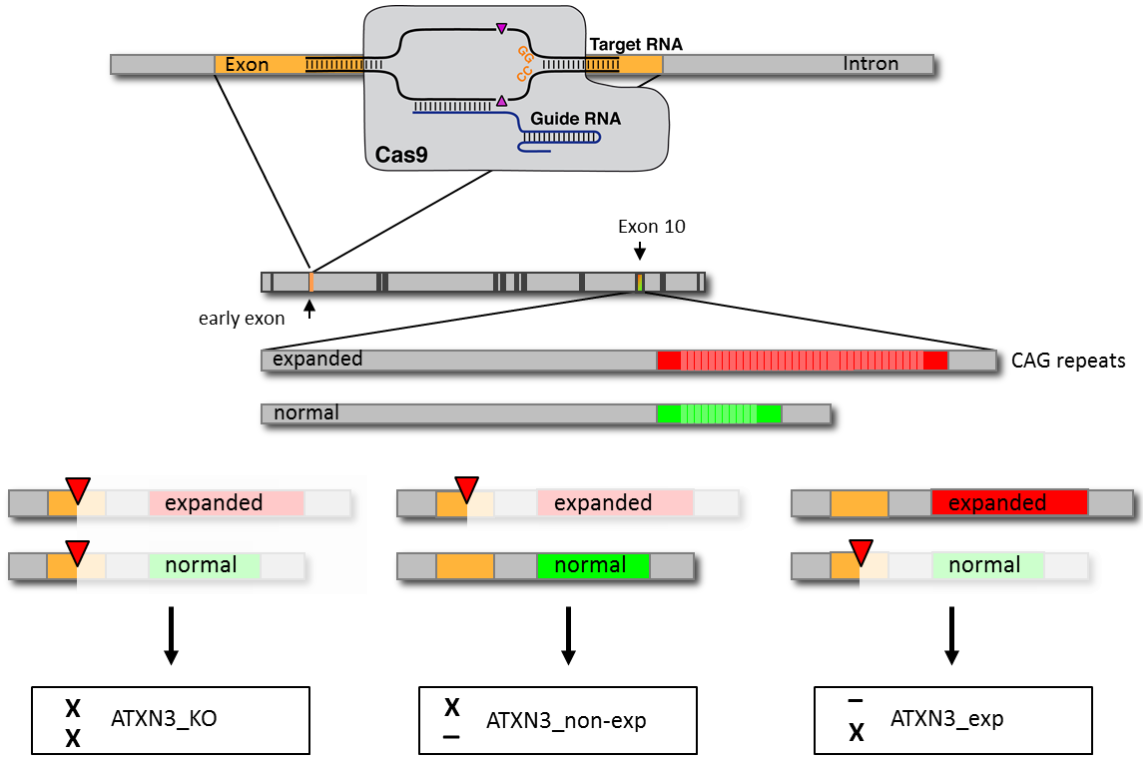

Figure 4.1: CRISPR/Cas9 strategy for the generation of isogenic iPSC-derived clones with differences in the expression of ATXN3.

Patient-derived small molecule neural precursor cells were nucleofected with the CRISPR/Cas9 plasmid system. Depending on which allele CRISPR/Cas9 cuts, the corresponding clones retained no ATXN3 (ATXN3_KO), the non-expanded (ATXN3_non-exp) or the expanded (ATXN3_exp) allele. Consequently, the translated protein Ataxin 3 varies in these clones.

Nucleofected cells were seeded in clonal density following by selection with puromycin (Fig. 4.2 A). After 30 days clones were picked, expanded to clonal cell lines and validated. Western blot analysis and PCR were performed to screen, which colonies express the non-expanded/healthy (ATXN3_non-exp), expanded/disease (ATXN3_exp) allele or no ATXN3 (KO) (Fig. 4.2 B-D). ATXN3_non-exp (healthy = H1, H2) and ATXN3_exp (disease = D1, D2)

neural stem cell clones express only the normal or the expanded allele, respectively. Ataxin 3 of the ATXN3_exp cell lines has a higher molecular weight because of the prolonged poly-glutamine stretch as the non-expanded form and thus displays a higher band in western immuno blots and PCR compared to the non-expanded protein. In the knockout situation (KO1, KO2), no ATXN3 is detectable.

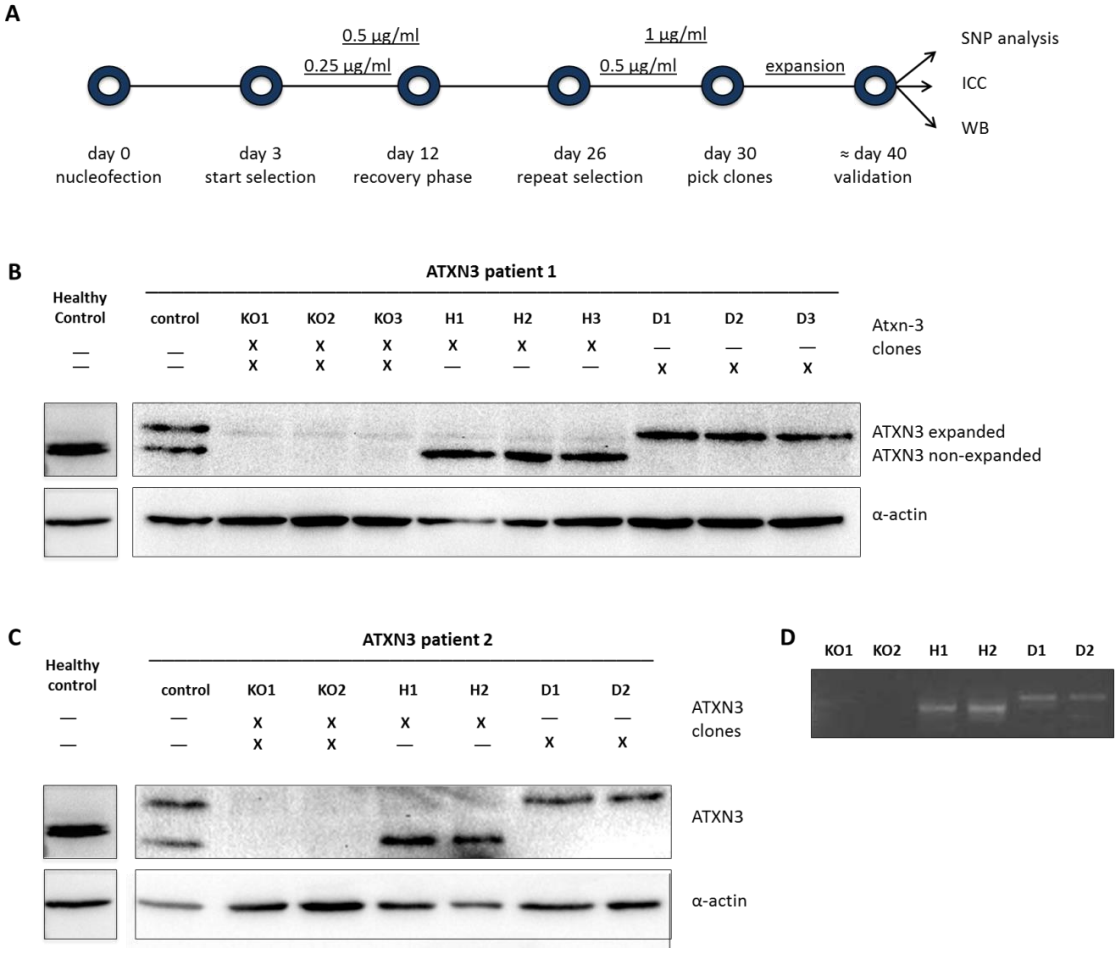

Figure 4.2: Depiction of identities of the generated isogenic neural stem cell lines compared to a non-patient and a patient control regarding their expression of ATXN3.

A: *Timeline for generation of CRISPR/Cas9 ATXN3 clones based on smNP cells. Nucleofection of smNP cells was followed by a recovery phase for three days. Puromycin initially was applied at 0.25 µg/ml at day three and increased to 0.5 µg/ml at day seven of the first selection interval. After a recovery phase of 14 days, a second selection interval with 0.5 µg/ml (3 days) and 1 µg/ml for one day was performed, followed by a second recovery phase for four days. Afterwards, cells were picked, expanded and evaluated by western blot, ICC and stainings for marker expression. In order to identify the status of Ataxin3 in clonally expanded cell lines, western blot analysis and PCR were performed.* ***B-D:*** *ATXN3_non-exp/healthy (H1, H2) and ATXN3_exp/diseased (D1, D2) clones express only the normal or the expanded allele, respectively and display* ***B/C*** *on the western blot and* ***D*** *in the PCR as one band for ataxin 3. Disease clones contain the expanded polyQ allele and therefore appear higher on the gels because of their larger size.*

By using a CRISPR/Cas9 system, isogenic cell lines were generated expressing different states of Ataxin 3. This enables to investigate how an expansion and/or loss of ATXN3 might affect gene expression in human iPSC SCA3 patient-derived neurons. Those clones expressing ATXN3, express either the expanded or the non-expanded allele. That makes this system especially appealing since the effects and functions of the expanded and non-expanded form of ATXN3 can clearly be discriminated without interfering with each other. Additionally the isogenic cell lines could further be used for disease modeling since the ATXN3_exp clones could “mimic” a homozygous state of Machado-Joseph Disease in which both alleles code for the expanded form only.

4.1.1 Genetic engineering by using CRISPR/Cas9 does not induce chromosomal aberrations in neural stem cells

As previously reported the application of CRISPR/Cas9 is associated with off-target cleavage events resulting in karyotypic abnormalities (Kim et al., 2015; Schaefer et al., 2017). To exclude such events in the generated cell lines, high-resolution SNP-analysis was performed. SNP analysis revealed that, in both cell lines, no significant karyotypic alterations were generated (Fig. 4.3 A). Since the normal and expanded alleles of ATXN3 are hemizygously expressed in ATXN3_non-exp and ATXN3_exp clones, respectively, those clones were additionally sequenced to ensure that the remaining allele is without any genetic defects in order to code for a functional protein. The sequencing results revealed an intact and correct protein sequence for *ATXN3* with no off-target alterations (Fig. 4.3 B). One single nucleotide exchange was found in the sequencing of all investigated clones as well as in the original smNPC lines. Thus, the SNP is not related to the nucleofection of the smNPCs with the CRISPR/Cas9 system. It is located at position 561 in the *ATXN3* gene and categorized as a single nucleotide variation with no clinical significance (rs16999141**,** see NCBI dsSNP data base; Fig. 4.3 B/C). Two clones of each group from both patient-derived cell lines were chosen to proceed with experiments (n=12).

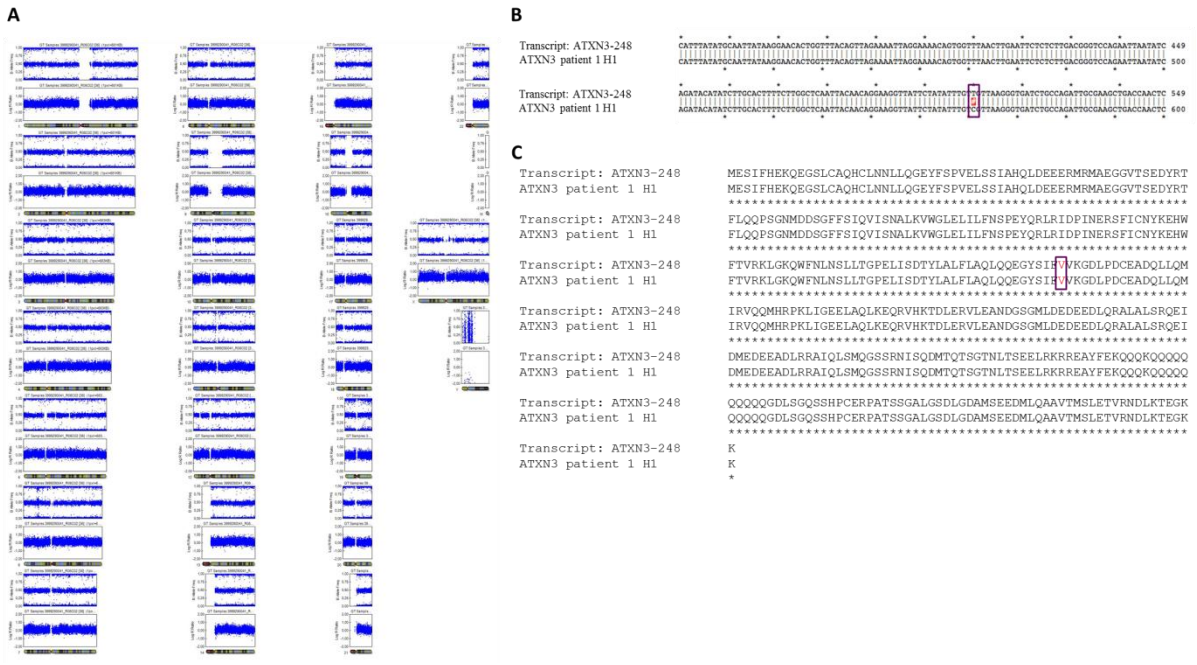

Figure 4.3: The remaining ATXN3 allele of the hemizygous isogenic cell lines shows no off-target effects ***A:*** *Full genome SNP analysis of the patient-derived cell line without detectable alterations.* ***B:*** *Sequencing revealed a complete and correct sequence for ATXN3. One SNP was found which exchanges T→C, both coding for the amino acid valine.* ***C:*** *Alignment of the protein template of the transcript ATXN3-248 (www.ensembl.org) with the protein sequences of the ATXN3 clones revealed no abnormalities in the protein sequence of the clones (shown for the clone H1).*

4.1.2 Isogenic neural stem cells express stem cell-specific markers and differentiate into neurons and glia

The isogenic neural stem cells and their differentiated neuronal progeny were further characterized for the expression of typical stage-specific proteins and transcription factors indicative for their regional identity in the brain axes. Homogenous smNPC lines were cultured in the presence of the small molecules CHIR and purmorphamine to stimulate WNT signaling and the SHH pathway, respectively, in order to promote the capacity of self-renewal. To differentiate smNPCs into neurons, the cells were exposed to the growth factors FGF2 and EGF for 24h to generate rosette-type neural stem cells (ltNES) and then differentiated in the absence of growth factors for five weeks (Fig. 4.4).

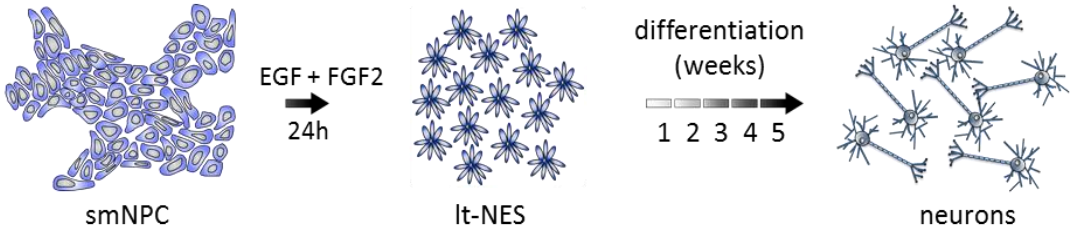

4.4 Scheme of the differentiation protocol

Schematic overview showing the protocol for differentiation of iPS cell-derived smNPCs into cultures of postmitotic human neurons, which were monitored over five weeks.

Immunocytochemical analysis revealed that all investigated smNPCs homogenously express the transcription factors SOX2, PAX6, PLZF and DACH1 in the nucleus, the intermediate filament nestin and the tight-junction marker ZO-1, which is spatially localized to the apical surface (Fig. 4.5 A/C).

After withdrawal of growth factors, cultures incrementally changed there cellular morphology and gave rise to a major number of β-III tubulin as well as MAP2ab-positive postmitotic human neurons and a minor number of GFAP- positive astrocytes within five weeks (Fig. 4.5 B/D). This means that the cells kept their preserved neuronal differentiation potential. Growth capacity as well as the differentiation potential in these neurons can be stable for more than 100 passages.

Since the cells expressed all typical stem cell markers and markers for the differentiated stage, the CRISPR/Cas9 targeting strategy, selection and propagation of clones did not significantly alter the characteristics of the modified cells.

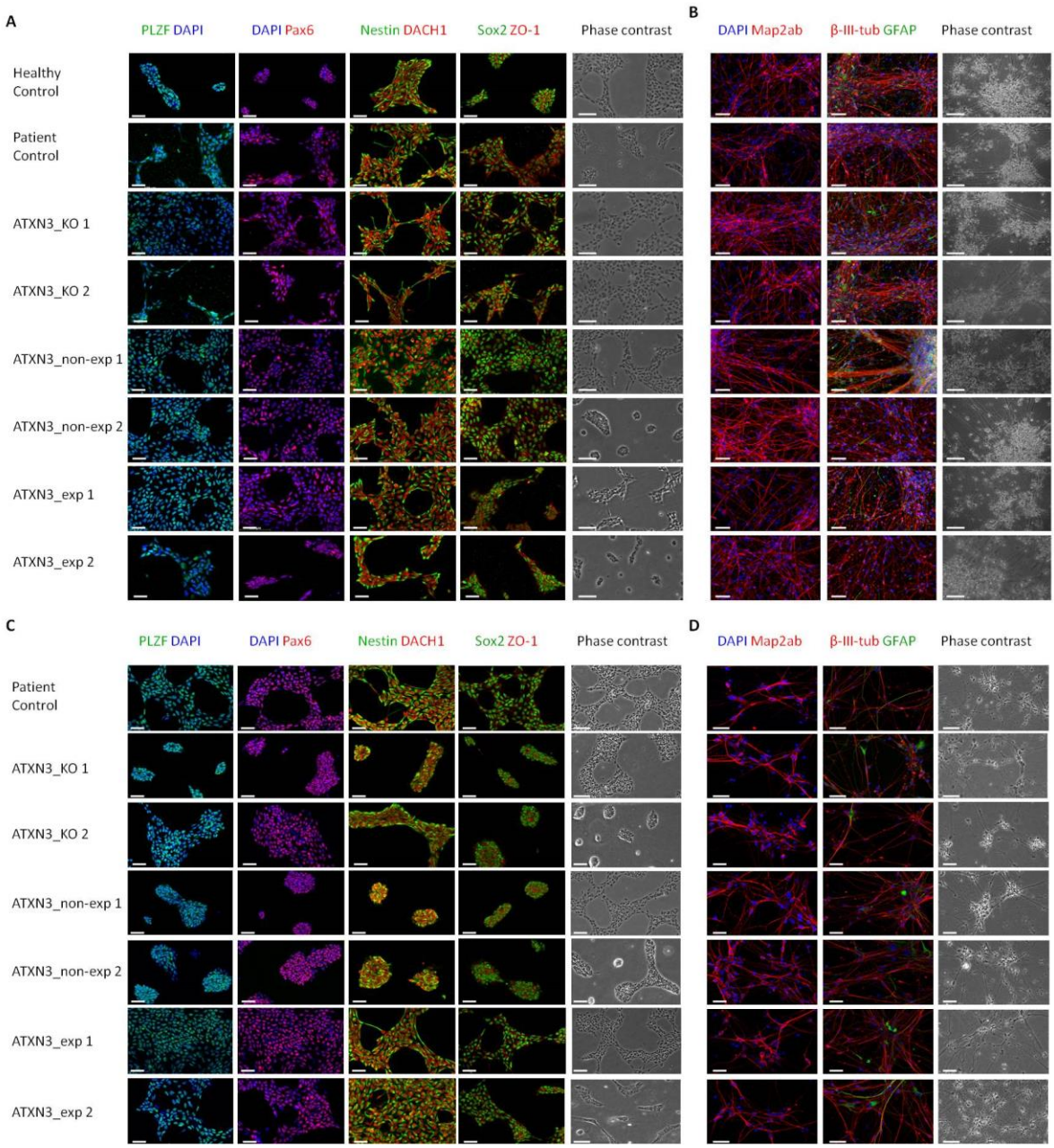

Figure 4.5: The isogenic smNPC clones expressed marker for the proliferative as well as for the differentiated state of cell development equally to the non-clonal healthy and patient controls and can be allocated to the hindbrain region

A/C: *Immunofluorescence staining of ATXN3 clones from two cell lines expressing the nuclear marker SOX2, PLZF, PAX6 and DACH1, nestin as an intermediate filament and the tight junction marker ZO-1 for the proliferative state (scale bar=100µM and 250µM for phase contrast).* ***B/D:*** *Neuronal cultures from two iPS cell-derived smNPCs clones, differentiated for five weeks, expressing the neural marker β-III tubulin and MAP2ab as well as the astrocytic marker GFAP for the differentiated state (scale bar=100µM and 250µM for phase contrast).*

Since ATXN3 is a major contributor to the induction of the pathology of SCA3, a disease that affects mainly the hindbrain (e.g. cerebellum), it was interesting to know which regional identity the clones express. All smNPC-derived neural cell lines showed a prominent expression of the anterior hindbrain markers HoxA2 and HoxB2, whereas HoxB4 was not detectable indicating an anterior hindbrain identity (Fig. 4.6; Koch et al., 2009; Reinhardt et al., 2013).

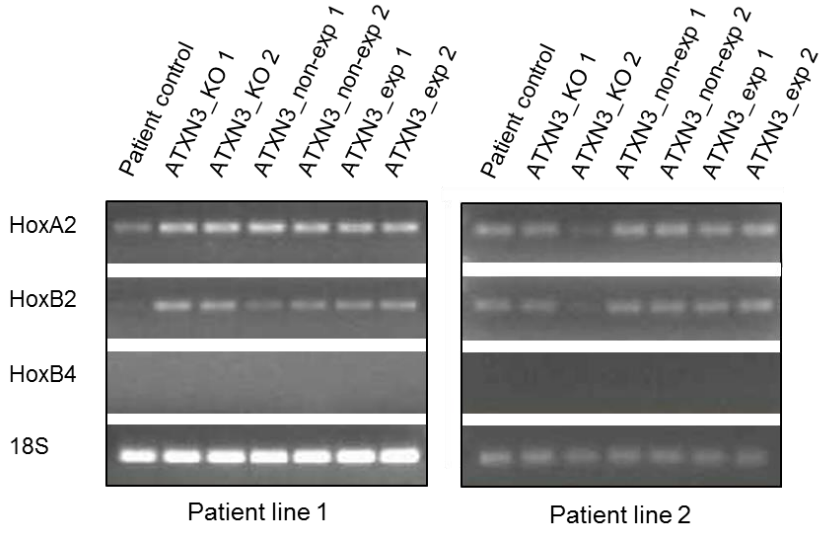

Figure 4.6: Isogenic neurons display an anterior hindbrain identity

Neuronal cultures were differentiated for five weeks and cDNA was generated. PCR revealed an expression of the rostrocaudal markers HOXA2 and HOXB2, but no expression of HoxB4 in clones derived from both cell lines and their non-isogenic controls. This expresson pattern marks an anterior hindbrain identity.

In summary, the ATXN3 clones did not develop karyotypic aberrations, sequencing revealed no alterations in the sequence of the remaining allele (KOs were excluded), marker for the proliferative state (PAX6, NESTIN, SOX2) as well as for the differentiated state (e.g. betaIII-tubulin, Map2ab) were expressed and an anterior hindbrain identity can be concluded.

4.2 Transcriptional analysis of isogenic human neurons identified metallothioneins to be differentially expressed depending on the state of Ataxin 3

Recent data suggest that either conformational changes of the expanded ATXN3 protein and/or a loss of free available ATXN3 due to recruitment of ATXN3 into aggregates leads to the dysregulation of multiple cellular pathways such as ubiquitination or transcriptional regulation (Evert et al., 2006; Haacke et al., 2006). To study the influence of expanded and/or loss of ATXN3 on gene expression in patient-specific and CRISPR/Cas9 edited

neurons, a gene expression analysis was performed. For the analysis neuronal cultures from three clones of each condition in biological duplicates were used. These clones were harvested under normal culture conditions and following exposure of the cultures to 100 µM L-glutamate to promote a glutamate-induced excitation of patient-derived neurons initiating Ca2+-dependent proteolysis of ATXN3 and a subsequent formation of SDS-insoluble aggregates (Koch et al., 2011). That allowed not only a genetic-dependent but also a treatment-dependent comparison between the clones regarding their response to L-glutamate as an aggregation-promoting stressor.

Gene expression analysis revealed 47194 genes of which 14532 remained after pooling samples into *ATXN3_KO, ATXN3_exp* and *ATXN3_non-exp* groups (n=6/group). The remaining 14,532 genes were analyzed to identify transcripts that were differentially expressed in ATXN3_KO, ATXN3_exp and ATXN3_non-exp samples with the minimum threshold level $p<0.001$ and and an up- or downregulation of 1.5-fold in gene counts.

First, a cluster analysis was done which clearly separated L-glutamate treated neurons from non-treated neurons. In addition, within both groups, those cultures where ATXN3 remained (ATXN3_non-exp and ATXN3_exp) cluster together and separate from the same branch whereas the ATXN3_KO clones are branching before (Fig. 4.7 A).

The more detailed gene expression analysis revealed a number of differentially expressed genes between the ATXN3 clones (Fig. 4.7 A-J) and that the strongest differences in the number of differentially expressed genes in the untreated condition are between ATXN3_KO and ATXN3_non-exp (Fig. 4.7 B/E), followed by ATXN3_KO versus ATXN3_exp (Fig. 4.7 C/F). In comparison, the differences between ATXN3_non-exp and ATXN3_exp are minor (Fig. 4.7 D/G). Following L-glutamate treatment, the number of differentially expressed genes between ATXN3_KO and ATXN3_non-exp is similar to that between ATXN3_KO and ATXN3_exp (Fig. 4.7 H/I). Still, the lowest number is observed when comparing gene expression between ATXN3_non-exp and ATXN3_exp neuronal cultures (Fig. 4.7 J).

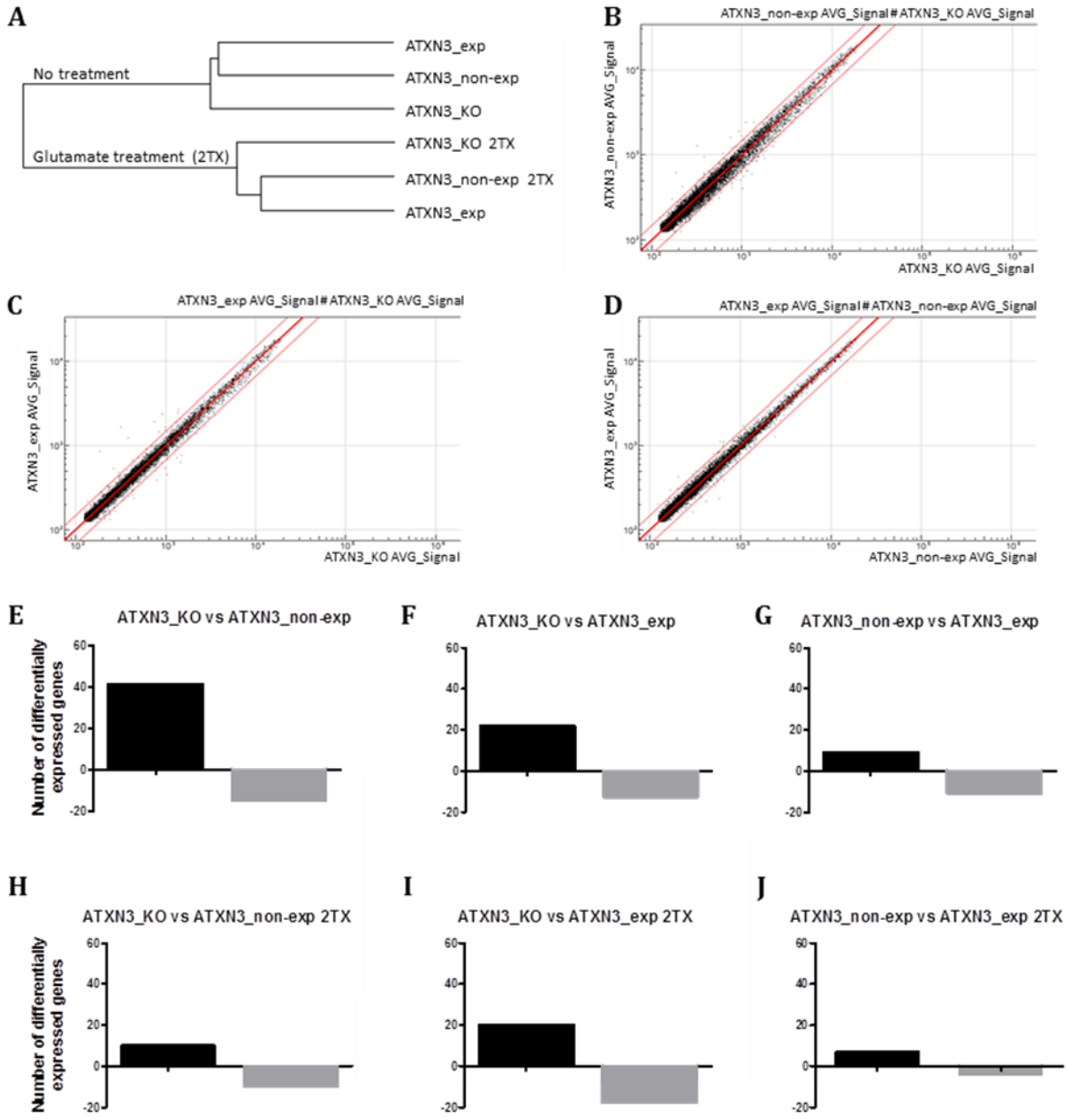

Figure 4.7: Differentially expressed genes in isogenic neuronal cultures

Gene expression studies were performed on five-week-old neuronal cultures from three clones of each condition (ATXN3 KO, expanded, non-expanded) in biological duplicates under normal culture conditions and following exposure of the cultures to 100 µM glutamate (2TX). All clones of each condition were pooled into a corresponding group **A:** Cluster analysis showing an allocation of the cell lines into a L-glutamate- and a non-treated cluster. In both clusters, ATXN3_exp and ATXN3_non-exp neuronal cultures are genetically closer related to each other than to ATXN3_KO**. B-G:** Several genes are differentially regulated under non-treated experimental conditions and **(H-J)** L-glutamate treatment between ATXN3_KO and the two other clone groups, with the most apparent differences between ATXN3_KO and ATXN3_non-exp. (n=6 for each group)

Differently expressed genes did not show significant enrichment for a specific pathway using gene ontology analysis. However, four of the most significant downregulated genes in ATXN_KO cells compared to ATXN3_non-exp cells belonged to the same functional cluster of metallothioneins (MT1A, MT1E, MT1G and MT2A; Fig. 4.8 A-I).

All four MT genes were significantly downregulated in ATXN3_KO compared to ATXN3_non-exp and ATXN3_exp neurons. Additionally, these genes seem to display a higher expression in ATXN3_exp than ATXN3_non-exp neurons but this trend was not significant (Fig. 4.8 A-D).

After L-glutamate treatment, the expression levels of all MTs increased in all cell lines, but again, remained comparatively downregulated in ATXN3_KO neuronal cultures (Fig. 4.8 E-H). Also under treated experimental conditions a non-significant trend of higher expression levels in ATXN3_exp compared to ATXN3_non-exp cells was observable for each gene.

The up-regulation of metallothioneins after glutamate-treatment is also shown in a heatmap displaying MT expression (Fig. 4.8 I). MT1F and MT1X were excluded from further studies since their expression profile does not significantly differ between the clonal groups.

Metallothioneins play a crucial role in the cellular response towards metal stress and maintenance of metal homeostasis (Hidalgo et al., 2001; Margoshes and Vallee, 1957; Thirumoorthy et al., 2011). In addition to the regulation of metal levels, metallothioneins are also involved in the cellular stress response by protecting against oxidative stress (Takahashi et al., 2012; Ruttkay-Nedecky et al., 2013).

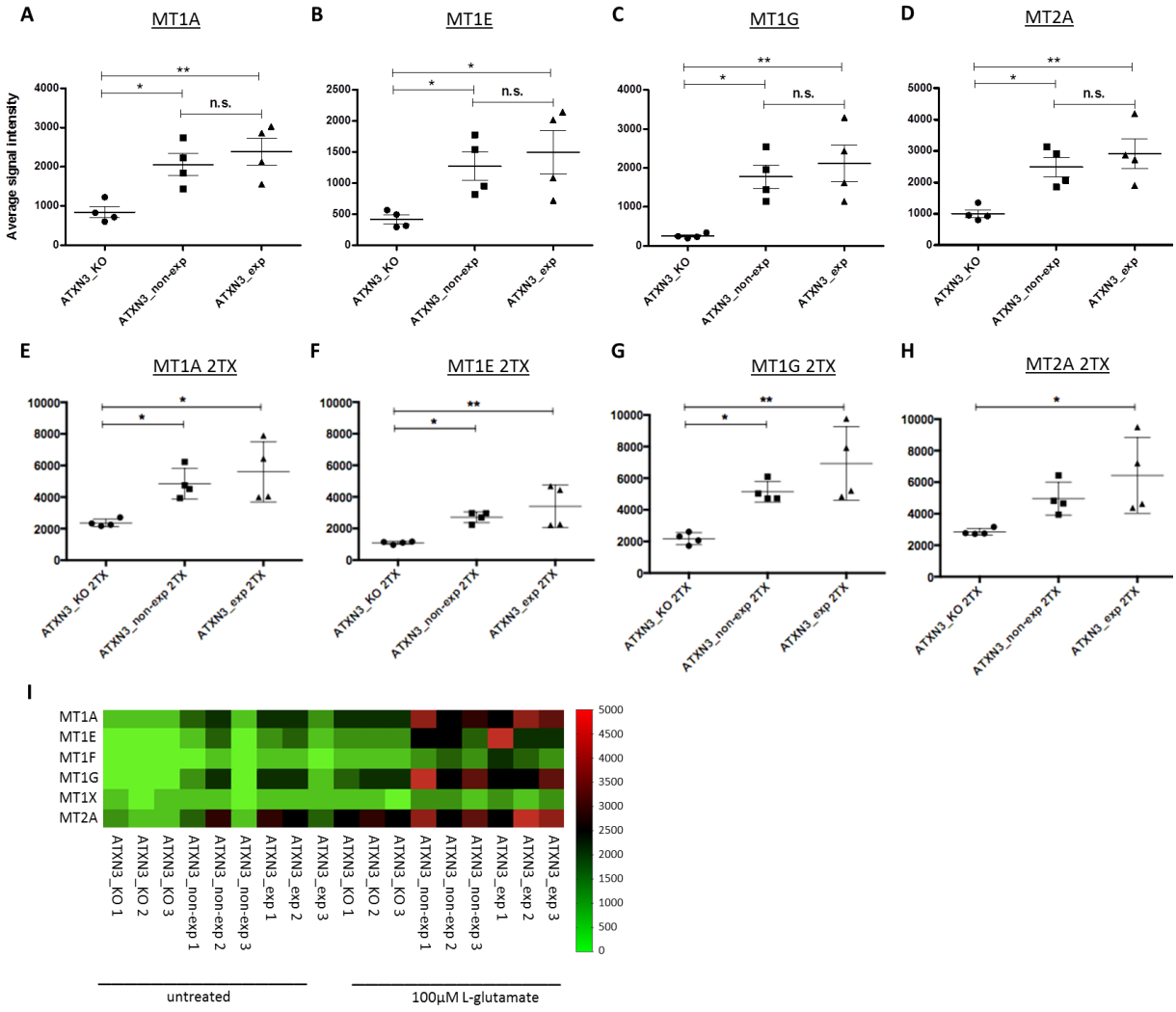

Figure 4.8: Gene expression analysis revealed a downregulation of a metallothionein cluster in ATXN3_KO neurons compared to neurons expressing the expanded or non-expanded allele

A-D: *Gene expression level depicted as average signal intensity for the metallothioneins MT1A, MT1E, MT1G and MT2A (n=6 for each group).* ***E-H:*** *Expression levels after application of 100 µM L-glutamate. (n=6 for each group).* ***I:*** *Heat map of the MT gene cluster expression for each clone (duplicates pooled). P < 0.05 and delta > 1.5. Each column represents a clone and each row represents a single gene. The left half of the heat map shows gene expression I the untreated condition, the right half shows expression after applying 100 µM L-glutamate. Expression levels are colored green for low intensities and red for high intensities (n=36 in total). *p<0.05; **p<0.01*

4.2.1 Quantitative real-time PCR verifies the metallothionein gene cluster to be differentially expressed depending on the state of Ataxin3 in isogenic human neurons

In order to verify the results of the gene expression analysis, quantitative real-time PCR was performed for *MT1A*, *MT1E*, *MT2A* and *MT1G.* This analysis confirmed that the cluster of metallothioneins is downregulated in ATXN3_KO neurons compared to ATXN3_non-exp and

ATXN3_exp cells and that the highest expression of MTs is detected in ATXN3_exp neurons (Fig. 4.9 A-D). Furthermore, the analysis confirmed that the application of L-glutamate increases the expression of all four metallothioneins in comparison to the untreated condition. Again, a similar pattern was observed with the lowest expression in ATXN3_KO and the highest expression in ATXN3_exp neurons (Fig. 4.9 E).

Since MTs are important for cellular metal homeostasis, the isogenic clones were further treated with the heavy metal $CdCl_2$ [25µM]. The treatment with 25µM $CdCl_2$ had an even stronger impact on the expression levels of MTs (Fig. 4.9 F). Furthermore, it changed the expression levels in ATXN3_non-exp and ATXN3_exp cultures to the effect that ATXN3_non-exp neurons now displayed the highest levels of metallothionein expression and the expression levels of ATXN3_exp neurons were comparable to ATXN3_KO cells.

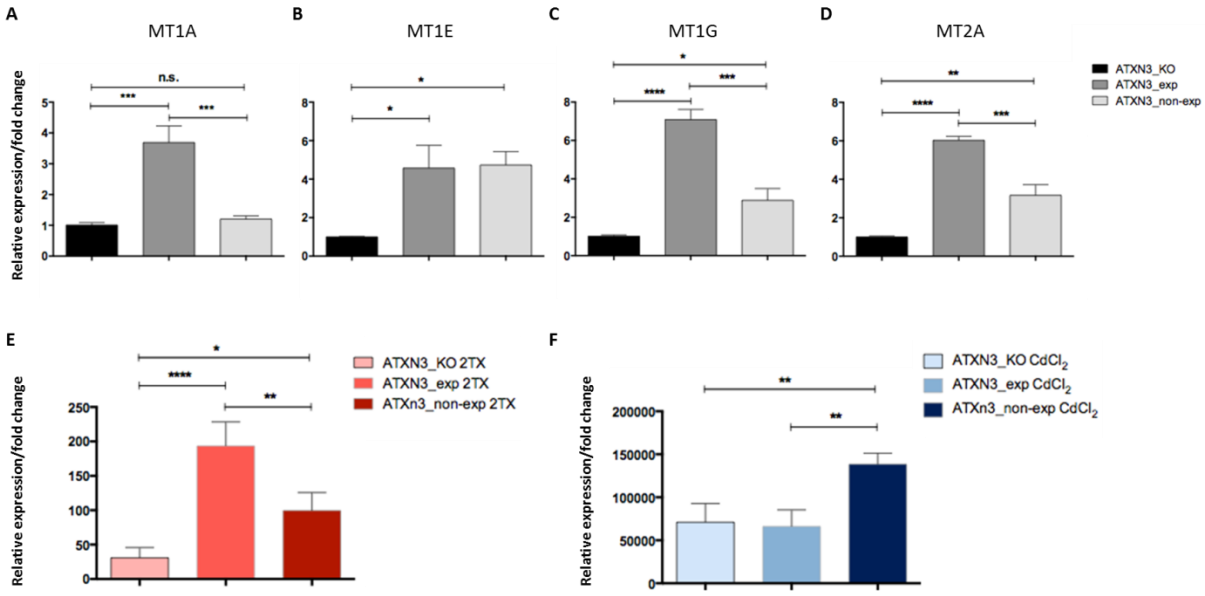

Figure 4.9 Metallothionein expressions in the isogenic cell lines derived from patient 2

A-D: qPCR was done for MT1A, MT1E, MT1G and MT2A. For all genes, the data show that they are significantly downregulated in ATXN3_KO compared to the two other groups and that the expression is highest in ATXN3_exp neurons. **E:** Cells which were treated with 100 µM glutamate (2TX) showed in general a higher expression of the gene compared to non-treated cells (here with MT1G) but still with the highest expression in clones with the expanded allele. **F:** After treatment with 25 µM $CdCl_2$, the expression level further increased and the pattern between ATXN3_exp and ATXN3_non-exp neurons was exchanged, with the highest expression now in those clones with the non-expanded allele (n=6 for each group). *Bar graphs show mean ± SD of each group. *p<0.05; **p<0.01; ***p<0.001; ****p<0.0001.*

The qPCR analysis was further repeated on isogenic neurons derived from the second patient. Interestingly, ATXN3_exp neurons derived from patient two showed an expression profile more similar to ATXN3_KO than to ATXN3_non-exp clones already in the untreated

condition (Fig. 4.10 A-D). In line with the results from the previous patient cell line the expression level of MTs increased with the treatment of L-glutamate and even more with $CdCl_2$ (Fig. 4.10 E/F). Under all conditions, the expression of MTs was lowest in ATXN3_KO and highest in ATXN3_non-exp neurons, with ATXN3_exp in between.

Together, these data demonstrate that, for both cell lines, the expression levels of MTs are lowest in ATXN3_KO neurons compared to the ATXN3-containing neurons and that the expression pattern of ATXN3_exp and ATXN3_non-exp neuronal cultures varies between the two patient-derived isogenic clones under non-treated and L-glutamate-treated conditions. This variation disappears after the application of a strong stressor such as the heavy metal $CdCl_2$ with the result that the MT-expression is highest in ATXN3_non-exp neurons in both cell lines.

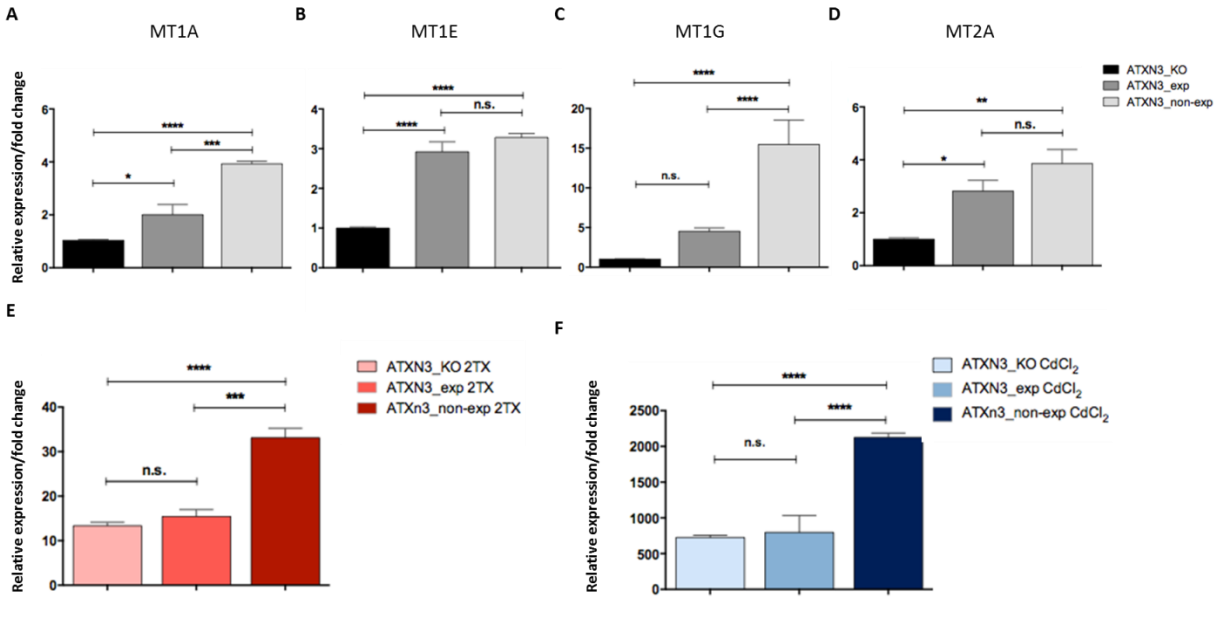

Figure 4.10 Metallothionein expression in the isogenic cell lines derived from patient 2

A-D: qPCR was performed for MT1A, MT1E, MT1G and MT2A on a second patient-derived cell line. The genes are significantly downregulated in ATXN3_KO compared to ATXN_exp and ATXN3_non-exp neurons, with the highest expression in clones with the non-expanded allele. **E:** Cells, which were treated with 100µM glutamate (2TX), showed in general a higher expression of the MTs compared to non-treated cells (here with MT1G) but still with the highest expression in the non-expanded clone condition. **F:** The highest expression of MTs was achieved after treatment with 25 µM $CdCl_2$, with the same expression pattern as in untreated and L-glutamate treated cells (n=6 for each group). *Bar graphs show mean ± SD of each group. *p<0.05; **p<0.01; ***p<0.001; ****p<0.0001.*

4.3 Loss of ATXN3 increases neuronal susceptibility to stress

Since metallothioneins are important regulators of cell homeostasis and participate in an array of protective stress responses such as metal and oxidative stress, it was inevitable to investigate if the loss of ATXN3, either due to a KO or due to the formation of aggregates (ATXN3_exp), results in an influence on the regulation of cell homeostasis by increasing the susceptibility to oxidative, metal-, or excitotoxicity-related stress conditions. To test this, five-week-old neurons of two patient-derived neural cell lines were exposed to rotenone, $CdCl_2$, $ZnCl_2$ and L-glutamate for 48 h in different concentrations. Afterwards, a cell viability assay was performed which demonstrated that ATXN3_exp and ATXN3_KO neurons were indeed more susceptible to several types of cellular stress than ATXN3_non-exp, resulting in a higher number of cell survival in ATXN3_non-exp neurons (Fig. 4.11 A-D).

After rotenone treatment the cell survival rate of ATXN3_non-exp neurons was significantly higher than in ATXN3_KO and ATXN3_exp at 5 µM (38,86% ± 17,13% vs 16,36% ± 5,56% and 24,34% ± 8,07%), 25 µM (26,7% ± 13,21% vs 13,43% ± 4,21% and 19,19% ± 6,14%) and 50 µM (19,25% ± 7,85% vs 10,75% ± 2,52% and 13,33% ± 3,14%).

Similar results were achieved with the administration of the metals $CdCl_2$ 10 µM (110,54% ± 3,99% vs 90,20% ± 12,44% and 104,32% ± 7,16%), 25 µM (80,29% ± 12,09% vs 42,51% ± 11,27% and 54,62% ± 10,47%), 50 µM (35,37% ± 13,70% vs 13,6% ± 5,78% and 20,86% ± 7,46%) and $ZnCl_2$ 100 µM (99,81% ± 12,77% vs 77,32% ± 14,64% and 89,36% ± 7,06%); 150 µM (72,11% ± 14,39% vs 41,04% ± 11,83% and 61,17% ± 12,57%) 200 µM (42,34% ± 10,92% vs 12,56% ± 5,52% and 24,31% ± 12,18%).

Finally, also after treatment with the exitotoxicity stressor L-glutamate 2 mM (92,6% ± 7,12% vs 89,05% ± 6,26% and 93,06% ± 20,12%), 5 mM (83,82% ± 4,82% vs 59,48% ± 15,92% and 76,46% ± 11,28%) and 7.5 mM (50,47% ± 12,14% vs 23,06% ± 12,75% and 25,96% ± 16,44%) ATXN3_non-exp neurons displayed a higher cell survival rate than the two other groups. No significant differences were found for the treatment with rotenone 50µM and $ZnCl_2$ 200 µM.

Overall, the cell survival assay demonstrates that ATXN3 is crucial for the cellular response towards oxidative, metal and excitotoxic stress.

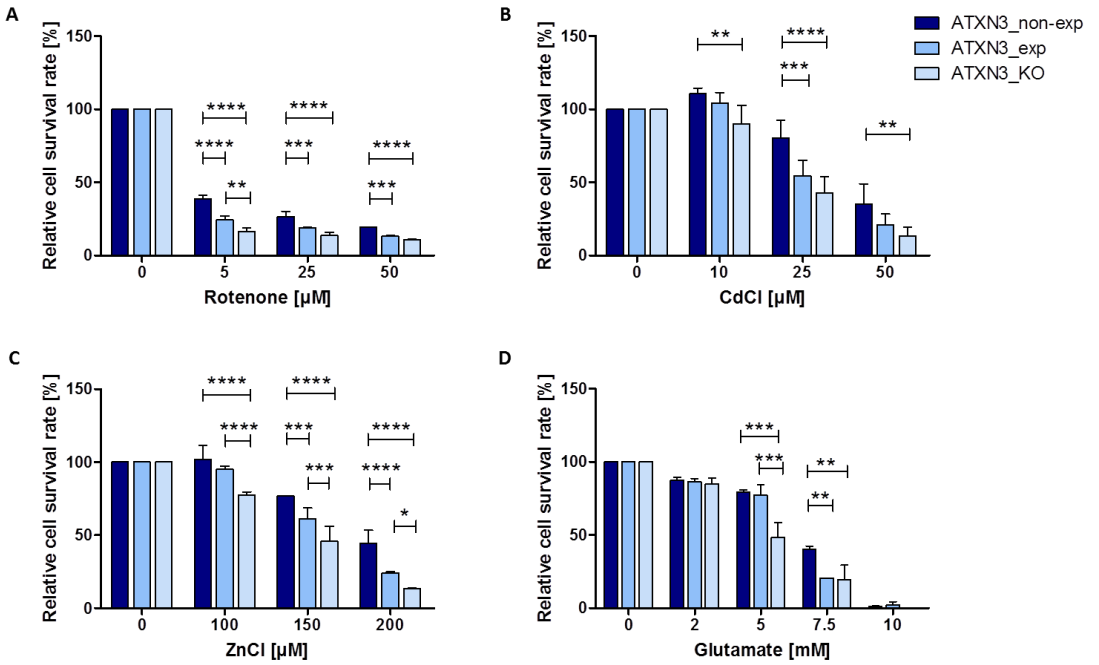

Figure 4.11: Neurons expressing either the expanded or no ATXN3 are more sensitive to oxidative, metal and excitotory stress than neurons, which express the non-expanded allele

Neuronal cultures were seeded in 96-well plates and cultured for four weeks, followed by a treatment of neural cultures with different stressors ***(A-D)*** *Afterwards, a cell survival assay was performed. Graphs show the relative cell survival rate [%] of ATXN3_non-exp, ATXN3_exp and ATXN3_KO neurons after exposure to* ***A:*** *Rotenone 5, 25 and 50 µM,* ***B:*** *$CdCl_2$ 10, 25 and 50 µM,* ***C:*** *$ZnCl_2$ 100,150 and 200 µM and* ***D:*** *Glutamate 2, 5 and 7.5 mM for 48 hours, respetively. For each group two clones with technical triplicates were used (n=6 / group). Bar graphs show mean ± SD of each group. *p<0.05; **p<0.01; ***p<0.001; ****p<0.0001*

The same experiment was performed on ATXN3_KO, ATXN3_exp and ATXN3_non-exp neurons of a second iPSC-derived patient cell line, displaying comparable results (Fig. 4.12 A-D).

ATXN3_non-exp neurons showed a significantly higher survival rate than ATXN3_KO and ATXN3_exp neurons after treatment with rotenone 5 µM (33,3% ± 7,8% vs 21,16% ± 8,48% and 24,75% ± 6,39%), 25 µM (31,31% ± 5,91% vs 17,57% ± 8,05% and 17,49% ± 5,1%) and 50 µM (22,42% ± 6.04% vs 11.51% ± 5,91% and 14,64% ± 5,23%).

The number of surviving ATXN3_non-exp neurons was also higher compared to ATXN3_KO and ATXN3_exp cells after exposure to the metals $CdCl_2$ 10 µM (100,7% ± 11,56% vs 68,56% ± 9,2% and 66,59% ± 13,84%), 25 µM (52,24% ± 12,74% vs 36,97% ± 4,9% and 41,55% ± 6,67%) and 50 µM (31,63% ± 11,67% vs 20,93% ± 9,2% and 16,29% ± 4,91%), and $ZnCl_2$ 100 µM (88,49% ± 10,91% vs 66,26 ± 5,35% and 75,77% ± 10,13%), 150 µM (71,13% ± 13,97% vs 39,9% ± 14,07% and 45,15% ± 10,16%) and 200 µM (30,65% ± 10,62% vs 17,46% ± 11,53% and 22,95% ± 4,92%) as well as the exitotoxicity stressor L-glutamate at 2 mM (98,67% ± 0,72% vs 61,57% ± 1,02% and 89,22% ± 6,14%) 5 mM

(64,91% ± 7,21% vs 49,96% ± 0,42% and 56,79% ± 3,74%) and 7.5 mM (42,71% ± 4,52% vs 27,39% ± 1,67% and 31,04% ± 2,6%).

No significant differences were found for the treatment with 2 mM glutamate.

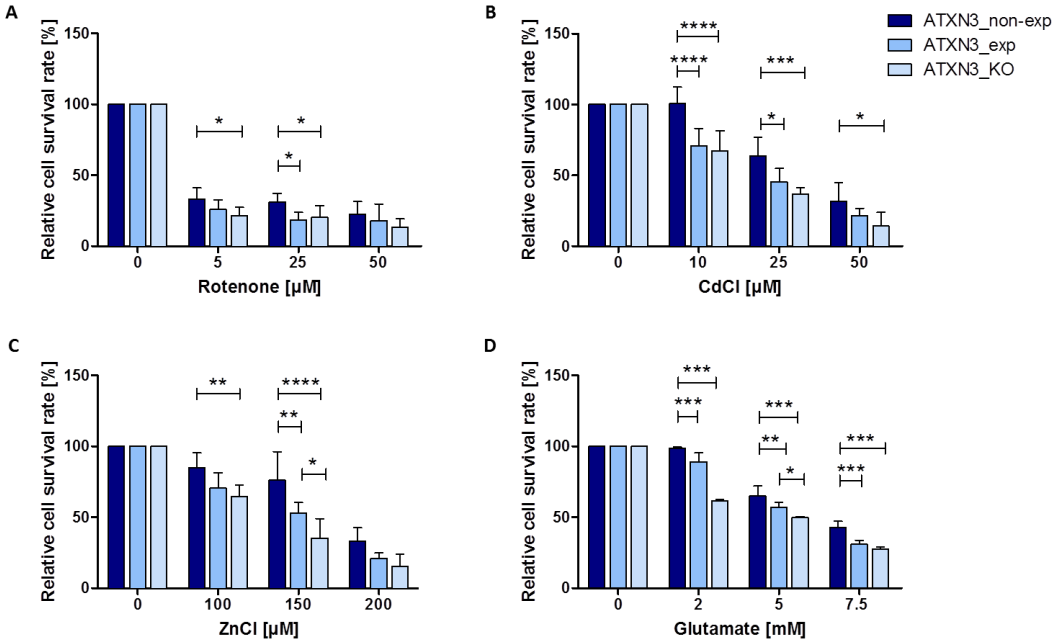

Figure 4.12: Neurons derived from a second patient line expressing either the expanded or no ATXN3 are as compared to the first patient line as well more sensitive to different stressors than neurons which express the non-expanded allele

Graphs show the relative cell survival rate [%] of ATXN3_non-exp, ATXN3_exp and ATXN3_KO neurons, derived from a second patient line, after exposure to ***A:*** *Rotenone 5, 25 and 50 µM,* ***B:*** *$CdCl_2$ 10, 25 and 50 µM,* ***C:*** *$ZnCl_2$ 100,150 and 200 µM and* ***D:*** *Glutamate 2, 5 and 7.5 mM for 48 hours, respetively. For each group two clones with technical triplicates were used (n=6 / group). Bar graphs show mean ± SD of each group. *p<0.05; **p<0.01; ***p<0.001; ****p<0.0001*

Based on the result that in comparison to ATXN3_non-exp neurons, ATXN3_KO and ATXN3_exp neurons showed a disturbance of the neuronal homeostasis and an increased susceptibility to stress, it was evaluated if such a phenotype can also be found when comparing neurons from a patient with that of healthy controls in a non-isogenic scenario. For that purpose, two iPSC-derived patient and two control neuronal cell lines were exposed to the same stressors.

The two healthy control cell lines showed a higher number of surviving cells compared to the two patient control cell lines after treatment with rotenone 5 µM (60,02 ± 0,64% vs 30,48% ±2,09%), 25 µM (48,74% ± 5,61% vs 18,01% ± 3,07%) and 50 µM (39,04% ± 6,28% vs 15,44% ± 0,96%), $CdCl_2$ 10 µM (92,31% ± 28,12% vs 93,28% ± 3,51%), 25 µM (87,93% ±

14,11% vs 48,0% ± 4,08%) and 50 µM (60,66% ± 3,51% vs 22,45% ± 5,66%), $ZnCl_2$ 100 µM (93,0 ± 2,05% vs 88,73%± 4,53%), 150 µM (72,15% ± 5,0% vs 62,37% ± 2,37%) and 200 µM (41,96% ± 8,81% vs 22,99% ± 3,58%), as well as the excitotoxicity stressor L-glutamate at 2 mM (87,03% ± 0,82% vs 70,47% ± 2,55%), 5 mM (73,82% ± 1,61% vs 53,35% ± 0,59%) and 7.5 mM (41,9% ± 0,01% vs 32,94% ± 0,45%) (Fig. 4.13 A-D).

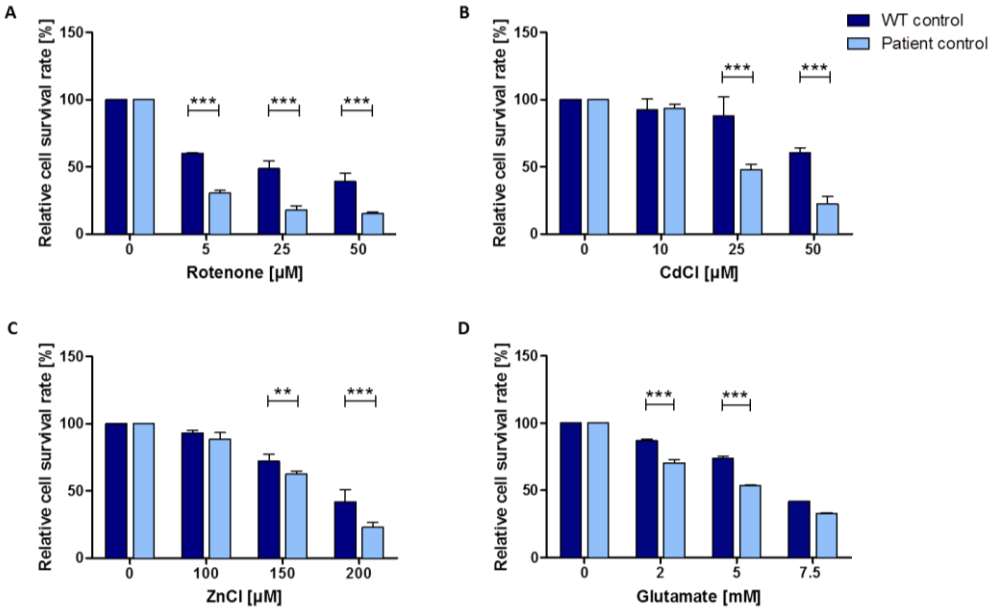

Figure 4.13: Patient iPSC-derived neurons react more sensitive to oxidative, metal and excitotory stress than the healthy control neurons.

Graphs show the relative cell survival rate [%] of two healthy and two patient control neurons after exposure to ***A:*** *Rotenone 5, 25 and 50 µM,* ***B:*** *CdCl 10, 25 and 50 µM,* ***C:*** *ZnCl 100,150 and 200 µM and* ***D:*** *Glutamate 2, 5 and 7.5 mM for 48 hours, respetively. For each group two clones with technical triplicates were used (n=6 / group). Bar graphs show mean ± SD of each group. *p<0.05; **p<0.01; ***p<0.001; ****p<0.0001*

Since the ATXN3_exp neurons as well as the patient derived non-clonal neurons displayed a lower cell survival rate than their control cell lines with a non-expanded allele of ATXN3, it was interesting to address the question of possible consequences resulting from induced aggregation in healthy control neurons. To answer this question, a lentiviral construct was generated overexpressing the polyQ fragment of ATXN3 since this fragment is believed to be a toxic species and responsible for the aggregation of ATXN3. It was assumed that neurons transfected with a construct expressing only the c-terminal polyQ fragment of ATXN3, might show a lower cell survival rate than the control neurons. Therefore, healthy control smNPCs were transduced with a lentiviral Tet-On 3G inducible expression system and the lentiviral vector pLVXTP-ATXN3_C71 expressing the truncated form of ATXN3 (Fig. 4.14 A). Before the accession of the cell viability, progenitors as well as their arising five-week-old neural

cultures were stained for ATXN3-containing aggregates after treatment with doxycycline. Non-treated cells were taken as a negative control for the formation of aggregates. Both, progenitors and neurons, displayed aggregates, which were only visible after doxycycline treatment in immunocytochemical stainings and a slot blot assay (Fig. 4.14 B/C). In both cell populations, smNPCs and neurons, the number of cells containing aggregates was around 40-45 % (Fig. 4.14 D/E).

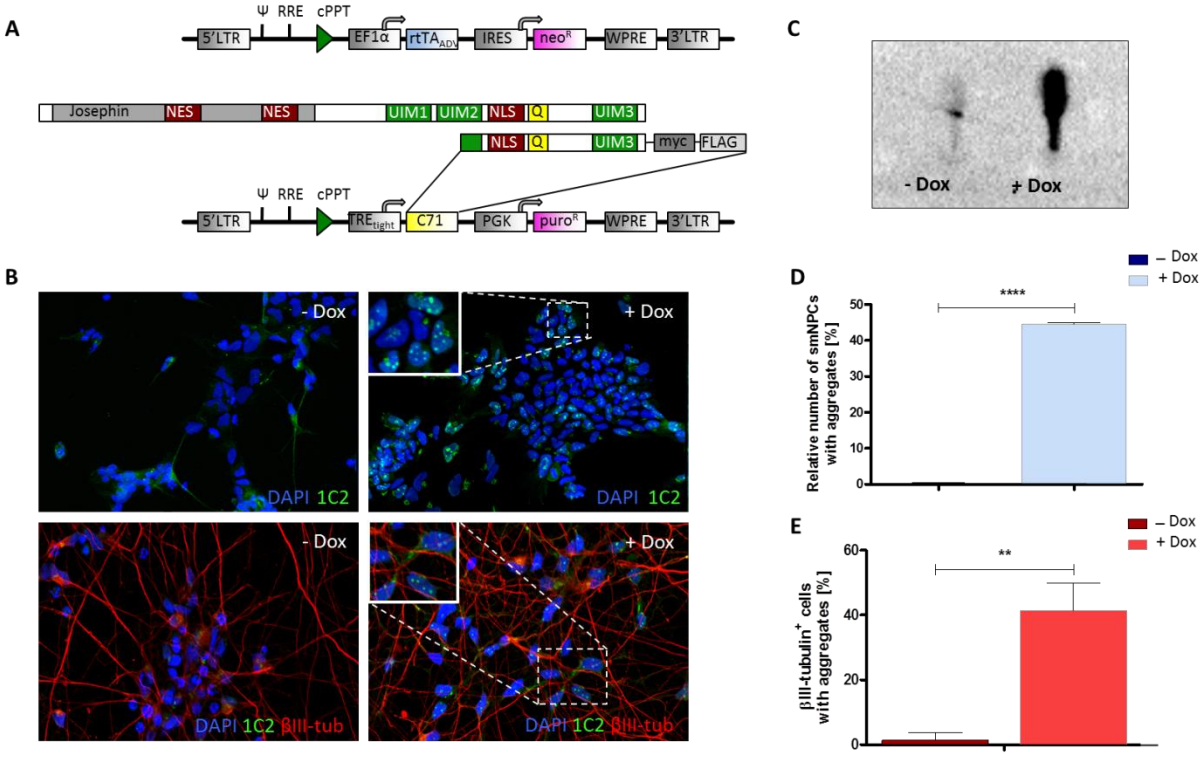

Figure 4.14: smNPCs and neurons transduced with a viral vector of an ATXN3 construct, expressing a truncated, only c-terminus containing form, efficiently formed intranuclear aggregates.

A: *Schematic representation of the lentiviral constructs for doxycycline-inducible overexpression of ATXN3_C71: The pLVX-EtO vector carries the tetOn protein rtTAAdv and an IRES-linked neomycin resistance gene (neoR), which are both controlled by an EF1α promoter (upper panel). The lower panel shows the full-length and the truncated form of the ATXN3 gene. The truncated form was cloned into a pLVXTP vector and the resulting pLVXTP-ATXn3_C71 vector contains the coding sequence for ATXN3_C71 under the control of the inducible TREtight promoter as well as a puromycin resistance gene (puroR) driven by aPGK promoter* ***B:*** *Immunocytochemistry of smNPCs and five-week-old differentiated neurons transfected with the truncated form of ATXN3 revealed the formation of ATXN3 positive inclusions under doxycycline induction (scale bar=100µm)* ***C:*** *Slot blot analysis using the polyQ-specific 1C2 antibody to detect aggregates after induction with doxycycline. Sample without doxycycline was used as a negative control.* ***D:*** *Bar graph shows the relative number of smNPCs containing intranuclear aggregates.* ***E:*** *Bar graph shows the relative number of β-II-tubulin positive neurons expression aggregates. Bar graphs show mean ± SD of each group. **p<0.01; ****p<0.0001*

Following a five-week differentiation period, the cell viability of neuronal cultures was evaluated in the presence and absence of cellular stress. The cell viability assay revealed that those cultures, forming lentiviral-induced aggregates after doxycyline treatment, showed decreased cell survival numbers compared to neurons without doxycycline treatment after application of different stressors such as rotenone 5 µM (44,33% ± 9,92% vs 36,45% ± 7,61%), 25 µM (44,21% ± 7,64% vs 30,08% ± 2,24%) and 50 µM (32,88% ± 7,00% vs 22,96% ± 1,78%).

Similar results were achieved with the administration of the metals $CdCl_2$ 25 µM (78,86% ± 9,77% vs 76,96% ± 8,17%), 50 µM (51,29% ± 4,04% vs 31,90% ± 4,72%) and 100 µM (25,93% ± 7,30% vs 23,88% ± 8,21%) as well as $ZnCl_2$ 100 µM (85,15% ± 7,30% vs 90,00% ± 11,66%), 150 µM (79,88% ± 9,01% vs 50,63% ± 18,44%) and 200 µM (30,00% ± 9,50% vs 27,33% ± 12,01% and the exitotoxicity stressor L-glutamate at 2 mM (87,91% ± 5,08% vs 67,09% ± 10,04%), 5 mM (68,54% ± 12,17% vs 49,44% ± 1,12%) and 7.5 mM (26,16% ± 7,35% vs 16,96% ± 7,42%) (Fig. 4.15 A-D).

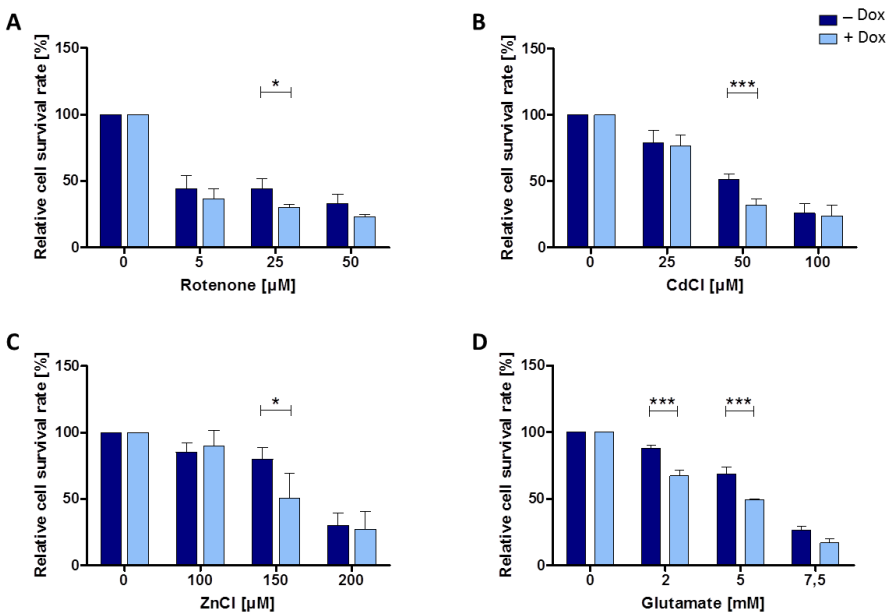

Figure 4.15: Doxycycline-dependent cells expressing the truncated form of ATXN3 display the same phenotype that was observed in ATXN 3 clones and their non-clonal controls

A-D: *Graphs show the relative cell survival rate [%] of neurons without (-DOX) and with (+DOX) doxycycline treatment after exposure to* ***A:*** *Rotenone 5, 25 and 50 µM,* ***B:*** *$CdCl_2$ 10, 25 and 50 µM,* ***C:*** *$ZnCl_2$ 100,150 and 200 µM and* ***D:*** *Glutamate 2, 5 and 7.5 mM for 48 hours, respectively. For each group technical triplicates were used (n=3 / group). Bar graphs show mean ± SD of each group. *p<0.05; **p<0.01; ***p<0.001.*

Additionally, the cell numbers of untreated controls were compared between doxycycline-dependent and non-dependent cells. No significant differences in the cell survival rates were found (Fig. 4.16). This indicates that the aggregates are not toxic to the neurons and that the

differences in the number of surviving cells are related to the absence or presence of ATXN3, which supports the hypothesis of ATXN3 being involved in the cellular response to stress.

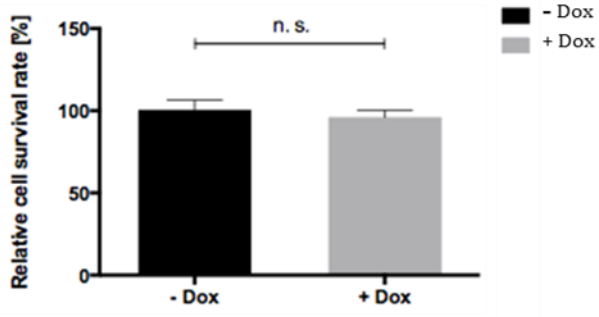

Figure 4.16: Aggregates inherently are not toxic to doxycycline-dependent neurons expressing the truncated form of ATXN3
Graphs show the relative cell survival rate [%] of neurons without (-DOX) and with (+DOX) doxycycline treatment under normal culture conditions. For each group technical triplicates were used (n=3 / group). Bar graphs show mean ± SD of each group.

4.4 Depletion of Ataxin3 in human neurons results in an increased susceptibility towards total ROS and superoxide formation

Loss of or defective ATXN3 in neurons might critically affect vital cellular functions and thus cell survival as it was shown in the section 4.5. Considering that metallothioneins are crucially involved in the generation and clearance of reactive oxygen species (ROS; Ruttkay-Nedecky et al., 2013; Sato et al., 1993), it was investigated if the ATXN3_ KO neurons might have a lower capacity to cope with increasing amounts of total ROS and superoxide during oxidative stress. For this, level of total ROS and superoxides were measured in five weeks differentiated neurons after exposure to oxidative stress. As antioxidants are present in standard media conditions (B27 supplement contains high levels of multiple antioxidants such as sodium pyruvate, catalase and superoxide dismutase) these experiments were performed under basal culture conditions not containing any antioxidants (medium without B27 supplement).

ROS and superoxide production were induced by exposing neural cultures to pyocyanin in different concentrations [0 µM, 150 µM, 300 µM and 500 µM] for 1h. Levels were measured by a fluorescent assay (Fig. 4.17 A/B, right graphs).

The pyocyanine-induced increase of ROS/superoxide at all concentrations was significantly highest in ATXN3_KO neurons (total ROS: 160,28% ± 2,20%, 199,02% ± 2,62% and 251,47% ± 15,35%; superoxide: 165,67% ± 5,86%, 191,20% ± 14,09% and 201,98% ± 23,61%), followed by ATXN3_exp (total ROS: 158,38% ± 11,61%, 170,31% ± 6,59% and 232,09% ± 21,22%; superoxide: 138,60% ± 3,10%, 136,39% ± 14,4% and 165,61% ± 31,27%) and lowest in ATXN3_non-exp neurons (total ROS: 111,11% ± 5,05%, 126,5% ± 13,09% and 251,47% ± 28,34%; superoxide: 106,99% ± 1,51%, 116,95% ± 2,88% and

125,49% ± 6,06%) compared to the control (Fig. 4.17). These data indicate that ATXN3 plays an important role in the processing of oxidative stress and the accompanied regulation of total ROS and superoxide levels by mediating the expression of metallothioneins.

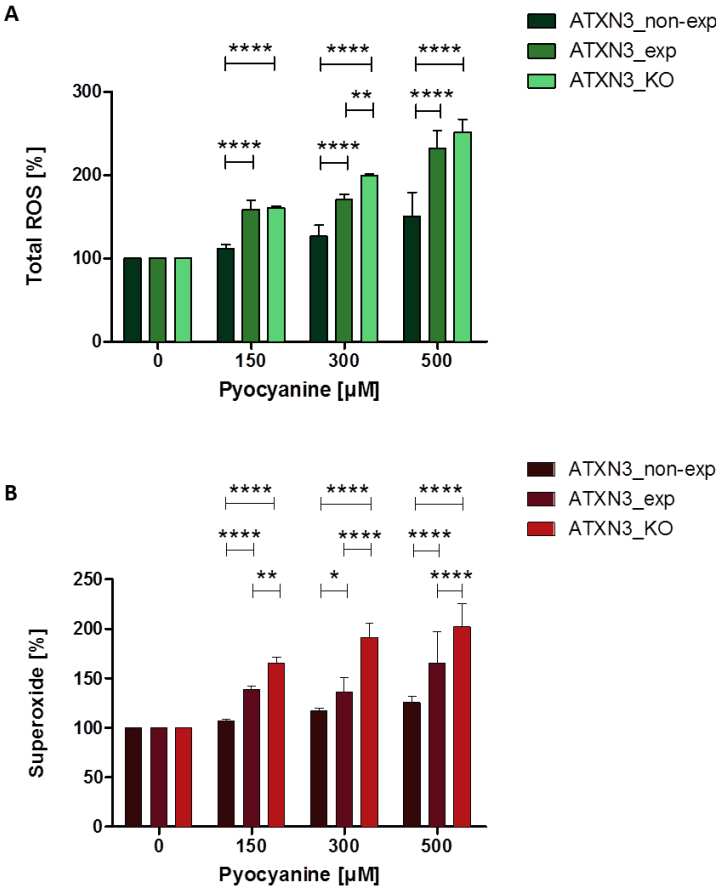

Figure 4.17: Ataxin3_KO neurons are more sensitive to oxidative stress than ATXN3_exp and ATXN3_non-exp neurons

A/B: *Induction of total ROS (green) and superoxide (red) after pyocyanin treatment (0 µM,150 µM, 300 µM und 500µM, 1 h) is highest in ATXN3_KO clones and lowest in ATXN3_non-exp clones. Bar graphs show mean ± SD of each group.*

**p <0.05; **p<0.01; ***p <0.001; **** p<0.0001.*

4.5 The metal regulatory transcription factor 1 expression does not differ between isogenic clones

Since the clones displayed a strong phenotype regarding the ATXN3-dependent cellular stress response, it was important to decipher a possible underlying mechanism. It was shown before that the expression of metallothioneins is induced through the transcription factor *MTF-1* (metal regulatory transcription factor 1). This transcription factor directly responds to metal and oxidative stress by binding to the metal-responsive element of the *MT* gene, which initiates its transcription. This autoregulatory loop is mandatory for the regulation of a normal intracellular level of metals and to reduce oxidative stress in cells (Fujie et al., 2016; Heuchel et al., 1994; Pamiter et al., 1994; Ruttkay-Nedecky et al., 2013). Therefore, MTF-1 was chosen as a candidate to decipher the mechanism of an ATXN3-dependent regulation of MTs. The cDNA expression levels of *MTF-1* between the three groups and between single clones were compared. qRT-PCR and PCR revealed no significant

differences in the expression profile between groups and single clones (Fig. 4.18 A-C). Conclusively, the stress response and concomitant the regulation of the metallothionein cluster might occur posttranscriptionally on protein level.

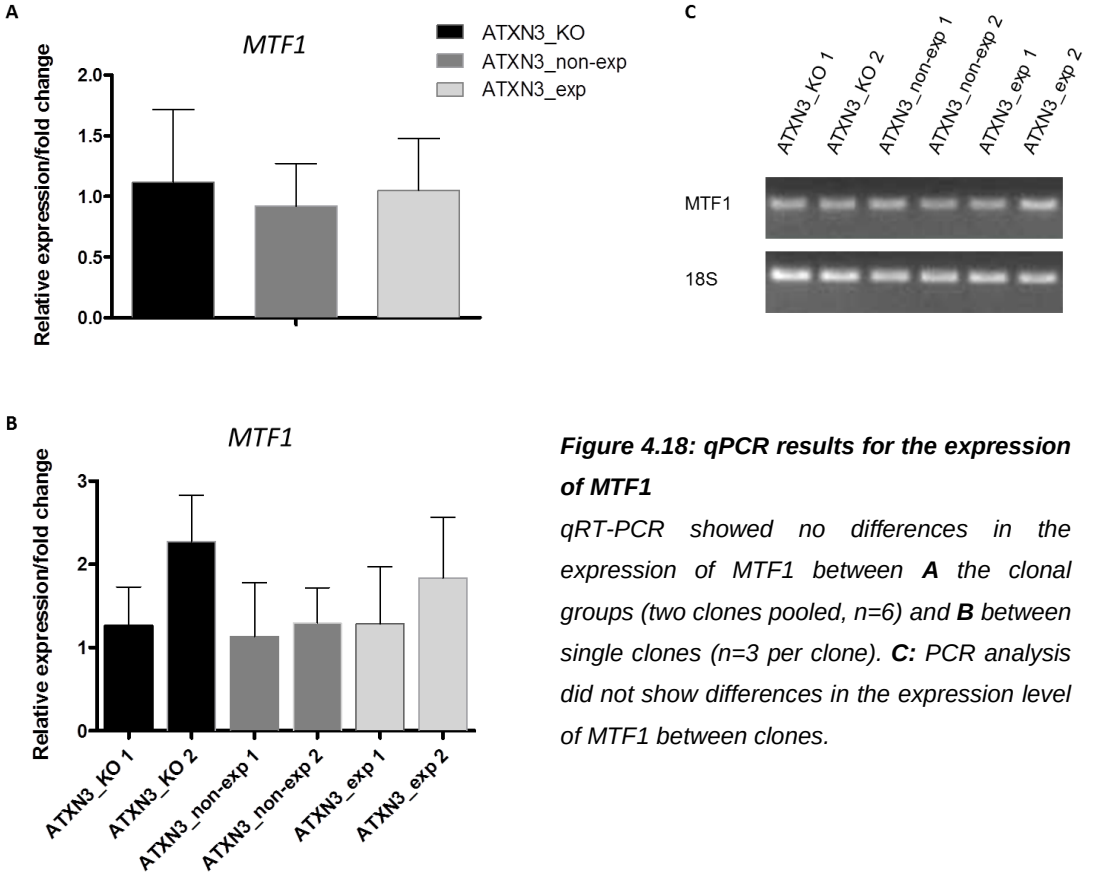

Figure 4.18: qPCR results for the expression of MTF1

qRT-PCR showed no differences in the expression of MTF1 between ***A*** *the clonal groups (two clones pooled, n=6) and* ***B*** *between single clones (n=3 per clone).* ***C:*** *PCR analysis did not show differences in the expression level of MTF1 between clones.*

To exclude the possibility that other metallothionein interaction partners except MTF-1 might contribute to the clonal phenotype, the expression of genes that are known to interact with metallothioneins were analyzed.

By using the transcription tool of enrichr (http://amp.pharm.mssm.edu/Enrichr/enrich), a cluster was generated that constitutes different factors whose pathways are connected to metallothioneins (Fig. 4.19 A). For all of these genes, except for *MTF-1*, the expression data of the neural cultures revealed an expression level beneath the significance border, which means, according to the array of the gene expression study, those genes are not expressed in the neural cultures (Fig. 4.19 B). One exception is the aryl hydrocarbon receptor (AHR), which is highly expressed in the neural cultures (Fig. 4.19 C). Sato et al. (2013) described a mechanism whereby *AHR* modulates expression of human MT2A via the glucocorticoid response element and protein-protein interactions with GR. Since the interaction of *AHR* in this study is restricted to *MT2A* and none of the other members of the metallothionein family, this gene was excluded as a candidate gene.

Therefore, MTF-1 remained as a candidate gene for further experiments regarding the

understanding of a mechanism how ATXN3 might be involved in the regulation of metallothionein expression.

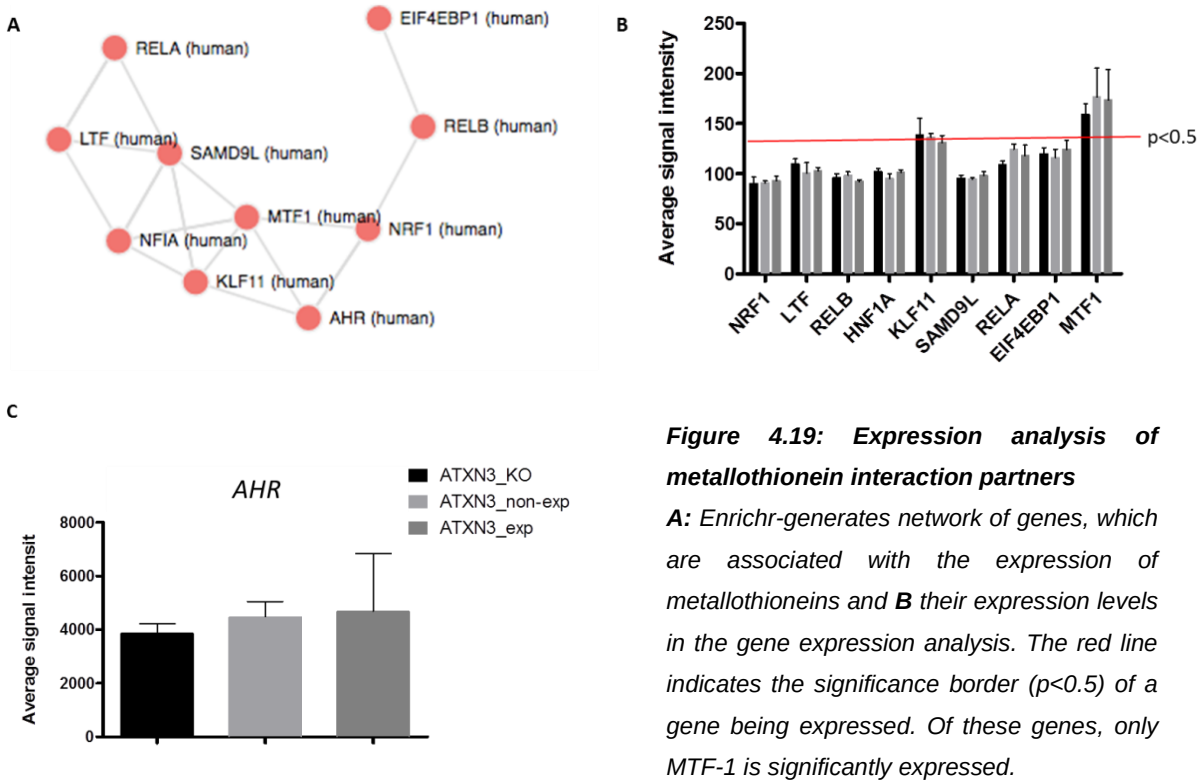

Figure 4.19: Expression analysis of metallothionein interaction partners

A: *Enrichr-generates network of genes, which are associated with the expression of metallothioneins and* ***B*** *their expression levels in the gene expression analysis. The red line indicates the significance border (p<0.5) of a gene being expressed. Of these genes, only MTF-1 is significantly expressed.*

C: Gene expression of the aryl hydrocarbon receptor (AHR). *There are no significant differences in its expression between the three groups of clones.*

4.6 Metal stress-induced nuclear translocation of MTF-1

The activation of MT expression is only possible when MTF-1 migrates into to nucleus in order to bind to the metal-regulated enhancer element (MRE) of MT promoters, before and after cell stress induction. To test for this, neural cultures transduced with the doxycycline dependent lentiviral VSV tagged MTF-1 were exposed to 25 µM $CdCl_2$ and harvested after 24 h. The obtained cell lysates were fractionated into a cytoplasmic and nuclear fraction by centrifugation and a western immunoblot analysis was performed (Fig. 4.20). Indeed, MTF-1_VSV was also found in the nucleus before stress application, but the highest amount of MTF-1_VSV was present in the nuclear fraction in those cells that were cultured in doxycycline conditions and exposed to the $CdCl_2$ stress. This suggests that MTF-1 translocates into the nucleus under stress conditions. In contrast, ATXN3 could not be detected in the nucleus at all.

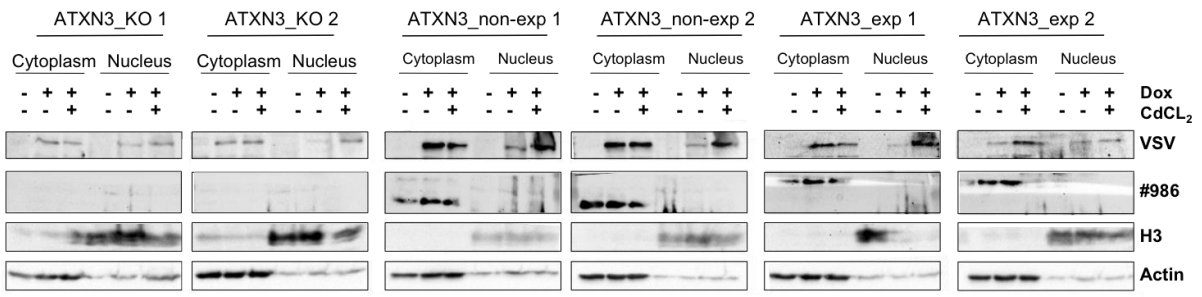

Figure 4.20: Nuclear fractioning of cell lysates obtained from neural cultures displays a translocation of MTF-1 into the nucleus after applying 25 µM $CdCl_2$.

Upper lane shows the signal for the VSV-tagged MTF-1 whose expression is doxycycline-dependent. After treatment with 25 µM $CdCl_2$, MTF-1 translocates, in all clones, into the nucleus. Whereas ATXN3 (#986, second lane) cannot be found in the nucleus in treated or untreated condition. The histone antibody H3 is the marker for the nuclear fraction. Actin is the loading control.

4.7 ATXN3 might be involved in the regulation of the metallothioneins e.g. by transcriptional control via its deubiquitinating function

ATXN3 is classified as a deubiquitinating enzyme (Amerik et al., 2004). As that, ATXN3 might also regulate the activity of MTF-1 via its deubiquitinating function. Following this hypothesis, a difference in the stability of MTF-1 would be expected between those clones expressing ATXN3 and ATXN3_KO since MTF-1 should be protected from proteasomal degradation due to ATXN3-mediated deubiquitination. To test this hypothesis, a cycloheximide chase experiment was performed. Cycloheximide blocks the synthesis of new proteins, which allows tracking the degradation of MTF-1 in neural cultures over a defined period of time. As commercial available antibodies did not show any specific band of the expected size in protein western blots, a VSV-tagged MTF-1 was cloned into a lentiviral vector (similar to Fig. 4.14, upper panel). By using an antibody against the VSV tag, western immunoblotting revealed that in ATXN3_KO and ATXN3_exp cultures MTF-1_VSV was degraded significantly faster after 24h as in clones with the non-expanded allele (ATXN3_KO vs. ATXN3_non-exp: 49,8% ± 11,26% vs. 84,99% ± 13.82%, ****p<0.0001; ATXN3_exp vs. ATXN3_non-exp: 67,8 ± 15% vs. 84,99% ± 13.82%, *p<0.05; ATXN3_KO vs. ATXN3_exp: 49,8% ± 11,26% vs. 67,8 ± 15%, **p<0.01). Also after 48h of chase the amount of MTF-1_VSV was significantly lower in ATXN3_KO but not ATXN3_exp neurons compared to ATXN3_non-exp neurons (38,75% ± 13,39% vs. 55,2% ± 15,76%, *p<0.05). After 72h no significant differences in the remaining MTF-1_VSV between groups could be observed (Fig. 4.21).

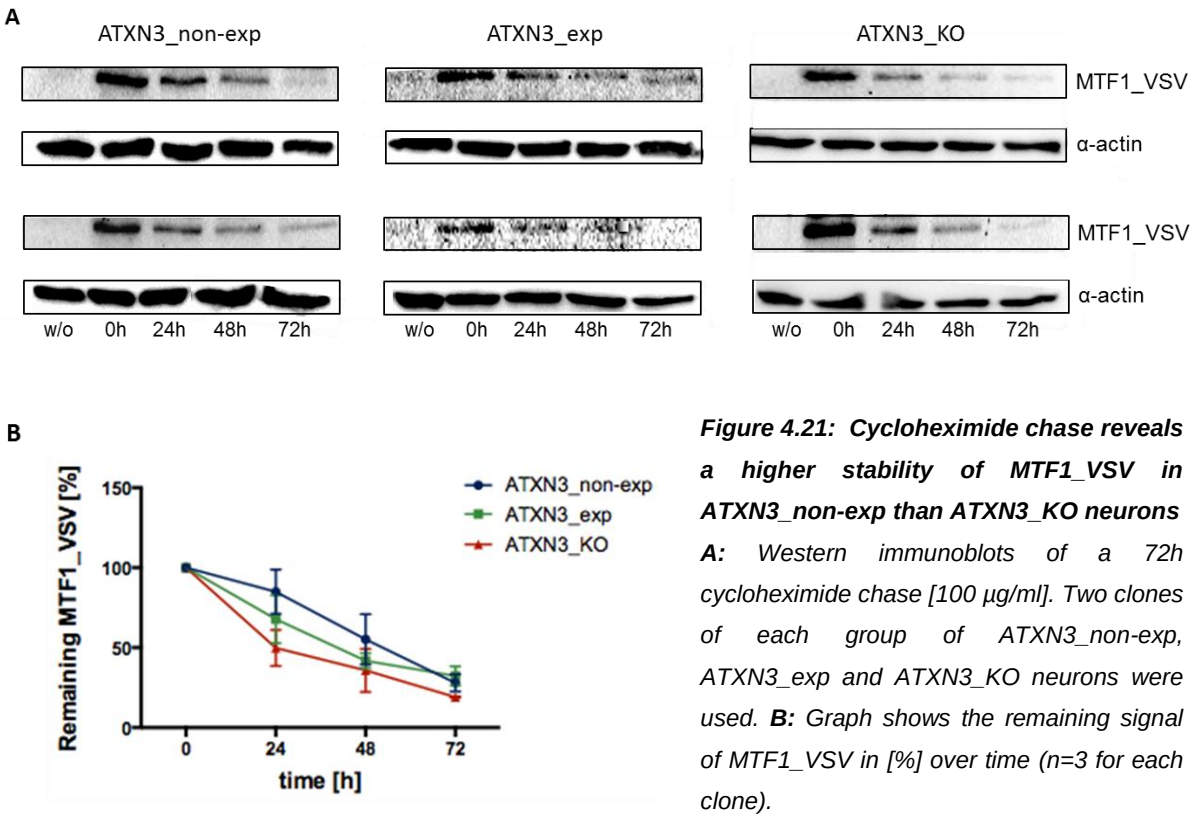

Figure 4.21: Cycloheximide chase reveals a higher stability of MTF1_VSV in ATXN3_non-exp than ATXN3_KO neurons ***A:*** *Western immunoblots of a 72h cycloheximide chase [100 µg/ml]. Two clones of each group of ATXN3_non-exp, ATXN3_exp and ATXN3_KO neurons were used.* ***B:*** *Graph shows the remaining signal of MTF1_VSV in [%] over time (n=3 for each clone).*

If ATXN3 interacts with MTF-1 in order to regulate the expression of MTs e.g. due to deubiquitination of MTF-1, an overexpression of MTF-1 in ATXN3_KO should lead to an improvement of cell survival rates. Therefore, neuronal cultures were transduced with a doxycycline-dependent lentivirus overexpressing VSV-tagged MTF-1. After five weeks of differentiation, the cell viability was evaluated after exposure to $CdCl_2$ at different concentrations to access cell survival rates. The cell viability assay revealed that MTF-1_VSV overexpression significantly increased cell survival rates in ATXN3_non-exp and ATXN3_KO but not in ATXN3_exp cells after applying $CdCl_2$ at the lowest concentration [10 µM]. At 25 µM $CdCl_2$ only a non-significant trend towards an increased cell survival under doxycycline conditions could be observed in all groups. However, 50 µM $CdCl_2$ does not affect the cell survival rates between MTF-1_VSV expressing and non-expressing neurons (Fig. 4.22).

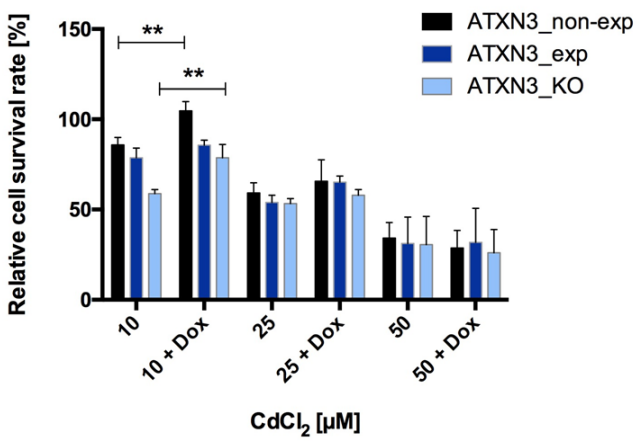

Figure 4.22: MTF-1_VSV overexpression significantly increases cell survival rates in ATXN3_non-exp and ATXN3_KO but not in ATXN3_exp neurons after application of $CdCl_2$ at low concentrations

Neuronal cultures were transduced with a lentivirus overexpressing MTF-1_VSV, seeded in 96-well plates and cultured for five weeks. Cells were cultivated in medium containing doxycycline, whereas controls maintained in doxycycline-free medium.

*Graphs show the relative cell survival rates [%] of ATXN3_non-exp, ATXN3_exp and ATXN3_KO neurons after exposure to $CdCl_2$ 10, 25 and 50 µM for 24 hours. For each group two clones with technical triplicates were used (n=6 / group). Bar graphs show mean ± SD of each group. *p<0.05; **p<0.01.*

5 Discussion

Transcription is the first step for gene expression and is influenced by epigenetic modifications (DNA-methylation or histone-modification) or transcriptional regulators including transcription factors and co-regulators. Depending on the regulation mechanism, transcriptional regulators are able to interfere in an activating or inhibiting manner and thus allowing the cell to react to changes in environmental conditions in order to maintain homeostasis.

Results from previous studies indicate that Ataxin 3 is involved in the progress of gene regulation, for instance by regulating the stability of transcriptional regulators via its deubiquitinating function. Transcription factors of transcriptional co-regulators might also be recruited to nuclear inclusions resulting in an unavailability of these proteins to fulfill their physiological tasks (Chai et al., 2001; McCampbell et al., 2000). Another hypothesis suggests that the non-expanded, but not the expanded form of ATXN3 acts as a transcriptional co-repressor due to formation of repressor complexes and histone deacetylation (Evert et al., 2006).

Metallothioneins were discovered in 1957 by Margoshes and Vallee and identified as low-molecular weight and cysteine rich proteins. The metallothionein family is evolutionarily conserved and proteins are localized in cytoplasm and cell organelles, predominantly in mitochondria (Banerjee et al., 1982). MTs are substantial to homeostasis of the essential micronutrients zinc and copper, and further for the detoxification of the toxic metal cadmium. Additionally, they play a role in radical scavenging, maintenance of cellular redox state and oxidative stress response against reactive oxygen species (Babula et al. 2012; Bremner and Beattie 1990; Isani and Carpene 2014; Vasak and Meloni 2011). The expression of metallothioneins can be induced by a variety of physiological and environmental stresses such as heavy metals, oxidizing agents, oxidative stress and hypoxia (Babula et al., 2012; Ruttkay-Nedecky et al., 2013; Saydam et al., 2003).

The present thesis showed that ATXN3 might be involved in the transcriptional regulation of the gene expression of metallothioneins, which is mandatory for the cell to respond to different stress events. Gene expression analysis and qRT-PCR results revealed reduced expression levels of MTs in ATXN3_KO and ATXN3_exp neurons compared to ATXN3_non-exp neurons. Consistent with this, the cell survival rate after exposure to metal, oxidative or excitotoxic stress was higher in ATXN3 non-exp neurons compared to the two other groups. Furthermore, ROS and superoxide levels were elevated in ATXN3_KO and ATXN_exp neurons compared to ATXN3_non-exp neurons, indicating that ATXN3 is involved to cope with increasing amounts of total ROS and superoxide during cell stress.

5.1 CRISPR/Cas9 for the generation of isogenic patient-derived stem cell-derived neural stem cells

The recent emergence of CRISPR/Cas9 technology provides a promising tool to overcome obstacles such as difficulties of protein design, synthesis and validation that occurred when using zinc finger nucleases (ZFNs) and TAL effector nucleases (TALENs). It is a straightforward two-component system, operating via Watson-Crick base pairing by a guide RNA to identify target DNA sequences and allows precise alterations of any target site.

Since the isogenic populations produced with CRISPR/Cas9 technology ideally only differ in one specific locus, they offer possibilities to overcome cell line specific differences and genetic variations of non-isogenic controls, which might mask disease-relevant changes. Often, control cells for experiments with patient-specific iPS-cell derived populations are obtained from healthy individuals, such as siblings, without knowing if those individuals will suffer from a late-onset neurodegenerative disease later in their lives. Furthermore, also monogenetic diseases such as Machado-Joseph disease display variation in its time of onset or severity within patients. For instance, the CAG repeat of ATXN3 in patients can be comparably low with 55 in number, while the average pathogenic number of repeats is 68. For repeat numbers in-between it is not possible to predict weather an individual will have MJD symptoms. This overlapping region illustrates that the number of repeats alone is not sufficient to predict the development of the disease. In this case, a multifactorial nature is seen, which includes single nucleotide polymorphisms (SNPs) within the genome, of which many are either not known or they are not well-studied enough to derive relations towards the disease. Therefore, an isogenic control population might help to obtain results, which are actually related to the gene of interest and not influenced by other non-related factors, sophisticating the outcome.

This assumption is supported by a study published by Reinhardt et al. (2013) investigating the link between Leucine-rich repeat kinase 2 (*LRRK2)* and Parkinson's Disease (PD) by using cultures of midbrain dopaminergic (mDA) neurons differentiated from isogenic human induced pluripotent stem cell (hiPSC) lines. The authors stated that since the pathology of PD is not only associated with *LRRK2* mutations such as G2019S but also with α-synuclein (SNCA) and microtubule associated protein tau (MAPT), patients with *LRRK2* mutations will exhibit variable phenotypes when additional polymorphisms are present in either SNCA or MAPT. Additionally the study showed that derivation of hiPSC lines from patients that were age and gender matched did not result in closely related gene expression patterns and instead displayed large variability in the genetic backgrounds between individuals. But gene correction resulted consistently in similar expression pattern within the isogenic *LRRK2* G2019S hiPSC-derived mDA neuronal cell line. Therefore, the authors concluded that it is

only possible to detect changes specifically associated with *LRRK2* G2019S by generating gene corrected isogenic cell lines.

In the course of this study, a CRISPR/Cas9 system for gene targeting in human neural stem was used. The aim was to generate isogenic cell lines with differences in the expression of ATXN3 in order to search for differentially expressed genes, which might be attributed to the expanded and non-expanded allele or a complete KO of ATXN3. Therefore a multiple plasmid system with two major components was incorporated into smNPCs via nucleofection: first, the CRISPR/Cas9 knockout plasmids consisting of a pool of three plasmids each encoding the Cas9 nuclease and a target-specific 20 nt guide RNA (gRNA) and second, a homology directed repair (HDR) plasmid providing a specific DNA repair template for a double strand break (DSB). The HDR plasmid incorporates a puromycin resistance gene for selection of cells where Cas9-induced DNA cleavage has occurred. Dependent on the cutting efficiency of Cas 9, multiple monoclonal cell lines derived from two patients were gained: cells expressing no ATXN3 (ATXN3_KO), only the non-expanded (ATXN3_non-exp) or the expanded allele (ATXN3_exp), respectively. Those monoclonal cell lines were selected with puromycin and could be validated by using western blot and PCR.

In the two KO scenarios either expressing the expanded or the non-expanded allele, ATXN3 is hemizygously expressed. This does not represent a physiologically occurring state but the ATXN3_exp clones could “mimic” a homozygous state of Machado-Joseph Disease in which both alleles code for the expanded form only. Furthermore, this system has the advantage that, in contrast to most studies investigating ATXN3, the effects and functions of the expanded and non-expanded form of ATXN3 can clearly be discriminated without interfering with each other.

Also, in order to gain isogenic clones with variances in the expression of *ATXN3,* the CRISPR/Cas9 system was highly efficient. Over 95 % of selected clones were either KO or hemizygous ATXN3 clones and less than 5 % still wild-type clones. The fact that wild type clones have been screened might be due to non-homologous integration of the HDR plasmids. Additionally to the high efficiency of this CRISPR/Cas9 system, it is further fast and straightforward in usage to generate KOs. After nucleofection of the designed plasmids (Santa Cruz) into neural precursor cells, within a month, these cells could be selected with puromycin, clones were picked and expanded and western blot analysis revealed the state of ATXN3 for each clone.

Since the Cas9 induced break can subsequently lead to wrong corrections by the cellular DNA repair machinery, all obtained cell lines were validated regarding their karyotype and the DNA sequence of the remaining allele in ATXN3_non-exp and ATXN3_exp clones. No karyotypic alterations could be observed and sequencing results revealed that only a minority of clones showed alterations in the sequence of the remaining *ATXN3* gene. These clones

were excluded from further experiments. Such a genome editing system could also bear the risk of off-target effects, for instance caused by random HDP plasmid integration, which can be detected by whole genome sequencing (WGS). Off-target effects cannot be excluded with certainty and testing would be mandatory e.g. for cell therapeutic studies.

Immunofluorescence stainings showed that all cell lines express the nuclear marker SOX2, PLZF, PAX6 and DACH1, nestin as an intermediate filament and the tight junction marker ZO-1 for the proliferative state. Also, all cell lines could be differentiated into neurons within five weeks expressing β-III tubulin and MAP2ab as well as the astrocytic marker GFAP. Additionally, these cultures display an anterior hindbrain identity as only HOXA2 and HOXB2 were highly expressed.

The use of neural stem cells allowed, due to their clonal growth and shorter differentiation periods, a fast and easy generation of several monoclonal patient-derived cell lines. Additionally, by nucleofecting those precursor cells with a CRISPR/Cas9 system in order to knock out either both alleles, only the expanded or the non-expanded allele of ATXN3, an ideal isogenic control population was created to decipher possible changes in the transcriptional regulation of MJD neurons dependent of the presence or absence of ATXN3.

5.2 Ataxin 3 as a regulator for the metallothionein-expression

ATXN3 has been proposed to function as a transcriptional co-repressor and to further regulate the expression of genes such as *MMP2* via histone deacetylation and chromatin modification. As a transcription regulator ATXN3 interacts with histones or in transcription complexes with co-regulators such as CBP, TBP, NCoR and HDAC3 (Evert et al., 2006; Li et al., 2002). Furthermore, it was shown that under oxidative stress, ATXN3 interacts with the forkhead box O (FOXO) transcription factor FOXO4 and activates the FOXO4-dependent transcription of the manganese superoxide dismutase (SOD2) gene by binding to the SOD2 gene promoter. In contrast to normal ATXN3, mutant ATXN3 displayed a reduced capability to activate the FOXO4-mediated SOD2 expression and interferes with binding of FOXO4 to the SOD2 gene promoter (Araujo et al., 2011). Considering the possibility that mutant and normal ATXN3 differentially interfere with transcription factors and diversely regulate transcriptional regulation, a gene expression analysis with the CRSPR/Cas9-derived cell lines was performed in order to screen for differentially expressed genes between ATXN3_KO, ATXN3_non-exp and ATXN3_exp neural cultures.

Comparing the three groups, some genes were depicted with the most dominant differences between ATXN3_KO and ATXN3_non-exp, whereas the number of differentially expressed genes was lower when comparing ATXN3_KO and ATXN3_exp neurons. Although the comparison between ATXN3_KO and ATXN3_non-exp cells helps to reveal functions of

ATXN3, the KO situation does not naturally occur. Therefore, the differences in the gene expression between cells with the expanded versus non-expanded ATXN3 might be more important to reveal a relevant phenotype and to provide the opportunity to make assumptions about the gain of function or loss-of-function theory.

In general, the gene expression analysis revealed only a small number of differentially expressed genes, which supports the isogeny of the two patient-derived cell lines. Among these few genes a whole cluster of metallothioneins (MT) was discovered. In mammals, MTs are divided into four subfamilies (MT-1 – MT-4). All known human MT genes are located in the q13 locus on chromosome 16 and encode seven functional MT-1 genes (MT-1A, B, E, F, G, H, X) and one functional gene for MT-2, MT-3 and MT-4, respectively. Whereas MT-1 and –2 are expressed throughout all tissues of the body, MT-3 is specifically expressed in the normal human brain, predominantly in glutamatergic neurons. MT-4 is specifically localized in the buccal mucosa and pseudostratified squamous epithelial lining of the uterine cavity (Montoliu et al., 2000; Vasak et al., 2011).

Interestingly, the revealed MT cluster consisted only of MT-1 genes and the MT-2 isoform, but no differences in the expression of MT-3 were found. MT-3 differs from MT-1 and -2 as it responds to metal levels in neurons differentially, even though the promoter region of MT-3 has several regions that are similar to the MRE regulating MT-1 and MT-2 levels. An explanation for this might be that metal transcription factor 1 (MTF-1), involved in the regulation of MT expression, does not bind to the MRE sequence in the MT-3 promoter region, suggesting that MT-3 is differently regulated from other metallothioneins (Bousleimann et al., 2017). Furthermore, induction of metallothioneins by several inducers was found to be due to an increase in MT-1 and -2 gene expression but not MT-3 gene expression, because MT-3 cannot be induced in brain (Kramer at al., 1996; Palmiter et al., 1992; Zheng et al. 1995). These results indicate that in neurons, MT-1 and –2, but not MT-3 genes are coordinately regulated.

Under normal conditions and after treatment with 100 µM L-glutamate, the cluster of MTs was found to be downregulated in ATXN3_KOs compared to the two other groups in the first patient-derived cell line that has been tested. Interestingly, the highest expression was observed in ATXN3_exp neurons. This was confirmed by quantitative real-time PCR. However, the qPCR data of a set of isogenic clones derived from a second patient cell line revealed a different expression pattern for MTs. Still, the expression was lowest in ATXN3_KO, but in this cell line the highest expression was found in those cultures with the non-expanded allele instead of the expanded one, which would argue for a (partial) loss of function of Ataxin 3.

After the application of 25 µM $CdCl_2$ for 24 h, which is a much stronger stress stimulus than 100 µM L-glutamate (30 min.), the expression pattern of all MTs was the same in both cell

lines with the highest expression in the ATXN3_non-exp neural cultures. This might be explained by the fact that the patient one-derived cell line and its generated ATXN3 clones could be less prone to the formation of aggregates compared to the patient two-derived cell line. Therefore, in the former cell line compensatory mechanisms might still be active, which fail to work in the latter one because of a more severe aggregation potential and less availability of Ataxin 3 to cope with stress.

Conclusively, in ATXN3_exp neurons from patient line one forming less aggregates than patient line two, there might remain a larger amount of freely available and functional ATXN3 helping the cells to partially respond to stress. However, after the application of a strong stressor such as $CdCl_2$ in a high concentration, the compensatory mechanisms of the less aggregation-prone cell line one start to fail as well. In this case, the MT expression pattern changes and the highest expression was not found in ATXN3_exp neurons anymore but in ATXN3_non-exp neurons, which is the same expression pattern in ATXN3 clones generated from patient two.

This is the first time that an upregulation of metallothioneins is associated with Ataxin 3, a link that was revealed by doing a gene expression analysis of isogenic cell lines with differences in the state of ATXN3. Evert et al. (2001, 2003) worked on a gene expression profile of expanded and non-expanded ATXN3 before but they found other genes to be differentially regulated such as the matrix metalloproteinase 2 (MMP-2). Reasons for this can be that different cell systems than human neurons were used such as rat mesencephalic CSM14.1 clonal cell lines and that some genes such as MMP-2 are not expressed in human neurons. This argues for the system used within this study since human neuronal cultures were used and only altered in one specific locus to clearly distinguish between expanded and non-expanded as well as a loss of Ataxin 3 to screen for genes that are differentially expressed.

5.3 Ataxin 3 as a regulator of stress responses in human neural cell lines

So far, no link between ATXN3 and metallothioneins has been reported. However, it was proposed that copper-binding proteins, including MTs, are potential therapeutic targets for Huntington's disease (HD), which belongs together with MJD, to the polyglutamine (ployQ) diseases. A pathological hallmark of this disease is an abnormal copper accumulation in the postmortem HD brain. It was demonstrated that *in vitro* copper accelerates the fibrillization of an N-terminal fragment of huntingtin with an expanded polyQ stretch (httExon1) in HeLa cells and that the overexpression of metallothioneins known to bind copper, protect against httExon1 toxicity in a yeast model (Hands et al., 2010).

Initially, copper, as a potential metal stressor for the neuronal cultures, was tested in the present study as well, but did not show concentration-dependent numbers of surviving cells. Instead, the metals $CdCl_2$ and $ZnCl_2$ displayed a linear dose-response curve and were used to induce metallothionein expression since MTs play a crucial role in homeostasis of trace metals like zinc and detoxification of toxic metals such as cadmium. The oxidative stressor rotenone was used due to the protective functions of MTs against oxidative damage and L-glutamate was chosen as an excitotoxicity-inducer. Typically, MT studies are done by application of different metal concentrations and by induction of oxidative stress, but less often by induction of excitotoxicicity with glutamate since, in contrast to most of the cell systems, this can only be achieved in neuronal cultures. In this study human neuronal cultures were used to investigate the influence of L-glutamate-induced excitotoxicty on the cell viability of isogenic ATXN3 clones and the associated expression of metallothioneins.

For the experimental design of the present study all stressors were applied to the cultured neurons in three different concentrations for a period of 48h to access cell viability. In accordance with the working hypothesis that ATXN3 might be involved in the transcriptional regulation of the cellular response to stress, ATXN3_non-exp neurons of both patient-derived cell lines displayed the highest number of surviving cells after exposure to different stressors and concentrations for 48h. In comparison, ATXN3_KO cells showed a significantly decreased cell survival rate and those clones expressing the expanded allele of ATXN3 displayed a survival rate comparable to those of ATXN3_KO neurons. The numbers of surviving cells were all concentration-dependent.

Similar experiments were conducted in non-clonal cell lines in order to evaluate a comparable phenotype. Therefore, two patient-derived non-clonal cell lines and two healthy control lines were used for the cell survival assay and indeed in this experiment the healthy control neurons displayed a higher cell survival number than the patient-derived cell lines, which argues for a similar phenotype as found in the genetically modified cells.

Since both, the ATXN3_non-exp neurons as well as the healthy control non-clonal neurons, displayed a higher cell survival rate than those cell lines with expanded ATXN3, it was further determined what consequences arise when aggregates are induced in a healthy control cell line by using a lentiviral doxycycline-dependent system overexpressing the truncated aggregation-prone form of ATXN3. Interestingly, in the doxycycline treated cells, the induction of aggregates lead to a decrease in the cell survival rate compared to those cells under normal culture condition without addition of doxycycline.

Additionally, the numbers of surviving cells of the untreated doxycycline—dependent and non-dependent controls were compared and no differenced were found. This might indicate that the aggregates inherently are not toxic and not responsible for neuronal cell death within the cell survival assay. All these observations lead to the assumption that the depletion due

to recruitment of expanded ATXN3 into nuclear inclusions or a KO of ATXN3 and thus the failure of functionality of the protein hampers the cellular response to stress.
From the literature it is known that ATXN3 is involved in certain stress responses within the cell due to its deubiquitinating and transcriptional regulation functions. For instance, as a deubiquitinating enzyme ATXN3 regulates basal level of hsp70 and modulates the hsp70 protein level in response to a subset of cellular stresses (Reina et al., 2012), it plays a role in the FOXO4-mediated SOD2 expression (Araujo et al., 2011) and the presence of misfolded and/or aggregated expanded ATXN3 by itself might result in cellular stress (Bichelmeier et al., 2007; Breuer et al., 2010).
The present study suggests a link between the expression of metallothioneins and ATXN3 and supports the hypothesis that ATXN3 is involved in the regulation of the cellular stress response.

5.4 Ataxin 3 as a regulator of total ROS and superoxide levels after stress application

The hypothesis that MTs function as an antioxidant against reactive oxygen and nitrogen species in biological systems has been widely reported. The results of this thesis indicate that ATXN3_KO neurons, expressing the lowest amount of MTs, displayed higher amounts of total ROS and superoxides compared to ATXN3 expressing cells. Neurons with the non-expanded allele of ATXN3, expressing the highest amount of MTs, showed the lowest levels of total ROS and superoxides. Since the expression levels of MTs were dependent on the presence or absence of ATXN3, this indicates a functional role of ATXN3 in the response to cellular stress by regulating the MT expression, which in turn regulate the total ROS and superoxide levels. The function of MTs as proteins that protect against oxidative stress is especially important for the brain since it is highly susceptible to oxidative stress due to the high levels of oxygen consumption.
Moreover, cells in the brain contain high levels of zinc, elucidating the importance of MT in the central nervous system, since MTs are responsible for metal homeostasis. More than a thousand proteins have been discovered by human genome analyses that possibly contain zinc-binding motifs (Brayer et al., 2008). However, the majority binds zinc tightly, and hence might not be able to contribute to fast zinc dynamics in the cell. In contrast, other proteins, such as MTs, contain highly redox state sensitive zinc-binding sites (Cousins et al., 2006; Chung et al., 2007; Krezel et al., 2007; Maret, 2008; Pedersen et al., 2009). When cells are exposed to reducing conditions or when cellular free zinc levels rise, MTs may bind more zinc. Vice versa, under oxidative stress conditions or during signaling events involving ROS generation, MTs may act as zinc-donors, increasing the availability of free zinc (Chung et al.,

2007).

Studies using a cell-free system have demonstrated the ability of MTs to function as free radical scavengers (Abel and Deruiter, 1989; Cai et al., 2000; Thornalley and Vasak, 1985). Other studies suggested that MTs scavenge a variety of ROS including hydroxyl radicals and superoxide anions, nitric oxide radicals, radicals of reactive nitrogen species and hydrogen peroxide when oxidative stress levels increase (Kumari et al., 2006; Pedersen et al., 2009; Sato and Bremner, 1993; Thirumoorthy et al., 2011).

The majority of ROS inside the cell is produced in mitochondria as a consequence of the electron transport chain, the major cellular mechanism of ATP production. Correspondingly, MT-1/2 isoforms have mainly been found in cellular cytoplasm and in some organelles, with predominant expression in mitochondria (Banerjee et al. 1982; Dziegiel et al., 2016).

Antioxidant defense is a major task of cells and considered to be critical in the pathogenesis of most neurodegenerative diseases as well as in ageing. Defects in mitochondrial and peroxiosomal detoxification are followed by an increase of ROS levels, which has been demonstrated to trigger neurodegeneration (Halliwell, 2006; Reddy and Beal, 2005).

Concluding, the absence of functional ATXN3 in ATXN3_KOs and ATXN3_exp neurons and the correlated dysregulation of MTs might bear severe consequences for the cell including neurodegeneration.

5.5 Model of the Ataxin 3 activated, metal regulatory transcription factor 1-dependent metallothionein gene expression

The ability of cells in the body to respond to various stressors is crucial for their survival. There is a large number of proteins, enzymes and transcriptional factors known which participate in stress responses, including ATXN3. The results of this thesis showed that a cluster of metallothioneins is downregulated in ATXN3_KO and ATXN3_exp neurons compared to those cells expressing the non-expanded allele of ATXN3.

As discussed before, both ATXN3 and metallothioneins play an important role for the cells appropriate reaction towards stress. This was evidenced by cell viability assays, showing that after treatment of neurons with metal, oxidative and excitotoxic stressors, the number of surviving cells was highest in neurons with the non-expanded allele of ATXN3 and lowest in ATXN3_KO cells, whereas the cells with the expanded allele showed numbers of surviving cells in-between. Vice versa and consistently, after applying oxidative stress to the neuronal cultures, the formation of reactive oxygen species and superoxides was lowest in ATXN3_non-exp cells and highest in KO cells.

The present results indicate that ATXN 3 is apparently required for appropriate induction of

MT expression. A possible hypothesis how ATXN3 regulates the expression of MTs is that ATXN3 interacts with a stress sensor (e.g. transcription factor). Within the ATXN3_non-exp neurons the coordinated regulation of MT expression helps to prevent the cell from damage, thus regulating homeostasis. In the disease situation, in accordance with the loss of function theory, expanded ATXN3 is sequestered in nuclear inclusions and further recruits non-expanded ATXN3 into NIs, reducing the amount of free available ATXN3 within the cell. To a certain extent this mimics a KO situation of ATXN3. In both cases, ATXN3 is hampered in its functions and fails to upregulate MTs. As a consequence, neurons suffer from stress and eventually degenerate (Fig. 5.1).

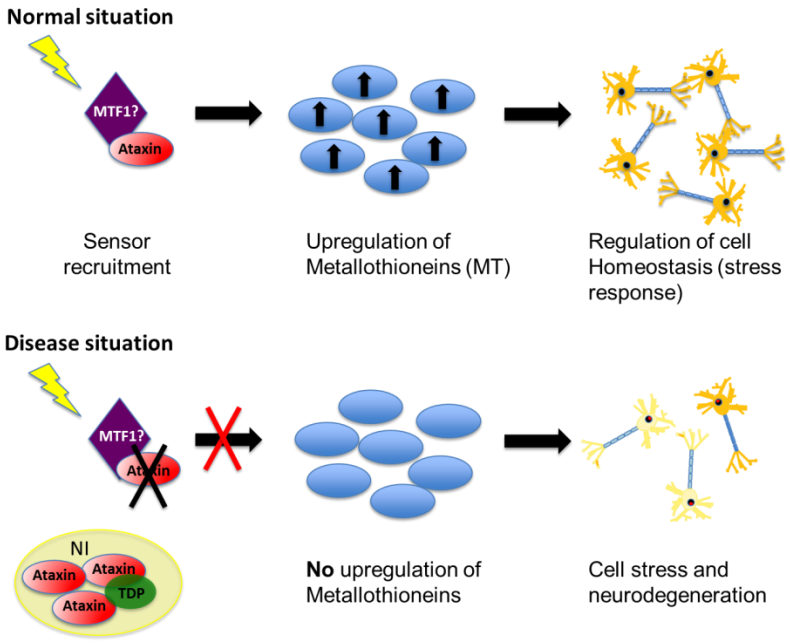

Figure 5.1: Scheme of a possible ATXN3 activated MTF-1-dependent stress response *The upper panel depicts the normal situation of a healthy cell to copy with cell stress. An interaction of MTF-1 and ATXN3 e.g. the ATXN3-mediated deubiquitination of MTF-1 might lead to an upregulation of MT genes due to transcriptional regulation of ATXN3. This stress response facilitates cell homeostasis and ensures neuronal survival. The lower panel displays the failure of MT upregulation under ATXN3 disease or KO condition. ATXN3 is captured and recruited into nuclear inclusions and thus not available for the cell to fulfill its biological functions. Hence, there is no interaction with MTF-1 possible, resulting in a failure of MT gene upregulation. This might cause cellular stress and neurodegeneration.*

It is known from literature that the expression of metallothineins is regulated by the transcription factor metal regulatory transcription factor 1. MTF-1 was identified in 1988, as a candidate protein for zinc-dependent binding of promoters containing a metal-responsive element (MRE; Westin and Schaffner, 1988). A few years later, in 1993 MTF-1 was cloned and further characterized (Radtke et al., 1993). MTF-1 is composed of 753 amino acids and contains six-zinc finger motifs. The protein is ubiquitously expressed and involved in cellular adaptation to various stress conditions, such as exposure to heavy metals, hypoxia and oxidative stress (Bonaventura et al., 2015; Lichten et al., 2011; Rutherford et al., 2004; Saydam et al., 2003). MTF-1 is a nucleocytoplasmic shuttling protein, which accumulates in the nucleus upon heavy metal exposure. Within the nucleus it binds DNA, recruits different

co-activators and was also shown to often rely on other transcription factors for the expression of certain target genes (Grzywacz et al., 2015; Ruttkay-Nedecky et al., 2013; Smirnova et al., 2000).

MTF-1 controls the expression of metallothioneins (MTs) after metal or oxidative stress, thereby maintaining the cellular homeostasis (Grzywacz et al., 2015; Ruttkay-Nedecky et al., 2013). Activation of metallothionein gene expression by MTF-1 is achieved by multiple MRE (metal response element) sequences of core consensus TGCRCNC upstream of the MT genes in the promoter regions of MT1 and MT2 genes (Palmiter 1994; Radtke et al., 1995; Saydam et al., 2003). Experiments with MTF-1 null-mutant mice revealed that MTF-1 is an essential gene, as these mice died in utero due to degeneration of the liver and further did not express MT1 and MT2 genes leading to an increased susceptibility to metal stress (Günes et al., 1998).

In order to exclude other factors than MTF-1 that might influence the expression of MTs, the comprehensive gene set enrichment analysis web server “Enrichr” was used to search for factors that were associated with the expression of MTs. Except MTF-1 and aryl hydrocarbon receptor (AHR), non of the revealed factors displayed significant expression levels in the gene expression study with isogenic neurons analyzed in this study. Since AHR was exclusively associated with MT2 in one study by Sato et al. (2013), it was excluded and MTF-1 was chosen as a possible candidate for mechanistic studies.

In order to initiate the expression of metallothioneins, MTF-1 binds to MREs upstream of the metallothionein genes. Therefore, MTF-1 has to migrate into the nucleus, which was shown for a VSV-tagged lentiviral overexpression construct of MTF-1 (MTF-1_VSV) by performing a fractioning protocol, separating total protein lysates into nuclear and cytoplasmic fractions. Under basal conditions MTF-1 is present in the cytoplasm and nucleus. After treatment with 25 µM $CdCl_2$ the amount of MTF-1_VSV increased within the nucleus and decreased within the cytoplasm, indicating a functional response towards stress. Additionally, the highest amount of the tagged protein MTF-1 was found in the ATXN3_non-exp clones, less was found in the ATXN3_exp cells and the KO cells displayed the lowest amount of MTF-1.

As stated before, qPCR results revealed no differences in the cDNA levels of MTF-1 in the isogenic neuronal cell lines, suggesting post-translational modifications of the transcription factor MTF-1 as a mechanistic explanation for the ATXN3-dependent regulation of the MT expression. The theory emerged that ATXN3 might deubiquitinate MTF-1 under stress conditions and thereby preventing it from proteasomal degradation to fulfill its task as a regulator of metallothionein expression. In ATXN3_exp and ATXN3_KO cells, deubiquitination of MTF-1 might fail, because of the dysfunction of ATXN3, resulting in the degradation of MTF-1 by the proteasome and the subsequent disturbance in the metallothionein expression.

Accordingly, an increased proteasomal degradation of MTF-1 in ATXN3_exp and ATXN3_KO neurons should reveal a lower amount of the protein MTF-1 within these cells compared to ATXN3 non-exp neurons. To determine the protein stability of overexpressed MTF-1_VSV for all cell lines, a cycloheximide chase was performed. Cycloheximide blocks the synthesis of new proteins, enabling the observation of protein degradation over time and the amount of remaining protein can be detected via western immuno blot. Indeed, after 24h and 48h ATXN3_KO neurons revealed a decreased protein stability of MTF-1_VSV than the neurons with the non-expanded allele, which might indicate that ATXN3 is involved in posttranslational modifications of MTF-1.

Restoring MTF-1 levels in ATXN3_KO and ATXN3_exp neurons to normal levels should improve cell survival. Therefore, neuronal cultures were transduced with a doxycycline-dependent lentivirus overexpressing VSV-tagged MTF-1. After five weeks of differentiation, the cell viability was evaluated after exposure to $CdCl_2$ at different concentrations to access neuronal survival rates. MTF-1_VSV expressing ATXN3_non-exp as well as ATXN3_KO but not in ATXN3_exp cells displayed significantly improved numbers of cell survival after treatment with 10 µM $CdCl_2$.

To conclude it was shown that the steady state amount of MTF-1 stability was highest in ATXN3_non-exp neurons compared to ATXN3_KO and ATXN3_exp neurons by doing a cycloheximide chase to determine protein stability. Also, a cell survival assay revealed that by overexpressing a VSV-tagged form of MTF-1, the number of surviving cells improved in ATXN3_KO and ATXN3_non-exp neurons. So far these are preliminary data and no conclusions can be made if this is actually related to the deubiquitinating function of ATXN3. Future experiments need to be done to reveal the ubiquitinating status of each cell line and to determine if there is an interaction between ATXN3 and MTF-1.

5.6 The role of metallothionein expression in neurodegenerative diseases

The brain is highly susceptible to oxidative stress, which increases with age and can therefore be considered as a major causative factor in neurodegenerative diseases. Furthermore, the brain contains a large amount of zinc, an essential trace metal whose dysregulation of homeostasis has been associated with neurodegeneration as well (Juárez-Rebollar et al., 2017). Metallothioneins are important for the regulation of both processes, scavenging free radicals to prevent oxidative stress and zinc homeostasis, hence showing the importance of MT in the central nervous system. Consistently, different studies have depicted that oxidative damage and abnormal Zn concentrations are associated with the pathophysiology of neurodegenerative diseases (Huntington's disease, Alzheimer’s disease

and Parkinson's disease) and other brain disorders such as cerebral ischemia and epilepsy (Carrasco et al., 2006; Hands et al., 2010; Juárez-Rebollar et al., 2017; Kim et al., 2012).

As mentioned before, there is no evidence in the literature that metallothioneins are associated with ATXN3 and MJD. However a link between MTs and another polyQ disease, Huntngton's disease (HD), was found. For the pathology of HD a dysregulation of copper homeostasis seems to be crucial. Hands et al. (2010) showed that in vitro copper accelerates the fibrillization of an N-terminal fragment of huntingtin with an expanded polyQ stretch and polyQ aggregation and that overexpression of MTs in mammalian cells significantly reduced polyQ aggregation and toxicity.

In reactive astrocytes of patients with Alzheimer's disease, an overinduction of MT-1 and MT-2 has been observed, which was stimulated primarily by the presence of free radicals, metal ions, and cytokines. This overinduction was considered to be a cellular defense mechanism against inflammatory signals supporting the idea of MT to be neuroprotective (Hidalgo et al., 2001). Furthermore, a study by Valko et al. (2007) suggested that especially upregulated MT-1 in reactive astrocytes has a neuroprotective effect in AD, directly by decreasing the neurotoxicity of Aβ and indirectly due to inhibition of Aβ-induced microglial activation by MT-1 and consequential neurotoxicity.

With regard to MJD, especially the recruitment of ATXN3 by dysfunctional expanded ATXN3 into nuclear inclusions and the subsequent dysregulation of metallothioneins within the ATXN3_exp neurons, provides a possible explanation why reactive oxygen species accumulate within patients neurons, enhancing neurodegenerative effects in MJD (Araujo et al., 2011; de Assis et al., 2017; Pacheco et al., 2013; Weber et al., 2014). This would also argue for MJD to account for a loss of function disease. By overexpressing the aggregation-prone truncated form of ATXN3 into a healthy control cell line, aggregates were formed, which were not toxic per se, but those cells forming aggregates showed a lower number of surviving cells after application of different stressors than those cells without aggregates. In accordance with a loss of function ATXN3 is sequestered into these aggregates and is thus hampered in its function to cope with cellular stress by regulating the metallothionein expression, which might lead to cell death and neurodegeneration.

Metallothioneins are important for the homeostasis of essential metals such as zinc, the detoxification of metals such as cadmium and for scavenging of reactive oxygen species such as ROS and superoxides. Potentially, all these processed might be disturbed if Ataxin 3 fails to regulate the expression of metallothioneins e.g. due to an interaction with MTF-1.

As a consequence it is mandatory to find an ATXN3-independent way to regulate the expression of metallothioneins in patients suffering from MJD. To this account different approaches might apply e.g. to avoid exposition to certain noxa, to control for a balanced supplementation of trace metals due to nutrients and potential therapeutic drugs. Possible

noxa to avoid can be heavy metals such as cadmium and mercury, and also exogenous ROS produced from pollutants, tobacco, smoke, drugs, xenobiotics, or radiation. Trace metals that are important for health and regulated by metallothioneins are for example iron, zinc, copper and manganese.

There are only a few potential drugs known, which induce the expression of metallothioneins: the polyphenol compound quercetin has been found to increase metallothionein expression in a rat model for experimental chronic cadmium nephrotoxicity (Morales et al., 2006), the açai fruit has been demonstrated to influence expression of MTs in *Drosophila* (Sun et al., 2010) as well as the neuroprotective drug resveratrol increasing MT protein levels by 65% in the hippocampus of rats following ischemic damage (Yousuf et al., 2009).

The latter, resveratrol is a polyphenolic stilbene that is widely distributed in red grapes, berries, and nuts with low bioavailability. It is known to cross the blood-brain barrier and has been shown to be neuroprotective in Huntington's Diseasae, belonging to the polyglutamine diseases (Parker et al., 2005). Resveratrol was shown to rescue mutant polyglutamine cytotoxicity in nematode and mammalian neurons (Parker et al., 2005), to improve motor deficits and imbalance in SCA3 transgenic mice by pharmacological activation of sirtuin1 (SIRT1), to protect against cell death in primary cortical neurons containing truncated ataxin-3 with 79 glutamine repeats and to alleviate oxidative stress induced neurotoxicity in cell and *Drosophila* models of MJD (Cunha-Santos et al., 201; Wu et al., 2017).

In conclusion, MTs are involved in a number of diseases in the central nervous system, indicating a multifunctional role over a wide range of cellular processes. Therefore, future studies on the expression and regulation of MT genes are mandatory to elucidate the molecular mechanisms involving MT in the nervous system and their role is in the pathophysiology of brain disorders. Within this study, a new approach is suggested comprising a possible regulation of the expression of metallothioneins by ATXN3. It was shown that depletion of ATXN3 due to nuclear inclusions or a KO, in accordance with the loss of function hypothesis, leads to a decreased expression of metallothioneins, accompanied by a decreased response to cellular stress and an impaired regulation of total ROS as well as superoxides, both facilitating neurodegeneration.

5.7 General conclusion

This thesis introduces isogenic CRISPR/Cas9-mediated iPSC-derived isogenic neural precursor cell lines with different allele expression profiles of ATXN3 for the study of its role as a transcriptional regulator and as a mediator of cellular stress. These cell lines could be differentiated into mature neurons and the present results revealed that ATXN3 plays an important role in the transcriptional regulation of the metallothionein expression in these neurons. Also, the regulation of MT expression by ATXN3 seems to be important to mediate the cellular response to metal, oxidative and excitotoxic stressors. Vice versa, the depletion of ATXN3 in ATXN3_KO and partially loss within ATXN3_exp neurons led to an impaired response of neuronal cultures to cellular stress resulting in cell death. Additionally, ATXN3 seems to be important for the cell to cope with total ROS and superoxides after exposure of neuronal cultures to different forms of cellular stress.

The upregulation of MT gene expression as a response of cells towards stress might be mediated by an interaction between ATXN3 and the transcription factor MTF-1. The more precise underlying mechanism remains to be demonstrated. However, this study supports the idea that ATXN3 is involved in the transcriptional regulation of metallothioneins and thus fulfills an important part in regulating the cellular stress response. It is further suggested that an impaired function of ATXN3 and consequently a dysregulation of the MT gene cluster leads to an increased susceptibility towards stress, which might contribute to the pathogenesis of Machado-Joseph-Disease.

6. Abbreviations

Abbreviation	Full name
AA	Ascorbic acid
AD	Alzheimer's Disease
ATXN3	Ataxin 3
cAMP	Cyclic adenosine monophosphate
Cd	Cadmium
CHIP	C-terminus of Hsc70 interacting protein
CNS	Central nervous system
CRISPR	Clustered regulatory interspaced palindromic repeats
Dach1	Dachshund homolog 1
DABCO	1,4-Diazabicyclo[2.2.2]octan
DAPI	4',6-Diamidino-2-phenylindole
DAPT	N-[N-(3,5-Difluorophenacetyl)-L-alanyl]-S-phenylglycine t-butyl ester DMSO Dimethyl suphoxide
DEPC	Diethyl pyrocarbonate
DMSO	Dimethyl sulfoxide
dNTPs	Nucleoside triphosphate
Dox	Doxycycline
DSB	Double strand break
DUB	Deubiquitinating enzyme
EDTA	Ethylenediaminetetraacetic acid
EF1α	Flongation factor α
EGF	Epidermal growth factor
ER	Endoplasmatic reticulum
ERAD	Endoplasmatic reticulum associated degragdation
FCS	Fetal calf serum
FGF2	Fibroblast growth factor 2
GFAP	Glial fibrillary acidic protein

Abbreviation	Full name
hES cell	Human embryonic cell
HD	Huntington's Disease
hPS cell	Human pluripotent stem cell
HDR	Homology-directed repair
HEK	Human embryonic kidney
ICC	Immunocytochemistry
ICM	Inner cell mass
Hsp	Heat shock protein
iPS cell	Induced pluripotent stem cell
IRES	Internal ribosomal entry site
Ln	Laminin
ltNES cell	long-term self-renewing neuroepithelial stem cell
MAP	Microtubuli-associated protein
mDA	Midbrain dopaminergic neurons
MEF	Mouse embryonic fibroblast
MJD	Machado-Joseph disease
GT	GelTrex
mRNA	messenger RNA
PAGE	Polyacrylamid gel electrophoresis
PAX6	Paired box 6
PBS	Phosphate buffered saline
PCR	Polymerase chain reaction
PD	Parkinson's Disease
PFA	Paraformaldehyde
PLZF	Promyelocytic leukemia-associated zinc finger
PO	Poly-ornithine
polyQ	Poly-glutamine
puroR	Puromycin resistance

Abbreviation	Full name
RNA	Ribonucleic acid
ROS	Reactive oxygen species
RT-PCR	Reverse-transcriptase PCR
SCA3	Spinocerebellar ataxia type 3
SDS	Sodium dodecyl sulphate
SOX2	Sex determing region Y-box 2
TALEN	Transcription activator-like effector nuclease
TC	Tissue culture
TE	Trypsin/EDTA
TEMED	Tetramethylethylenediamine
tetOn	Tetracycline regulatable gene induction system
TF	Transcription factor
TI	Trypsin inhibitor
TREtight	Tetracyclin-responsive element
Ub	Ubiquitin
VCP	Valosin containing protein
ZO-1	Zona occludens-1
Zn	Zinc
ZNF	Zinc finger

7 Abstract

Ataxin-3 (ATXN3), the disease-causing protein for Machado Joseph Disease (MJD) is functionally involved in the protein quality control and transcriptional regulation of various genes. Recent data suggest that either conformational changes of the expanded ATXN3 protein and/or a loss of free available ATXN3 due to recruitment of ATXN3 into aggregates leads to the dysregulation of multiple cellular pathways such as ubiquitination or transcriptional regulation. In this study, induced pluripotent stem cells (iPSCs) were used to decipher the influence of expanded and/or lost ATXN3 on gene expression in patient-specific neurons. To that end isogenic iPSC-derived neural stem cell lines were generated, expressing the normal (ATXN3_non-exp), the expanded (ATXN3_exp) or no ATXN3 (ATXN3_KO) using CRISPR/Cas9-mediated gene editing. This approach allowed a direct comparison of the gene expression profiles between the expanded/KO and non-expanded allele of ATXN3 within an isogenic genetic background. By transcriptional profiling of neurons generated from these lines identified several genes were identified, which were dysregulated in ATXN3_exp and ATXN3_KO neurons. Among those a cluster of metallothioneins (MTs) was found, which was significantly downregulated in ATXN3_exp and ATXN3_KO neurons compared to those cells with the non-expanded form of ATXN3. Physiologically, MTs are important regulators of cell homeostasis and participate in an array of protective responses against oxidative, metal and excitotoxic stress. Consequently, it was discovered that ATXN3_exp and ATXN3_KO neurons are more susceptible to several types of cellular stress. Furthermore, these neurons displayed a higher level of total ROS and superoxide under oxidative stress compared to ATXN3_non-exp neurons.

As a possible underlying mechanism this thesis suggests a posttranslational interaction between ATXN3 and metal transcription factor 1 (MTF-1) for the regulation of the gene expression of MTs via the deubiquitinating function of ATXN3. So far, increased MTF-1 protein levels in ATXN3_non-exp neurons in comparison to ATXN3_KOs support this idea. But these are preliminary data and whether ATXN3 regulates responses to various stressors by interacting with MTF-1 remains to be demonstrated, however in the frame of this work a strong genetic neuronal model was generated that supports a correlation between ATXN3 and MT expression. Furthermore, this work confirms that ATXN3 plays an important role in regulating the cellular stress response and that an increased susceptibility towards stress and the correlating decreased anti-oxidative defense contributes to neuronal cell death and thus to the pathogenesis of Machado Joseph Disease.

8 Zusammenfassung

Ataxin-3 (ATXN3), das Protein, welches für die Entstehung der Machado Joseph Krankheit verantwortlich ist, ist funktionell an der zellulären Qualitätskontrolle von Proteinen und der transkriptionellen Regulation von verschiedenen Genen beteiligt. Bisherige Studien unterstützen die Annahme, dass eine Änderung in der Konformation des Proteins und/oder der Verlust von nicht-expandiertem ATXN3 durch die Rekrutierung in nucleäre Inklusionen zu einer Dysregulierung von diversen zellulären Prozessen so wie der Ubiquitinierung oder der transkriptionellen Regulation führen.

In der vorliegenden Arbeit wurden induzierte pluripotente Stammzellen (iPS-Zellen) verwendet, um den Einfluss von expandiertem ATXN3 oder einem KO von ATXN3 auf die Genexpression innerhalb patientenspezifischer Neurone zu entschlüsseln. Dafür wurden, unter Verwendung einer CRISPR/Cas9-vermittelten Geneditierung, isogene iPS-abgeleitete Stammzellen generiert, welche entweder das normale (ATXN3_non-exp), das expandierte (ATXN3_exp) oder einen KO von ATXN3 (ATXN3_KO) ausbilden. Die resultierenden isogenen Zelllinien erlauben einen direkten Vergleich der Genexpression zwischen Zellen, welche entweder die expandierte/KO oder normale Form von ATXN3 exprimieren. Durch Genexpressionsanalysen der durch diese Zelllinien abgeleiteten Neurone konnten einige Gene identifiziert werden, welche in ATXN3_exp- und ATXN3_KO-Neuronen dysreguliert waren. Unter diesen befand sich eine Gruppe von Metallothioneinen, welche im Vergleich zu ATXN3_nicht-expandierten Neuronen in ATXN3_expandierten und ATXN3_KO signifikant runterreguliert waren.

Physiologisch gesehen sind Metallothioneine wichtige Regulatoren der Zellhomöostase und der zellulären Antwort auf oxidativen, excitotoxischen und Metallstress. Dementsprechend ergaben Ergebnisse dieser Arbeit eine erhöhte Anfälligkeit auf Stress in Neuronen, die entweder den KO von ATXN3 oder die expandierte Form ausbildeten. Außerdem wurde in diesen Zellen ebenfalls erhöhte Level an reaktiven Sauerstoffspezies and Superoxiden gefunden.

Ein möglicher Mechanismus dafür könnte eine posttranslationale Interaktion zwischen ATXN3 und dem Transkriptionsfaktor MTF-1 sein, wobei die deubiquitinierende Funktion von ATXN3 eine wichtige Rolle spielen könnte. Vorläufige Ergebnisse dieser Arbeit zeigen eine erhöhte MTF-1-Proteinstabilität in Neuronen mit dem nicht-expandiertem ATXN3 im Vergleich zu den anderen Zelllinien, was diese Hypothese unterstützt. Für eine genauere Untersuchung dieses Mechanismus müssen weitere Experimente vorgenommen werden. Dennoch wurde im Rahmen dieser Arbeit ein genetisch editiertes Zellmodell geschaffen, welches einen Zusammenhang zwischen der Genexpression von ATXN3 und der Expression von Metallothioneinen darstellt. Außerdem unterstützen die Ergebnisse dieser

Arbeit die Involvierung von ATXN3 in der Regulierung von zellulärem Stress und dass eine erhöhte Stressanfälligkeit der Zelle und einer damit einhergehenden Verringerung der antioxidativen Abwehr zu Zelltod und folglich zu der Pathogenese von Machado Joseph Krankheit beitragen kann.

9 References

Abel, J. and de Ruiter, N. (1989). Inhibition of hydroxyl-radical-generated DNA degradation by metallothionein. Toxicology Letters *47*, 191–196.

Adamsa, S. V., Barrickb, B., Freneya, E. P., Shaferc, M. M., Makard, K., Songd, X., Lampea, J., Vilchise, H., Uleryb, A., and Newcomb, P. A. (2015). Genetic variation in metallothionein and metal-regulatory transcription factor 1 in relation to urinary cadmium, copper, and zinc. Toxicology and Applied Pharmacology *289*, 381–388.

Albrecht, M., Golatta, M., Ullrich Wullner, U., and Lengauer, T. (2004). Structural and functional analysis of ataxin-2 and ataxin-3. European Journal of Biochemistry *271*, 3155-3170.

Ambjorn, M., Asmussen, J.W., Lindstam, M., Gotfryd, K., Jacobsen, C., Kiselyov, V.V., Moestrup, S.K., Penkowa, M., Bock, E., Berezin, V. (2008). Metallothionein and a peptide modeled after metallothionein, EmtinB, induce neuronal differentiation and survival through binding to receptors of the low-density lipoprotein receptor family. Journal of Neurochemistry *104*, 21-37.

Amerik, A.Y., and Hochstrasser, M. (2004). Mechanism and function of deubiquitinating enzymes. Biochimica et Biohysica Acta *29*, 189-207.

Andrews, G. K. (2000). Regulation of metallothionein gene expression by oxidative stress and metal ions. Biochemical Pharmacology *59*, 95–104.

Anokye-Danso, F., Trivedi, C., Juhr, D., Gupta, M., Cui, Z., Tian, Y., Zhang, Y., Yang, W., Gruber, P., Epstein, J.*, et al.* (2011). Highly Efficient miRNA-Mediated Reprogramming of Mouse and Human Somatic Cells to Pluripotency. Cell stem cell *8*, 376-388.

Antony, P.M., Mantele, S., Mollenkopf, P., Boy, J., Kehlenbach, R.H., Riess, O., and Schmidt, T. (2009). Identification and functional dissection of localization signals within ataxin-3. Neurobiology of Disease *36*, 280–292.

Araujo, J., Breuer, P., Dieringer, S., Krauss, S., Dorn, S., Zimmermann, K., Pfeifer, A., Klockgether, T., Wuellner, U., and Evert, B.O. (2011). FOXO4- dependent upregulation of superoxide dismutase-2 in response to oxidative stress is impaired in spinocerebellar ataxia type 3. Human Molecular Genetics *20*, 2928–2941.

Asmussen, J. W., Sperling, M. L. V., and Penkowa M., (2009). Intraneuronal signaling pathways of metallothionein. Journal of Neuroscience Research *87*, 2926–2293.

de Assis, A.M., Saute, J.A.M., Longoni, A., Haas, C.B., Torrez, V.R., Brochier, A.W., Souza, G.N., Furtado, G.V., Gheno, T.C., Russo, A., et al. (2017). Peripheral Oxidative Stress Biomarkers in Spinocerebellar Ataxia Type 3/Machado-Joseph Disease. Frontiers in Neurology *8*, 485.

Babu, M.M., Luscombe, N.M., Aravind, L. Gerstein, M. and Teichmann, S.A. (2004). Structure and evolution of transcriptional regulatory networks. Current Opinion in Structural Biology *14* (3), 283-291.

Babula, P., Masarik, M., Adam, V., Eckschlager, T., Stiborova, M., Trnkova, L., Skutkova, H., Provaznik, I., Hubalekadi J., and Kizek R. (2012). Mammalian metallothioneins: properties and functions. Metallomics *4,* 739–750.

Baddour, J.A., Sousounis, K., and Tsonis, P.A. (2012). Organ repair and regeneration: an overview. Birth defects research Part C, Embryo today: Reviews *96*, 1-29.

Banerjee, D., Onosaka, S. and Cherian, M.G. (1982). Immunohistochemical localization of metallothionein in cell nucleus and cytoplasm of rat liver and kidney. Toxicology *24(2), 95-105.*

Barrangou, R. Fremaux, C., Deveau, H., Richards, M., Boyaval, P., Moineau, S., Romero, D.A., and Horvath, P. (2007). CRISPR provides acquired resistance against viruses in prokaryotes. Science *315*, 1709–1712.

Berke, S.J., Schmied, F.A., Brunt, E.R., Ellerby, L.M., and Paulson, H.L. (2004). Caspase-mediated proteolysis of the polyglutamine disease protein ataxin-3. Journal of Neurochemistry *89*, 908–918.

Berke, S.J., Chai, Y., Marrs, G.L., Wen, H., and Paulson, H.L. (2005). Defining the role of ubiquitin-interacting motifs in the polyglutamine disease protein, ataxin-3. Journal of Biological Chemistry *280*, 32026–32034.

Besenbacher, S., Liu, S., Izarzugaza, J. M. G., Grove, J., Belling, K., Bork-Jensen, J., Huang, S., Als, T.D., Li, S., Yadav, R. et al. (2015). Novel variation and *de novo* mutation rates in population-wide *de novo* assembled Danish trios. Nature Communications *6*, 5969.

Bettencourt, C., Santos, C., Montiel, R., Costa, M. do Carmo , Cruz-Morales, P., Santos, L.R., Simões, N., Kay, T., Vasconcelos, J., Maciel, P., and Lima, M. (2010). Increased transcript diversity: novel splicing variants of Machado-Joseph disease gene (ATXN3). Neurogenetics *11*, 193-202.

Bibikova, M., Carroll, D., Segal, D.J., Trautman, J.K., Smith, J., Kim, Y.G., and
Chandrasegaran, S. (2001). Stimulation of homologous recombination through targeted cleavage by chimeric nucleases. Molecular Cell Biology *21*, 289-297.

Bibikova, M., Beumer, K., Trautman, J. K., and Carroll, D. (2003). Enhancing gene targeting with designed zinc finger nucleases. Science *300*, 764.

Bichelmeier, U., Schmidt, T., Hubener, J., Boy, J., Ruttiger, L., Habig, K., Poths, S., Bonin, M., Knipper, M., Schmidt, W.J., et al., (2007). Nuclear localization of ataxin-3 is required for the manifestation of symptoms in SCA3: in vivo evidence. Journal of Neuroscience *27*, 7418–7428.

Boch, J., Scholze, H., Schornack, S., Landgraf, A., Hahn, S., Kay, S., Lahaye, T., Nickstadt, A., and Bonas, U. (2009). Breaking the code of DNA binding specificity of TAL-type III effectors. Science *326*, 1509–1512.

Boedderich, A., Gaumer, S., Haacke, A., Tzvetkov, N., Albrecht, M., Evert, B.O., Müller, E.C., Lurz, R., Breuer, P., Schugardt, N. et al. (2006). An arginine/lysine-rich mofit is crucial for VCP/p97-mediated modulation of ataxin-3 fibrillogenesis. The EMBO Journal *25*, 1547-1558.

Boehnke, K., Falkowska-Hansen, B., Stark, H.J., and Boukamp, P. (2012). Stem cells of the human epidermis and their niche: composition and function in epidermal regeneration and carcinogenesis. Carcinogenesis *33*, 1247-1258.

Bolotin, A., Quinquis, B., Sorokin, A., and Ehrlich, S.D. (2005). Clustered regularly interspaced short palindrome repeats (CRISPRs) have spacers of extrachromosomal origin. Microbiology *151*, 2551–2561.

Bonaventura, P., Benedetti, G., Albarede, F., Miossec, P. (2015). Zinc and its role in immunity and inflammation. Autoimmunity Reviews *14*, 277-285.

Bongso, A., Fong, C.Y., Ng, S.C., and Ratnam, S. (1994). Isolation and culture of inner cell mass cells from human blastocysts. Human reproduction (Oxford, England) *9*, 2110-2117.

Bousleiman, J., Pinsky, A., Ki, S., Su, A., Morozova, I., Kalachikov, S., Wiqas, A., Silver, R., Sever, M. and Austin, R. N. (2017). Function of Metallothionein-3 in Neuronal Cells: Do Metal Ions Alter Expression Levels of MT3? International Journal of Molecular Sciences, 18(6), 1133.

Brayer, K.J., Kulshreshtha, S., and Segal, D.J. (2008). The protein-binding potential of C2H2 zinc finger domains. Cell Biochemistry and Biophysics *51*, 9-19.

Bremner, I. and Beattie, I.H. (1990). Metallothionein and the trace metals. Annual Review of Nutrition *10*, 63,83.

Breuer, P., Haacke, A., Evert, B.O., and Wullner, U., 2010. Nuclear aggregation of polyglutamine-expanded ataxin-3: fragments escape the cytoplasmic quality control. Journal of Biological Chemistry *285*, 6532–6537.

Breunig, J.J., Haydar, T.F. and Rakic, P. (2011). Neural stem cells: historical perspective and future prospects. Neuron *70***,** 614-625.

Burnett, B., Li, F., and Pittman, R.N. (2003). The polyglutamine neurodegenerative protein ataxin-3 binds polyubiquitylated proteins and has ubiquitin protease activity. Human Molecular Genetics *12*, 3195-3205.

Burnett, B., Li, F., and Pittman, R.N. (2005). The polyglutamine neurodegenerative protein ataxin-3 binds polyubiquitylated proteins and has ubiquitin protease activity. Human Molecular Genetics *12*, 3195–3205.

Cai, L., Klein, J.B., and Kang, Y.J. (2000). Metallothionein inhibits peroxynitrite-induced DNA and lipoprotein damage. Journal of Biological Chemistry *275*, 38957–38960.

Cai, L. and Cherian, M. G. (2003). Zinc-metallothionein protects from DNA damage induced by radiation better than glutathione and copperor cadmium-metallothioneins. Toxicology Letters *136*, 193–198.

Cancel, G., Abbas, N., Stevanin, G., Durr, A., Chneiweiss, H., Neri, C., Duyckaerts, C., Penet, C., Cann, H.M., Agid, Y., and Brice, A. (1995). Marked phenotypic heterogeneity associated with expansion of a CAG repeat sequence at the spinocerebellar ataxia 3/Machado-Joseph disease locus. American Journal of Human Genetics *57*, 809–816.

do Carmo Costa, M., Bajanca, F., Rodrigues, A.J., Tome, R.J., Corthals, G., Macedo- Ribeiro, S., Paulson, H.L., Logarinho, E., and Maciel, P. (2010). Ataxin-3 plays a role in mouse myogenic differentiation through regulation of integrin subunit levels. PLoS One *5*, e11728.

Carrasco, J., Adlard, P., Cotman C., Quintana, A., Penkowa, M., Xu, F., van Nostrand, W.E. and Hidalgo, J. (2006). Metallothionein-I and -III expression in animal models of Alzheimer disease. Neuroscience, *143 (4)*, 911–922.

Carvalho, D.R., La Rocque-Ferreira, A., Rizzo, I.M., Imamura, E.U., and Speck-Martins, C.E. (2008). Homozygosity enhances severity in spinocerebellar ataxia type 3. Pediatric Neurology *38*, 296-299.

Chai, Y., Wu, L., Griffin, J.D., and Paulson, H.L. (2001). The role of protein composition in specifying nuclear inclusion formation in polyglutamine disease. Journal of Biological Chemistry *276*, 44889-44897.

Chai, Y., Shao, J., Miller, V.M., Williams, A., and Paulson, H.L. (2002). Livecell imaging reveals divergent intracellular dynamics of polyglutamine disease proteins and supports a sequestration model of pathogenesis. Proceedings of the National Academy of Sciences of the USA *99*, 9310–9315.

Chambers, S., Fasano, C., Papapetrou, E., Tomishima, M., Sadelain, M. and Studer, L. (2009). Highly efficient neural conversion of human ES and iPS cells by dual inhibition of SMAD signaling. Nature Biotechnology *27***,** 275-280.

Choulika, A., Perrin, A., Dujon, B., & Nicolas, J. F. (1995). Induction of homologous recombination in mammalian chromosomes by using the I-SceI system of Saccharomyces cerevisiae. Molecular and Cellular Biology *15*, 1968–1973.

Chow, M.K., Mackay, J.P., Whisstock, J.C., Scanlon, M.J. and Bottomley, S.P. (2004). Structural and functional analysis of the Josephine domain of the polyglutamine protein ataxin-3. Biophysical and biochemical research communications *322*, 387-394.

Christian, M., Cermak, T., Doyle, E.L., Schmidt, C., Zhang, F., Hummel, A., Bogdanove, A. J. and Voytas, D.F. (2010). Targeting DNA double-strand breaks with TAL effector nucleases. Genetics *186*, 757–761.

Chung, R.S., Fung, S.J., Leung, Y.K., Walker, A.K., McCormack, G.H., Chuah, M.I., Vickers, J.C., and West, A.K. (2007). Metallothionein expression by NG2 glial cells following CNS injury. Cellular and Molecular Life Sciences. *64*: 2716-2722.

Clements, W.K., and Traver, D. (2013). Signalling pathways that control vertebrate haematopoietic stem cell specification. Nature reviews Immunology *13*, 336-348.

Colman A & Dreesen O. (2009). Pluripotent Stem Cells and Disease Modeling. Stem Cell *5***,** 244-247.

Conti, L., and Cattaneo, E. (2010). Neural stem cell systems: physiological players or in vitro entities? Nature Review Neuroscience *11*, 176–187.

Cousins, R.J., Liuzzi, J.P., and Lichten, L.A. (2006). Mammalian zinc transport, trafficking, and signals. Journal of Biological Chemistry *281*, 24085-24089.

Cunha-Santos, J., Duarte-Neves, J., Carmona, V., Guarente, L., Pereira de Almeida, L., and Cavadas, C. (2016). Caloric restriction blocks neuropathology and motor deficits in Machado–Joseph disease mouse models through SIRT1 pathway. Nature Communications 7, 11445.

Dalton, T. P., Qingwen, L., Bittel, D., Liang, L. and Andrews, G. K. (1996). Oxidative stress activates metal-responsive transcription factor-1 binding activity. Occupancy in vivo of metal response elements in the metallothionein-I gene promoter. The Journal of Biological Chemistry *271 (42)*, 26233–26241.

Deibel, M.A., Ehmann, W.D. and Markesbery, W.R. (1996). Copper, iron, and zinc imbalances in severely degenerated brain regions in Alzheimer's disease: possible relation to oxidative stress. Journal of the Neurological Science *143 (1-2)*, 137–142.

Donaldson, K.M., Li, W., Ching, K.A., Batalov, S., Tsai, C.C., and Joazeiro, C.A. (2003). Ubiquitinmediated sequestration of normal cellular proteins into polyglutamine aggregates. Proceedings of the National Academy of Sciences of the USA *100*, 8892-8897.

Doss-Pepe, E.W., Stenroos, E.S., Johnson, W.G., and Madura, K. (2003). Ataxin-3 interactions with rad23 and valosin-containing protein and its associations with ubiquitin chains and the proteasome are consistent with a role in ubiquitinmediated proteolysis. Molecular and Cellular Biology *23*, 6469–6483.

Doudna, J.A., and Charpentier, E. (2014). The new frontier of genome engineering with CRISPR-Cas9. Science *346*, 1258096.

Durr, A., Stevanin, G., Cancel, G., Duyckaerts, C., Abbas, N., Didierjean, O., Chneiweiss, H., Benomar, A., Lyon-Caen, O., Julien, J., et al. (1996). Spinocerebellar ataxia 3 and Machado-Joseph disease: clinical, molecular and neuropathological features. Annals of Neurology *4,* 490-499.

Dziegiel, P., Pula, B., Kobierzycki, C., Stasiolek, M., Podhorska-Okolow, M. (2016). Metallothioneins in Normal and Cancer Cells. Advances in
Anatomy, Embryology and Cell Biology *218*, 1:117.

Elkabetz, Y., Panagiotakos, G., Shamy Al, G., Socci, N.D., Tabar, V., and Studer, L. (2008). Human ES cell-derived neural rosettes reveal a functionally distinct early neural stem cell stage. Genes and Development *22*, 152–165.

Eriksson, P.S., Perfilieva, E., Björk-Eriksson, T., Alborn, A.M., Nordborg, C., Peterson, D.A. and Gage, F.H. (1998). Neurogenesis in the adult human hippocampus. Nature Methods *4***,** 1313-1317.

Evert, B.O., Wullner, U., Schulz, J.B., Weller, M., Groscurth, P., Trottier, Y., Brice, A., and Klockgether, T. (1999). High level expression of expanded full-length ataxin-3 in vitro causes cell death and formation of intranuclear inclusions in neuronal cells. Human Molecular Genetics *8*, 1169–1176.

Evert, B.O., Vogt, I.R., Vieira,_saecker, A.M., Ozimek, L., de Vos, R.A., Brunt, E.R., Klockgether, T., and Wüllner, U. (2003). Gene expression profiling in ataxin-3 expressing cell lines reveals distinct effects of normL nd mutant ataxin-3. Journal of Neuropathology and Experimental Neuroloy *62,* 1006-1018.

Evert, B.O., Araujo, J., Vieira-Saecker, A. M., de Vos, R. A. I., Harendza, S., Klockgether, T. and Wullner, U. (2006). Ataxin-3 Represses Transcription via Chromatin Binding, Interaction with Histone Deacetylase 3, and Histone Deacetylation. Journal of Neuroscience *26 (44)*, 11474-11486.

Falk, A., Koch, P., Kesavan, J., Takashima, Y., Ladewig, J., Alexander, M., Wiskow, O., Tailor, J., Trotter, M., Pollard, S.*, et al.* (2012). Capture of Neuroepithelial-Like Stem Cells from Pluripotent Stem Cells Provides a Versatile System for In Vitro Production of Human Neurons. PloS one *7*, e29597.

Fei, E., Jia, N., Zhang, T., Ma, X., Wang, H., Liu, C., Zhang, W., Ding, L., Nukina, N., and Wang, G. (2007). Phosphorylation of ataxin-3 by glycogen synthase kinase 3beta at serine 256 regulates the aggregation of ataxin-3. Biochemical and Biophysical Research Communications *357*, 487–492.

Formigari, A., Irato, P., and Santon, A. (2007). Zinc, antioxidant systems and metallothionein in metal mediated-apoptosis: biochemical and cytochemical aspects. Comparative Biochemistry and Physiology C. Toxicology and Pharmacology *146*, 443–459.

Friedman, J.H. (2002). Presumed rapid eye movement behavior disorder in Machado-Joseph disease (spinocerebellar ataxia type 3). Movement Disorders *17*, 1350–1353.

Fujie, T., Murakami, M., Yoshida, E., Yasuike, S., Kimura, T. , Fujiwara, Y., Yamamoto, C. and Kaji, T. (2016). Transcriptional Induction of Metallothionein by Tris(pentafluorophenyl)stibane in Cultured Bovine Aortic Endothelial Cells. International Journal of neuronal Sciences *17* (9), 1381.

Fusaki, N., Ban, H., Nishiyama, A., Saeki, K., and Hasegawa, M. (2009). Efficient induction of transgene-free human pluripotent stem cells using a vector based on Sendai virus, an RNA virus that does not integrate into the host genome. Proceedings of the Japan Academy Series B, Physical and biological sciences *85*, 348-362.

Futakawa, N., Kondoh, M., Ueda, S., Higashimoto, M., Takiguchi, M., Suzuki, S., and Sato, M. (2006). Involvement of oxidative stress in the synthesis of metallothionein induced by mitochondrial inhibitors. Biological and Pharmaceutical Bulletin *29*, 2016–2020.

Gage F. (2000). Mammalian Neural Stem Cells. *Science* **287,** 1433-1438.

Gatchel, J.R., and Zoghbi, H.Y. (2005). Diseases of unstable repeat expansion: mechanisms and common principles. Nature Reviews Genetics *6* (10), 743-755.

Ghoshal, K., Majumder, S., Li, Z., Bray, T. M. and Jacob, S. T. (1999). Transcriptional induction of metallothionein-I and -II genes in the livers of Cu,Zn-superoxide dismutase knockout mice. Biochemical and Biophysical Research Communications *264*, 735–742.

Gore, A., Li, Z., Fung, H.L., Young, J.E., Agarwal, S., Antosiewicz-Bourget, J., Canto, I., Giorgetti, A., Israel, M.A., Kiskinis, E.*, et al.* (2011). Somatic coding mutations in human induced pluripotent stem cells. Nature *471*, 63-67.

Goto, J., Watanabe, M., Ichikawa, Y., Yee, S.B., Ihara, N., Endo, K., Igarashi, S., Takiyama, Y., Gaspar, C., Maciel, P. et al. (1997). Machado-Joseph disease gene products carrying different carboxyl termini. Neuroscience Research *28*, 373-7.

Grzywacz, A., Gdula-Argasińska, J., Muszyńska, B., Tyszka-Czochara, M., Librowski, T., and Opoka W. (2015). Metal responsive transcription factor 1 (MTF-1) regulates zinc dependent cellular processes at the molecular level. Acta biochimica polonica *62*, 491–498.

Guarente, L. (2008). Mitochondria- A nexus for aging, calorie restriction and sirtuins? Cell *132* (2), 171-176.

Gunawardena, S., Her, L.S., Brusch, R.G., Laymon, R.A., Niesman, I.R., Gordesky-Gold, B., Sintasath, L., Bonini, N., and Goldstein, L.S.B. (2003). Disruption of axonal transport by loss of huntingtin or expression of pathogenic polyQ proteins in Drosophila. Neuron *40*, 25-40.

Gu, W., Ma, H., Wang, K., Jin, M., Zhou, Y., Liu, X., Wang, G., and Shen, Y. (2004). The shortest expanded allele of the MJD1 gene in a Chinese MJD kindred with autonomic dysfunction. European Neurology *52*, 107–11.

Gunawardena, S., Her, L.S., Brusch, R.G., Laymon, R.A., Niesman, I.R., Gordesky-Gold, B., Sintasath, L., Bonini, N.M., and Goldstein, L.S. (2003). Disruption of axonal transport by loss of huntingtin or expression of pathogenic polyQ proteins in Drosophila. Neuron *40*, 25–40.

Günes, C., Heuchel, R., Georgiev, O., Müller, K.H., Lichtlen, P., Blüthmann, H., Marino, S., Aquzzi, A., and Schaffner, W. (1998). Embryonic lethality and liver degeneration in mice lacking the metal-responsive transcriptional activator MTF-1. EMBO Journal *17*, 2846-2854.

Haacke, A., Broadley, S.A., Boteva, R., Tzvetkov, N., Hartl, F.U., and Breuer, P. (2006). Proteolytic cleavage of polyglutamine-expanded ataxin-3 is critical for aggregation and sequestration of non-expanded ataxin-3. Human Molecular Genetics *15*, 555–568.

Haberhausen, G., Damian, M.S., Leweke, F., and Müller, U. (1995). Spinocerebellar ataxia, type 3 (SCA3) is genetically identical to Machado-Joseph disease (MJD). Journal of the Neurological Science *132*, 71-75.

Haidara, K., Moffatt, P., and Denizeau, F. (1999) Metallothionein induction attenuates the effects of glutathione depletors in rat hepatocytes. Toxicological Sciences. *49*, 297–305.

Halliwell, B. (2006). Oxidative stress and neurodegeneration: where are we now? Journal of neurochemistry *97* (6), 1634-1658.

Han, S.S., Williams, L.A. and Eggan, K.C. (2011). Constructing and deconstructing stem cell models of neurological disease. Neuron *70***,** 626-644.

Hands, S.L., Mason, R., Sajjad, M.U., Giorgini, F., and Wyttenbach, A. (2010). Metallothioneins and copper metabolism are candidate therapeutic targets in Huntington's
Disease. Biochemical Society Transactions *38*, 552-558.

Harris, G.M., Dodelzon, K., Gong, L., Gonzalez-Alegre, P., and Paulson, H.L. (2010). Splice isoforms of the polyglutamine disease protein ataxin- 3 exhibit similar enzymatic yet different aggregation properties. PLoS One *5*, e13695.

Heuchel, R., Radtke, F., Georgiev, O., Stark, G., Aguet, M., and Schaffner, W. (1994). The transcription factor MTF-1 is essential for basal and heavy metal-induced metallothionein gene expression. EMBO Journal *13*, 2870-2875.

Hidalgo, J., Aschner, M., Zatta, P., and Vasak, M. (2001). Roles of the metallothionein family of proteins in the central nervous system. Brain Research Bulletin *55*, 133–145.

Hirabayashi, M., Inoue, K., Tanaka, K., Nakadate, K., Ohsawa, Y., Kamei, Y., Popiel, A.H., Sinohara, A., Iwamatsu, A., and Kimura, Y. et al. (2001). VCP/ p97 in abnormal protein aggregates, cytoplasmic vacuoles, and cell death, phenotypes relevant to neurodegeneration. Cell Death and Differentiation *8*, 977–984.

Hofmann, K., and Falquet, L. (2001). A ubiquitin-interacting motif conserved in components of the proteasomal and lysosomal protein degradation systems. Trends in Biochemical Sciences *26*, 347–350.

Hsu, P. D., Lander, E. S., and Zhang, F. (2014). Development and Applications of CRISPR-Cas9 for Genome Engineering. Cell *157*, 1262–1278.

Hussein, S.M., Batada, N.N., Vuoristo, S., Ching, R.W., Autio, R., Närvä, E., Ng, S., Sourour, M., Hämäläinen, R., Olsson, C.*, et al.* (2011). Copy number variation and selection during reprogramming to pluripotency. Nature *471*, 58-62.

Ikeda, H., Yamaguchi, M., Sugai, S., Aze, Y., Narumiya, S., Kakizuka, A. (1996). Expanded polyglutamine in the Machado–Joseph disease protein induces cell death in vitro and in vivo. Nature Genetics *13*, 196–202.

Ilic, D., and Ogilvie, C. (2017). Concise Review: Human Embryonic Stem Cells-What Have We Done? What Are We Doing? Where Are We Going? Stem Cells *35*, 17-25.

Ichikawa, Y., Goto, J., Hattori, M., Toyoda, A., Ishii, K., Jeong, S.-Y., Hashida, H., Masuda, N., Ogata, K., and Kanazawa, I. (2001). The genomic structure and expression of *MJD*, the Machado-Joseph disease gene. Journal of Human Genetics volume *46*, 413–422.

Isani, G., & Carpenè, E. (2014). Metallothioneins, Unconventional Proteins from Unconventional Animals: A Long Journey from Nematodes to Mammals. Biomolecules, *4*(2), 435–457.

Ishino, Y., Shinagawa, H., Makino, K., Amemura, M., and Nakata, A. (1987). Nucleotide sequence of the iap gene, responsible for alkaline phosphatase isozyme conversion in Escherichia coli, and identification of the gene product. J. Bacteriol. *169*, 5429–5433.

Jinek, M., Chylinski, K., Fonfara, I., Hauer, M., Doudna, J.A., and Charpentier, E. (2012). A programmable dual-RNA-guided DNA endonuclease in adaptive bacterial immunity. Science, *337*, 816-821.

Juárez-Rebollar, D., Manjarrez, J., Nava-Ruíz, C., Zaga-Clavellina, V., Flores-Espinosa, P., Heras-Romero, Y., Díaz-Ruíz, A. and Méndez-Armenta, M. (2015). Metallothionein expression in the rat brain following KA and PTZ treatment. Environmental Toxicology and Pharmacology *40 (2)*, 530–53.

Juárez-Rebollar, D., Rios, C., Nava-Ruíz, C., and Méndez-Armenta, M. (2017). Metallothionein in Brain Disorders. Oxidative Medicine and Cellular Longevity 2017, 5828056.

Kang, Y.J. (2006). Metallothionein redox cycle and function. Experimental Biology and Medicine *231*, 1459-67.

Karus, M., Blaess, S., and Brüstle, O. (2014). Self-organisation of neural tissue architectures from pluripotent stem cells. Journal of Comparative Neurology *522*, 2831-2844.

Kawaguchi, Y., Okamoto, T., Taniwaki, M., Aizawa, M., Inoue, M., Katayama, S., Kawakami, H., Nakamura, S., Nishimura, M., Akiguchi, I. (1994). CAG expansions in a novel gene for Machado-Joseph disease at chromosome 14q32.1. Nature Genetics *8*, 221 – 228.

Kelly, E. J. and Palmiter, R. D. (1996). A murine model of Menkes disease reveals a physiological function of metallothionein. Nature Genetics *13*, 219–222.

Kelly, E. J., Quaife, C. J., Froelick, G. J., and Palmiter, R. D. (1996). Metallothionein I and II protect against zinc deficiency and zinc toxicity in mice. Journal of Nutrition *126*, 1782–1790.
Kim, Y.-G., Cha, J., and Chandrasegaran, S. (1996). Hybrid restriction enzymes: zinc finger fusions to Fok I cleavage domain. Proceedings of the National Academy of Sciences of the USA *93*, 1156–1160.

Kim, D., Kim, E. H., Kim C. H., Sun, W., Kim, H.J., Uhm, C.-S., Park, S.-H. and Kim, H. (2003). Differential regulation of metallothionein-I, II, and III mRNA expression in the rat brain following kainic acid treatment. Neuroreport *14 (5)*, 679–682

Kim, H.S., Oh, S.K., Park, Y.B., Ahn, H.J., Sung, K.C., Kang, M.J., Lee, L.A., Suh, C.S., Kim, S.H., Kim, D.W., and Moon, S.Y. (2005). Methods for derivation of human embryonic stem cells. Stem Cells *23***,** 1228-1233.

Kim, H., Lee, G., Ganat, Y., Papapetrou, E., Lipchina, I., Socci, N., Sadelain, M., and Studer, L. (2011). miR-371-3 Expression predicts neural differentiation propensity in human pluripotent stem cells. Stem Cell *8*, 695-706.

Kim, J. H., Nam, Y. P., Jeon, S. M., Han, H. S. and Suk, K. (2012) Amyloid neurotoxicity is attenuated by metallothionein: dual mechanisms at work. Journal of Neurochemistry *121 (5)*, 751–762.

Kim, D., Bae, S., Park, J., Kim, E., Kim, S., Yu, H.R., Hwang, J., Kim, J.I., and Kim, J.S. (2015). Digenome-seq: genome-wide profiling of CRISPR-Cas9 off-target effects in human cells. Nature Methods *12* (3), 237-243.

Klockgether, T., Ludtke, R., Kramer, B., Abela, M., Burk, K., Schols, L., Riess, O., Laccone, F., Boesch, S., Lopes-Cendes, I., Brice, A., Inzelberg, R., Zilber, N., and Dichgans, J. (1998). The natural history of degenerative ataxia: a retrospective study in 466 patients. Brain *121*, 589–600.

Koch, P., Opitz, T., Steinbeck, J.A., Ladewig, J., and Brüstle, O. (2009). A rosette-type, self-renewing human ES cell-derived neural stem cell with potential for in vitro instruction and synaptic integration. Proceedings of the National Academy of Sciences of the United States of America *106*, 3225-3230.

Koch, P., Breuer, P., Peitz, M., Jungverdorben, J., Kesavan, J., Poppe, D., Doerr, J., Ladewig, J., Mertens, J., Tuting, T. et al. (2011). Excitation induced ataxin-3 aggregation in neurons from patients with Machado–Joseph disease. Nature *480*, 543–546.

Koeppen, A.H., Dickson, A.C., Lamarche, J.B., and Robitaille, Y. (1999). Synapses on the hereditary ataxias. Journal of Neuropathology and Experimental Neurology *58*, 748–764.

Kondo, Y., Rusnak, J. M., Hoyt, D. G., Settineri, C. E., Pitt, B. R., and Lazo, J. S. (1997). Enhanced apoptosis in metallothionein null cells. Molecular Pharmacology *52*, 195–201.

Kondoh, M., Inoue, Y., Atagi, S., Futakawa, N., Higashimoto, M., and Sato, M. (2001). Specific induction of metallothionein synthesis by mitochondrial oxidative stress. Life Sciences *69*, 2137–2146.

Kondrashov, A.S. (2002). Direct estimates of human per nucleotide mutation rates at 20 loci causing Mendelian diseases. Human Mutation *21*, 12–27.

Kramer, K.K., Zoelle, J.T., and Klaasen, C.D. (1996). Induction of metallothionein mRNA and protein in primary murine neuron cultures. Toxicology and applied pharmacology *141*, 1-7.

Krezel, A., Hao, Q., and Maret, W. (2007). The zinc/thiolate redox biochemistry of metallothionein and the control of zinc ion fluctuations in cell signaling. Archives of Biochemistry and Biophysics *463*: 188-200.

Kriegstein A & Alvarez-Buylla A. (2009). The glial nature of embryonic and adult neural stem cells. Annual Reviews of Neuroscience *32,* 149-184.

Kuhlbrodt, K., Janiesch, P.C., Kevei, E., Segref, A., Barikbin, R., and Hoppe, T. (2011). The Machado–Joseph disease deubiquitylase ATX-3 couples longevity and proteostasis. Nature Cell Biology *13*, 273–281.

Kuleshov, M.V., Jones, M.R., Rouillard, A.D., Fernandez, N.F., Duan, Q., Wang, Z., Koplev, S., Jenkins, S.L., Jagodnik, K.M., Lachmann, A. et al. (2016). Enrichr: a comprehensive gene set enrichment analysis web server 2016 update. Nucleic Acids Research *44,* W90-W97.

Kumari, M. V., Hiramatsu, M., and Ebadi, M. (1998). Free radical scavenging actions of metallothionein isoforms I and II. Free Radical Research *29*, 93–101.

LaRochelle, O., Gagné, V., Charron, J., Soh, J.W., Séguin, C., and Gagné, V. (2001). Phosphorylation is involved in the activation of metal-regulatory transcription factor 1 in response to metal ions. The Journal of Biological Chemistry *276*, 41879-41888.

Li, F., Macfarlan, T., Pittman, R.N., and Chakravarti, D. (2002). Ataxin-3 is a histone-binding protein with two independent transcriptional corepressor activities. Journal of Biological Chemistry *277*, 45004–45012.

Li X, Du Z, Zarnowska E, Pankratz M, Hansen L, Pearce R & Zhang S. (2005). Specification of motoneurons from human embryonic stem cells. Nature Biotechnology *23***,** 215-221

Li, W., Sun, W., Zhang, Y., Wei, W., Ambasudhan, R., Xia, P., Talantova, M., Lin, T., Kim, J., Wang, X., Kim, W.R., Lipton, S.A., Zhang, K., and Ding, S. (2011). Rapid induction and long-term self-renewal of primitive neural precursors from human embryonic stem cells by small molecule inhibitors. Proceedings of the National Acadamy Sciences USA *108*, 8299–8304.

Lichten, L.A., Ryu, M-S., Guo, L, Embury, J., and Cousins, R.J. (2011). MTF-1-mediated repression of the zinc transporter *Zip10* is alleviated by zinc restriction. PLoS ONE *6* (6), e1526.

Lichtlen, P., and Schaffner W. (2001). Putting its fingers on stressful situations: the heavy metal-regulatory transcription factor MTF1. BioEssays *23*, 1010-1017.

Lister, R., Pelizzola, M., Kida, Y.S., Hawkins, R.D., Nery, J.R., Hon, G., Antosiewicz-Bourget, J., O'malley, R., Castanon, R., Klugman, S*., et al.* (2011). Hotspots of aberrant epigenomic reprogramming in human induced pluripotent stem cells. Nature *471* (7336), 68-73..

Liu, Y., and Ye, Y. (2012). Roles of p97-associated deubiquitinases in protein quality control at the endoplasmic reticulum. Current Protein and Peptide Science *13*, 436–446.

Lovell-Badge R. (2001). The future for stem cell research. Nature *414***,** 88-91.

Macedo-Ribeiro S, Cortes L, Maciel P, Carvalho AL (2009). Nucleocytoplasmic shuttling activity of ataxin-3. PLoS One 4: e5834.

Maciel, P., Gaspar, C., DeStefano, A.L., Silveira, I., Coutinho, P., Radvany, J., Dawson, D.M., Sudarsky, L., Guimarães, J., and Loureiro, J.E. (1995). Correlation between CAG repeat length and clinical features in Machado-Joseph Disease. American Journal of Human Genetics *57,* 54-61.

Makarova, K. S., Grishin, N. V., Shabalina, S. A., Wolf, Y. I., and Koonin, E. V. (2006). A putative RNA-interference-based immune system in prokaryotes: computational analysis of the predicted enzymatic machinery, functional analogies with eukaryotic RNAi, and hypothetical mechanisms of action. Biology Direct, *1*, 7.

Mali, P., Yang, L., Esvelt, K. M., Aach, J., Guell, M., DiCarlo, J. E., Norville, J. E., and Church, G. M. (2013). RNA-Guided Human Genome Engineering via Cas9. Science *339*, 823–826.

Manoharan, S., Guillemin, G. J., Abiramasundari, R. S., Essa, M. M., Akbar, M., & Akbar, M. D. (2016). The Role of Reactive Oxygen Species in the Pathogenesis of Alzheimer's Disease, Parkinson's Disease, and Huntington's Disease: A Mini Review. Oxidative Medicine and Cellular Longevity *2016*, 8590578.

Mao, Y., Senic-Matuglia, F., Di Fiore, P. P., Polo, S., Hodsdon, M. E., & De Camilli, P. (2005). Deubiquitinating function of ataxin-3: Insights from the solution structure of the Josephin domain. Proceedings of the National Academy of Sciences of the United States of America *102*, 12700–12705.

Maret, W. (2008). Metallothionein redox biology in the cytoprotective and cytotoxic functions of zinc. Experimental Gerontology *43*: 363-369.
Margoshes, M., and Vallee, B.L. (1957). A cadmium protein from equine kidney cortex. Journal of the American Chemical Society *79*, 4813–4814.

Marteyn, A., Maury, Y., Gauthier, M., Lecuyer, C., Vernet, R., Denis, J., Pietu, G., Peschanski, M. and Martinat, C. (2011). Mutant Human Embryonic Stem Cells Reveal Neurite and Synapse Formation Defects in Type 1 Myotonic Dystrophy. Stem Cell *8***,** 434-444.

Masino, L., Musi, V., Menon, R.P., Fusi, P., Kelly, G., Frenkiel, T.A., Trottier, Y., and Pastore, A. (2003). Domain architecture of the polyglutamine protein ataxin-3: a globular domain followed by a flexible tail. FEBS Lett *549*, 21-25.

Masino, L., Nicastro, G., Menon, R.P., Dal Piaz, F., Calder, L., and Pastore, A. (2004). Characterization of the structure and the amyloidogenic properties of the Josephin domain of the polyglutamine-containing protein ataxin-3. J Mol Biol *344*, 1021-1035.

Matilla, T., McCall, A., Subramony, S.H., and Zoghbi, H.Y. (1995). Molecular clinical correlations in spinocerebellar ataxia type 3 and Machado-Joseph disease. Annals of Neurology *38*, 68–72.

Matos, C.A., Macedo-Ribeiro, S., Carvalho, A.L. (2011). Polyglutamine diseases: The special case of ataxin-3 and Machado–Joseph disease. Progress in Neurobiology *95* (1), 26-48.

Matsumoto, M., Yada, M., Hatakeyama, S., Ishimoto, H., Tanimura, T., Tsuji, S., Kakizuka, A., Kitagawa, M., and Nakayama, K.I. (2004). Molecular clearance of ataxin-3 is regulated by a mammalian E4. EMBO Journal *23*, 659–669.

Matsumura, R., Takayanagi, T., Fujimoto, Y., Murata, K., Mano, Y., Horikawa, H., and Chuma, T. (1996). The relationship between trinucleotide repeat length and phenotypic variation in Machado-Joseph disease. Journal of the Neurological Sciences *139*, 52–57.

Mazzucchelli, S., De Palma, A., Riva, M., D'Urzo, A., Pozzi, C., Pastori, V., Comelli, F., Fusi, P., Vanoni, M., Tortora, P., Mauri, P., and Regonesi, M.E., (2009). Proteomic and biochemical analyses unveil tight interaction of ataxin-3 with tubulin. International Journal of Biochemical and Cell Biology *41*, 2485–2492.

McCampbell, A., Taylor, J.P., Taye, A.A., Robitschek, J., Li, M., Walcott, J., Merry, D., Chai, Y., Paulson, H., Sobue, G., and Fischbeck, K.H. (2000). CREB-binding protein sequestration by expanded polyglutamine. Human Molecular Genetics *9*, 2197–2202.

Moscou, M. J., and Bogdanove, A. J. (2009). A simple cipher governs DNA recognition by TAL effectors. Science *326*, 1501.

Michalska, A. E. and Choo, K. H. (1993). Targeting and germ-line transmission of a null mutation at the metallothionein I and II loci in mouse. Proceedings of the National Acadamy Sciences USA *90*, 8088-8092.

Miyoshi, N., Ishii, H., Nagano, H., Haraguchi, N., Dewi, D.L., Kano, Y., Nishikawa, S., Tanemura, M., Mimori, K., Tanaka, F.*, et al.* (2011). Reprogramming of Mouse and Human Cells to Pluripotency Using Mature MicroRNAs. Cell stem cell *8*, 633-638.

Mojica, F.J., Díez-Villaseñor, C., Soria, E., and Juez, G. (2000). Biological significance of a family of regularly spaced repeats in the genomes of Archaea, Bacteria and mitochondria. Molecular Microbiology *36*, 244–246.

Mojica, F. J. M., Díez-Villaseñor, C., García-Martínez, J., and Soria, E. (2005). Intervening sequences of regularly spaced prokaryotic repeats derive from foreign genetic elements. Journal of Molecular Evolution *60*, 174–182.

Montoliu, C., Monfort, P., Carrasco, J., Palacios, O., Capdevila, M., Hidalgo, J. and Felipo, V. (2000). Metallothionein-III prevents glutamate and nitric oxide neurotoxicity in primary cultures of cerebellar neurons. Journal of Neurochemistry *75(1)*, 266-273.

Morales, A.I., Vicente-Sanchez, C., Jerkic, M., Santiago, J.M., Sanchez-Gonzalez, P.D., Perez-Barriocanal, F., and Lopez-Novoa, J.M. (2006). Effect of quercetin on metallothionein, nitric oxide synthases and cyclooxygenase-2 expression on experimental chronic cadmium nephrotoxicity in rats. Toxicology and Applied Pharmacology *210*, 128 – 135.

Moscou, M.J., and Bogdanoce, A.J. (2009). A simple cipher governs DNA recognition by TAL effectors. Science *326*, 1501.

Muchowski, P.J., Schaffar, G., Sittler, A., Wanker, E.E., Hayer-Hartl, M.K. and Hartl, F.U. (2000). Hsp70 and Hsp40 chaperones can inhibit self-assembly of polyglutamine proteins into amyloid-like fibrils. PNAS of the United States of America *97* (14), 7841-7846.

Mueller, T., Breuer, P., Schmitt, I., Walter, J., Evert, B.O., and Wullner, U. (2009). CK2-dependent phosphorylation determines cellular localization and stability of ataxin-3. Human Molecular Genetics *18*, 3334–3343.

Nakagawa, M., Koyanagi, M., Tanabe, K., Takahashi, K., Ichisaka, T., Aoi, T., Okita, K., Mochiduki, Y., Takizawa, N. and Yamanaka, S. (2008). Generation of induced pluripotent stem cells without Myc from mouse and human fibroblasts. Nature Biotechnology *26***,** 101-106.

Nakano, K.K., Dawson, D.M., and Spence, A. (1972). Machado disease. A hereditary ataxia in Portuguese emigrants to Massachusetts. Neurology *22*, 49-55.

Nemati, S., Hatami, M., Kiani, S., Hemmesi, K., Gourabi, H., Masoudi, N., Alaie, S. and Baharvand, H. (2010). Long-term Self-Renewable Feeder-Free Human Induced Pluripotent Stem Cell-derived Neural Progenitors. Stem Cells and Development *20* (3), 503-514.

Nicastro G, Masino L, Esposito V, Menon RP, De Simone A, et al. (2009) The josephin domain of ataxin-3 contains two distinct ubiquitin binding motifs. Biopolymer *91*: 1203–1214

Nicastro, G., Todi, S.V., Karaca, E., Bonvin, A.M., Paulson, H.L., and Pastore, A. (2010). Understanding the role of the Josephin domain in the PolyUb binding and cleavage properties of ataxin-3. PLoS ONE *5* (8), e12430.

Nishikawa, M., Mori, H., and Hara, M. (2015). Reduced zinc cytotoxicity following differentiation of neural stem/progenitor cells into neurons and glial cells is associated with upregulation of metallothioneins. Environmental Toxicology and Pharmacology *39*, 1170-1176.

Niwa, H., Burdon, T., Chambers, I. and Smith, A. (1998). Self-renewal of pluripotent embryonic stem cells is mediated via activation of STAT3. Genes & Development *12***,** 2048-2060.

Orr, H.T. (2012). Cell biology of spinocerebellar ataxia. Journal of Cell Biology *197*, 167–177.

Pacheco, L.S., Da Silveira, A.F., Trott, A., Houenou, L.J., Algarve, T.D., Bello C., et al. (2013) Association between Machado-Joseph disease and oxidative stress biomarkers. Mutatation Research *757*, 99–103.

Padiath, Q.S., Srivastava, A.K., Roy, S., Jain, S., and Brahmachari, S.K. (2005). Identification of a novel 45 repeat unstable allele associated with a diseasephenotype at the MJD1/SCA3 locus. American Journal of Medical Genetics B Neuropsychiatric Genetics *133*, 124–6.

Palmiter, R. D., Findley, S. D., Whitmore, T. E., and Durnam, D. M. (1992). MT-III, a brain-specific member of the metallothionein gene family. Proceedings of the National Academy of Sciences of the United States of America, *89*(14), 6333–6337.

Palmiter, R.D. (1994). Regulation of metallothionein genes by heavy metals appears to be mediated by a zinc-sensitive inhibitor that interacts with a constitutively active transcription factor, MTF-1. Proceedings of the National Acadamy Sciences USA *91*, 1219-1223.

Pardo, B., Gomez-Gonzales, B., and Aguilera, A. (2009). DNA repair in mammalian cells: DNA double-strand break repair: how to fix a broken relationship. Cellular and Molecular Life Sciences *66*, 1039–1056.

Paulson, H.L., Das, S.S., Crino, P.B., Perez, M.K., Patel, S.C., Gotsdiner, D., Fischbeck, K.H., and Pittman, R.N. (1997). Machado–Joseph disease gene product is a cytoplasmic protein widely expressed in brain. Annals of Neurology *41*, 453–462.

Paulson, H.L., Perez, M.K., Trottier, Y., Trojanowski, J.Q., Subramony, S.H., Das, S.S., Vig, P., Mandel, J.L., Fischbeck, K.H., and Pittman, R.N. (1997). Intranuclear inclusions of expanded polyglutamine protein in spinocerebellar ataxia type 3. Neuron *19*, 333–344.

Paulson, H.L. (2007). Dominantly inherited ataxias: lessons learned from Machado-Joseph disease/spinocerebellar ataxia type 3. Seminars in Neurology *27*, 133-142.

Paulson, H. (2012). Machado-Joseph disease/spinocerebellar ataxia type 3. Handbook of Clinical Neurology *103*, 437-449.

Pedersen, M.O., Larsen, A., Stoltenberg, M., and Penkowa, M. (2009). Cell death in the injured brain: roles of metallothioneins. Progress in Histochemistry and Cytochemistry *44*, 1-27.

Pedersen, M. Ø., Jensen, R., Pedersen, D. S., Skjolding A.D., Hempel, C., Maretty, L., and Penkowa, M. (2009). Metallothionein-I+II in neuroprotection. BioFactors *35*, 315–325.

Penkowa, M. (2006). Metallothioneins are multipurpose neuroprotectants during brain pathology. The FEBS Journal, *273*, 1857–1870.

Peura, T., Bosman, A., Chami, O., Jansen, R.P., Texlova, K. and Stojanov, T. (2008). Karyotypically normal and abnormal human embryonic stem cell lines derived from PGD-analyzed embryos. Cloning Stem Cells *10***,** 203-216.

Porteus, M. H., and Baltimore, D. (2003). Chimeric nucleases stimulategene targeting in human cells. Science *300*, 763-774.

Pourcel, C., Salvignol, G., and Vergnaud, G. (2005). CRISPR elements in Yersinia pestis acquire new repeats by preferential uptake of bacteriophage DNA, and provide additional tools for evolutionary studies. Microbiology *151*, 653–663.

Pozzi, C., Valtorta, M., Tedeschi, G., Galbusera, E., Pastori, V., Bigi, A., Nonnis, S., Grassi, E., and Fusi, P. (2008). Study of subcellular localization and proteolysis of ataxin-3. Neurobiology of Disease *30*, 190–200.

Radtke, F., Georgiev, O., Müller H.P., Brugnera, E., and Schaffner, W. (1995). Functional domains of the heavy metal-responsive transcription regulator MTF-1. Nucleic Acid Research *23*, 2277-2286.

Radtke, F., Heuchel, R., Georgiev, O., Hergersberg, M., Gariglio, M., Dembic, Z., and Schaffner W. (1993). Cloned transcription factor MTF-1 activates the mouse metallothionein-I promoter. EMBO Journal *12*, 1355-1362.

Radtke, F., and Clevers, H. (2005). Self-renewal and cancer of the gut: two sides of a coin. Science *307*, 1904-1909.

Rakic P. (1988). Specification of cerebral cortical areas. Science *241***,** 170-176.

Ranum, L.P.W., Lundgren, J.K., Schut, L.J., Ahrens, M.J., Perlman, S., Aita, J., Bird, T.D., Gomez, C., and Orr, H.T. (1995). Spinocerebellar ataxia type 1 and Machado-Joseph disease: incidence of CAG expansions among adult-onset ataxia patients from 311 families with dominant, recessive or sporadic ataxia. American Journal of Human Genetics *57*, 603–608.

Rao, M.V., Williams, D.R., Cocklin, S., and Loll, P.J. (2017). Interaction between the AAA+ ATPase p97 and its cofactor ataxin3 in health and disease: Nucleotide-induced conformational changes regulate cofactor binding. Journal of Biological Chemistry *292*, 18392-18407.

Reddy, P.H. and Beal, M.F. (2005). Are mitochondria critical in the pathogenesis of Alzheimer's Disease? Brain Research Reviews *49*. 618-632.

Reina, C.P., Zhong, X., and Pittman, R.N. (2010). Proteotoxic stress increases nuclear localization of ataxin-3. Human Molecular Genetics *19*, 235-49.

Reina, C.P., Nabet, B.Y., Young, P.D., and Pittman, R.N. (2012). Basal and stress-induced Hsp70 are modulated by ataxin-3. Cell Stress and Chaperones *17*, 729-742.

Reinhardt, P., Glatza, M., Hemmer, K., Tsytsyura, Y., Thiel, C. S., Höing, S., Moritz, S., Parga, J. A., Wagner, L. and Sterneckert, J. (2013). Derivation and Expansion Using Only Small Molecules of Human Neural Progenitors for Neurodegenerative Disease Modeling. PLoS ONE, *8*(3), e59252.

Reinhardt, P., Schmid, B., Burbulla, L.F., Schöndorf, D.C., Wagner, L., Glatza, M., Höing, S., Hargus, G., Heck, S.A., Dhingra, A. et al. (2013). Genetic correction of a LRRK2 mutation in human iPSCs links parkinsonian neurodegeneration to ERK-dependent changes in gene expression. Cell Stem Cell *12,* 354-367.

Reyes-Turcu, F.E., Ventii, K.H., Wilkinson, K.D., (2009). Regulation and cellular roles of ubiquitin-specific deubiquitinating enzymes. Annual Review of Biochemistry *78*, 363–397.

Reyes-Turcu, F.E., Wilkinson, K.D., (2009). Polyubiquitin binding and disassembly by deubiquitinating enzymes. Chemical Reviews *109*, 1495–1508.

Reynolds, B.A. and Weiss, S. (1992). Generation of neurons and astrocytes from isolated cells of the adult mammalian central nervous system. Science *255***,** 1707-1710.

Rodda, D.J., Chew, J.L., Lim, L.H., Loh, Y.H., Wang, B., Ng, H.H. and Robson, P. (2005). Transcriptional regulation of nanog by OCT4 and SOX2. Journal of Biological Chemistry *280***,** 24731-24737.

Rodrigues, A., do Carmo Costa, M., Silva, T., Ferreira, D., Bajanca, F., Logarinho, E., and Maciel, P. (2010). Absence of ataxin-3 leads to cytoskeletal disorganization and increased cell death. Biochim Biophys Acta *1803*, 1154-1163.

Rong, Y.S., Golic, K. G. (2000). Gene targeting by homologous recombination in Drosophila. Science *288*, 2013–2018.

Rouet, P., Smih, F., & Jasin, M. (1994). Introduction of double-strand breaks into the genome of mouse cells by expression of a rare-cutting endonuclease. Molecular and Cellular Biology, *14*, 8096–8106.

Rosenberg, R.N. (1992). Machado-Joseph disease: an autosomal dominant motor system degeneration. Movement Disorders *7*, 193-203.

Rub, U., Brunt, E.R., de Vos, R.A., Del Turco, D., Del Tredici, K., Gierga, K., Schultz, C., Ghebremedhin, E., Burk, K., Auburger, G., and Braak, H. (2004). Degeneration of the central vestibular system in spinocerebellar ataxia type 3(SCA3) patients and its possible clinical significance. Neuropathology and Applied Neurobiology *30,* 402–414.

Rub, U., Burk, K., Schols, L., Brunt, E.R., de Vos, R.A., Diaz, G.O., Gierga, K., Ghebremedhin, E., Schultz, C., Del Turco, D., Mittelbronn, M., Auburger, G., Deller, T., and Braak, H. (2004). Damage to the reticulotegmental nucleus of the pons in spinocerebellar ataxiatype 1, 2, and 3. Neurology. *63*, 1258–63.

Rudin, N., Sugarman, E., & Haber, J. E. (1989). Genetic and Physical Analysis of Double-Strand Break Repair and Recombination in *Saccharomyces Cerevisiae*. Genetics, *122*, 519–534.

Rutherford, J.C., and Bird, A.J. (2004). Metal-responsive factors that regulate iron, zinc, and copper homeostasis in eukaryotic cells. Eukaryotic Cell *3*, 1-13.

Ruttkay-Nedecky, B., Nejdl, L., Gumulec, J., Zitka, O., Masarik, M., Eckschlager, T., … Kizek, R. (2013). The Role of Metallothionein in Oxidative Stress. International Journal of Molecular Sciences *14*, 6044–6066.

Sander, J.D., and Joung, J.K. (2014). CRISPR-Cas systems for editing, regulating and targeting genomes. Nature Biotechnology *32*, 347–355.

Santos, C. R., Martinho, A., Quintela, T. and Gonçalves, I. (2012). Neuroprotective and neuroregenerative properties of metallothioneins. IUBMB Life *64 (2)*, 126–135.

Sasaki, H., Wakisaka, A., Fukazawa, T., Iwabuchi, K., Hamada, T., Takada, A., Mukai, E., Matsuura, T., Yoshiki, T., and Tashiro, K. (1995). CAG repeat expansion of Machado-Joseph disease in the Japanese: analysis of the repeat instability for parental transmission, and correlation with disease phenotype. Journal of the Neurological Sciences *133*, 128–133.

Sato, M., and Bremner, I. (1993). Oxygen free-radicals and metallothionein. Free Radical Biology and Medicine , *14*, 325–337.

Sato, M. and Kondoh M. (2002). Recent studies on metallothionein: protection against toxicity of heavy metals and oxygen free radicals. The Tohoku Journal of Experimental Medicine, *196*, 9–22.

Sato, S., Shirakawa, H., Tomita, S., Tohkin, M., Gonzales, F.J. and Komai, M. (2013). The aryl hydrocarbon receptor and glucocorticoid receptor interact to activate human metallothionein 2A. Toxicology and Applied Pharmacology *273* (1), 90-99.

Saydam, N., Steiner, F., Georgiev, O., and Schaffner, W. (2003). Heat and Heavy Metal Stress Synergize to Mediate Transcriptional Hyperactivation by Metal-responsive Transcription Factor MTF-1. The Journal of Biological Chemistry *278*, 31879–31883.

Scaglione, K.M., Zavodszky, E., Todi, S.V., Patury, S., Xu, P., Rodriguez- Lebron, E., Fischer, S., Konen, J., Djarmati, A., Peng, J. et al. (2011). Ube2w and ataxin-3 coordinately regulate the ubiquitin ligase CHIP. Molecular Cell *43*, 599–612.

Schaefer, K. A., Wu, W.-H., Colgan, D.F. Tsang, S. H., Bassuk A. G. and Mahajan, V. B. (2017). Unexpected mutations after CRISPR–Cas9 editing *in vivo.* Nature Methods *14* (6), 547-548.

Scheel, H., Tomiuk, S., and Hofmann, K. (2003). Elucidation of ataxin-3 and ataxin-7 function by integrative bioinformatics. Human Molecular Genetics *12*, 2845-52.

Scherer, S., and Davis, R. W. (1979). Replacement of chromosome segments with altered DNA sequences constructed in vitro. Proceedings of the National Academy of Sciences of the United States of America *76*, 4951–4955.

Schlaeger, T.M., Daheron, L., Brickler, T.R., Entwisle, S., Chan, K., Cianci, A., DeVine, A., Ettenger, A., Fitzgerlad, K., Godfrey, M., et al. (2015). A comparison of non-integrating reprogramming methods. Nature Biotechnology *33*, 58-63.

Schmidt, T., Landwehrmeyer, G.B., Schmitt, I., Trottier, Y., Auburger, G., Laccone, F., Klockgether, T., Volpel, M., Epplen, J.T., Schols, L., and Riess, O. (1998). An isoform of ataxin-3 accumulates in the nucleus of neuronal cells in affected brain regions of SCA3 patients. Brain Pathology *8*, 669–679.

Schmidt, T., Lindenberg, K.S., Krebs, A., Schols, L., Laccone, F., Herms, J., Rechsteiner, M., Riess, O., Landwehrmeyer, G.B. (2002). Protein surveillance machinery in brains with spinocerebellar ataxia type 3: redistribution and differential recruitment of 26S proteasome subunits and chaperones to neuronal intranuclear inclusions. Annals of Neurology *51*, 302–310.

Schmitt, I., Linden, M., Khazneh, H., Evert, B.O., Bruer, P. Klockgether, T. and Wuellner, U. (2007). Inactivation of the mouse *Atxn3* (ataxin-3) gene increases protein ubiquitination. Biochemical and Biophysical Research Communications *362* (3), 734-739.

Schöls, L., Bauer, P., Schmidt, T., Schulte, T., and Riess, O. (2004). Autosomal dominant cerebellar ataxias: clinical features, genetics, and pathogenesis. Lancet Neurol *3*, 291-304.

Seidel, K., den Dunnen, W.F.A., Schultz, C., Paulson, H., Frank, S., de Vos, R.A., Brunt, E.R., Deller, T., Kampinga, H.H. and Rüb, U. (2010). Axonal inclusions in spinocerebellar ataxia type 3. Acta Neuropathologica *120* (4), 449–460

Shao, J., and Diamond, M.I. (2007). Polyglutamine diseases: emerging concepts in pathogenesis and therapy. Human Molecular Genetics *16* (2), 115-123.

Shi, Y., Inoue, H., Wu, J.C., and Yamanaka, S. (2017). Induced pluripotent stem cell technology: a decade of progress. Nature Reviews Drug Discovery *16*, 115–130.

Shimohata, T., Nakajima, T., Yamada, M., Uchida, C., Onodera, O., Naruse, S., Kimura, T., Koide, R., Nozaki, K., Sano, Y. et al. (2000). Expanded polyglutamine stretches interact with TAFII130, interfering with CREB-dependent transcription. Nature Genetics *26*, 29–36.

Smirnova, I. V., Bittel, D. C., Ravindra, R., Jiang, H., and Andrews, G. K. (2000)**.** Zinc and cadmium can promote rapid nuclear translocation of metal response element-binding transcription factor-1. Journal of Biological Chemistry *275*, 9377–9384**.**

Smith, A.G. (2001). Embryo-derived stem cells: of mice and men. Annual Review of Cellular and Developmental Biology *17***,** 435-462.

Stankovic, R. K., Chung, R. S., and Penkowa, M. (2007). Metallothioneins I and II: neuroprotective significance during CNS pathology. International Journal of Biochemistry and Cell Biology *39*, 484–489.

Sternberg, S. H., Redding, S., Jinek, M., Greene, E. C., and Doudna, J. A. (2014). DNA interrogation by the CRISPR RNA-guided endonuclease Cas9. Nature *507*, 62–67.

Strelchenko, N., Verlinsky, O., Kukharenko, V., and Verlinsky, Y. (2004). Morula-derived human embryonic stem cells. Reproductive Biomedicine online *9*, 623-629.

Sun, X., Seeberger, J., Alberico, T., Wang, C., Wheeler, C.T., Schauss, A.G., and Zou, S. (2010). Açai palm fruit (Euterpe oleracea Mart.) pulp improves survival of flies on a high fat diet. Experimental Gerontology *45*, 243–51.

Tabar, V., and Studer, L. (2014). Pluripotent stem cells in regenerative medicine: challenges and recent progress. Nature Reviews Genetics *15*, 82-92.

Tait, D., Riccio, M., Sittler, A., Scherzinger, E., Santi, S., Ognibene, A., Maraldi, N.M., Lehrach, H., and Wanker, E.E. (1998). Ataxin-3 is transported into the nucleus and associates with the nuclear matrix. Human Molecular Genetics *7*, 991–997.

Takahashi, J., Tanaka, J., Arai, K., Funata, N., Hattori, T., Fukuda, T., Fujigasaki, H., and Uchihara, T. (2001). Recruitment of nonexpanded polyglutamine proteins to intranuclear aggregates in neuronal intranuclear hyaline inclusion disease. Journal of Neuropathology and Experimental Neurology *60*, 369-376.

Takahashi, T., Kikuchi, S., Katada, S., Nagai, Y., Nishizawa, M., and Onodera, O. (2008). Soluble polyglutamine oligomers formed prior to inclusion body formation are cytotoxic. Human Molecular Genetics *17*, 345–356.

Takahashi, K., Okita, K., Nakagawa, M. and Yamanaka, S. (2007). Induction of pluripotent stem cells from fibroblast cultures. Nature Protocols *2***,** 3081-3089.

Takahashi, S. (2012). Molecular functions of metallothionein and its role in hematological malignancies. Journal of Hematology & Oncology 2012, **5**-41.

Takiyama, Y., Okynagi, S., Kawashima, S., Sakamoto, H., Saito, K., Yoshida, M., Tsuji, S., Mizuno, Y., and Nishizawa, M. (1994). A clinical and pathologic study of a large Japanese family with Machado-Joseph disease tightly linked to the DNA markers on chromosome 14q. Neurology *44*, 1302–1308.

Takiyama, Y., Igarashi, S., Rogaeva, E.A., Endo, K., Rogaev, E.I., Tanaka, H., Sherrington, R., Sanpei, K., Liang, Y., Saito, M., et al. (1995). Evidence for intergenerational istability in the CAG repeat in the MJD1 gene and for conserved haplotypes at flanking markers amongst Japanese and Caucasian subjects with Machado-Joseph disease. Human Molecular Genetics *4*, 1137–1146.

Tamai, K. T., Gralla, E. B., Ellerby, L. M., Valentine, J. S. and Thiele, D. J. (1993). Yeast and mammalian metallothioneins functionally substitute for yeast copper-zinc superoxide dismutase. Proceedings of the National Acadamy Sciences USA *90*, 8013–8017.

Theocharis, S. E., Margeli, A. P., Klijanienko, J. T., and Kouraklis, G. P. (2004). Metallothionein expression in human neoplasia. Histopathology *45*, 103–118.

Thirumoorthy, N., Shyam Sunder, A., Manisenthil Kumar, K., Senthil kumar, M., Ganesh, G., and Chatterjee, M. (2011). A Review of Metallothionein Isoforms and their Role in Pathophysiology. World Journal of Surgical Oncology *9*, 54.

Thomson, J.A., Itskovitz-Eldor, J., Shapiro, S.S., Waknitz, M.A., Swiergiel, J.J., Marshall, V.S. and Jones, J.M. (1998). Embryonic stem cell lines derived from human blastocysts. Science *282***,** 1145-1147.

Thornalley, P.J., and Vasak, M. (1985). Possible role for metallothionein in protection against radiation-induced oxidative stress—Kinetics and mechanism of its reaction with superoxide and hydroxyl radicals. *Biochimica et Biophysica Acta 827*, 36–44.

Todi, S.V., Laco, M.N., Winborn, B.J., Travis, S.M., Wen, H.M., and Paulson, H.L. (2007). Cellular turnover of the polyglutamine disease protein ataxin-3 is regulated by its catalytic activity. Journal of Biological Chemistry *282*, 29348–29358.

Todi, S.V., Winborn, B.J., Scaglione, K. M; Blount, J. R., Travis, S.M., and Paulson, H.L. (2009). Ubiquitination directly enhances activity of the deubiquitinating enzyme ataxin-3. The EMBO Journal *28* (4), 372-382.

Todi, S. V., Scaglione, K. M., Blount, J. R., Basrur, V., Conlon, K. P., Pastore, A., Elenitoba-Johnson, K., and Paulson, H.L. (2010). Activity and Cellular Functions of the Deubiquitinating Enzyme and Polyglutamine Disease Protein Ataxin-3 Are Regulated by Ubiquitination at Lysine 117. The Journal of Biological Chemistry *285*, 39303–39313.

Trottier, Y., Cancel, G., An-Gourfinkel, I., Lutz, Y., Weber, C., Brice, A., Hirsch, E., and Mandel, J.L. (1998). Heterogeneous intracellular localization and expression of ataxin-3. Neurobiology of Disease *5*, 335–347.

Tzvetkov, N. and Bruer, P. (2007). Josephin domain-containing proteins from a variety of species are active de-ubiquitination enzymes. Biological Chemistry, *388*, 973–978

Uchihara, T., Fujigasaki, H., Koyano, S., Nakamura, A., Yagishita, S., and Iwabuchi, K. (2001). Non-expanded polyglutamine proteins in intranuclear inclusions of hereditary ataxias--triple-labeling immunofluorescence study. Acta Neuropathologica *102*, 149-152.

Unger, C., Skottman, H., Blomberg, P., Dilber. M.S., and Hovatta, O. (2008). Good manufacturing practice and clinical-grade human embryonic stem cell lines. Human Molecular Genetics *17***,** R48-R53.

Valko, M., Leibfritz, D., Moncol, J., Cronin, M.M., Mazur, M. and Telser J. (2007). Free radicals and antioxidants in normal physiological functions and human disease. The International Journal of Biochemistry and Cell Biology *39 (1)*, 44–84.

Vanacore, R. M., Eskew, J. D., Morales, P. J., Sung, L., and Smith, A. (2000). Role for copper in transient oxidation and nuclear translocation of MTF-1, but not of NF-kappa B, by the heme-hemopexin transport system. Antioxidants and Redox Signaling *2*, 739–752.

Van Alfen, N., Sinke, R., Zwarts, M., Gabreels-Festen, A., Praamstra, P., Kremer, B.P., and Horstink, M.W. (2001). Intermediate CAG repeat lengths (53,54) for MJD/SCA3 are associated with an abnormal phenotype. Annals of Neurology *49*, 805–808.

Van der Oost, J., Westra, E. R., Jackson, R. N., and Wiedenheft, B. (2014). Unravelling the structural and mechanistic basis of CRISPR–Cas systems. Nature Reviews. Microbiology *12*, 479–492.

Vašák, M., and Meloni, G. (2011). Chemistry and biology of mammalian metallothioneins. Journal of Biological Inorganic Chemistry *16*(7), 1067-1078.

Wang, G., Sawai, N., Kotliarova, S., Kanazawa, I., and Nukina, N. (2000). Ataxin-3, the MJD1 gene product, interacts with the two human homologs of yeast DNA repair protein RAD23, HHR23A and HHR23B. Human Molecular Genetics *9*, 1795–1803.

Wang, Q., Li, L., Ye, Y. (2006). Regulation of retrotranslocation by p97-associated deubiquitinating enzyme ataxin-3. Journal of Cell Biology *174*, 963–971.

Wang, H., Ying, Z., and Wang, G. (2012). Ataxin-3 Regulates Aggresome Formation of Copper-Zinc Superoxide Dismutase (SOD1) by Editing K63-linked Polyubiquitin Chains. The Journal of Biological Chemistry *287*, 28576–28585.

Wang,H., La Russa,M., and Lei S. Q (2016). CRISPR/Cas9 in genome editing and beyond. Annual Review of Biochemistry *85*, 227-264.

Warren, L., Manos, P., Ahfeldt, T., Loh, Y., Li, H., Lau, F., Ebina, W., Mandal, P., Smith, Z., and Meissner, A. (2010). Highly Efficient Reprogramming to Pluripotency and Directed Differentiation of Human Cells with Synthetic Modified mRNA. Cell Stem Cell *7*, 618-630.

Warrick, J.M., Chan H.Y., Gray-Board, G.L., Chai, Y., Paulson, H.L. and Bonini, N.M. (1999). Suppression of ploy glutamine-mediated neurodegeneration in Drosophila by the molecular chaperone HSP70. Nature Genetics *23*, 425-428.

Weber, J.J., Sowa, A.S., Binder, T., Hubener, J. (2014) From pathways to targets: understanding the mechanisms behind polyglutamine disease. BioMed Research International *2014,* 70175.

Weissman, I.L. (2000). Stem cells: units of development, units of regeneration, and units in evolution. Cell *100***,** 157-168.

West, A.K., Hidalgo, J., Eddins, D., Levin, E.D. and Aschner, M. (2008). Metallothionein in the central nervous system: roles in protection, regeneration and cognition. Neurotoxicology *3*, 488-502.

Westin, G., and Schaffner, W. (1988). A zinc-responsive factor interacts with a metalregulated enhancer element (MRE) of the mouse metallothionein-I gene. EMBO Journal *7*, 3763-3770.

Winborn, B.J., Travis, S.M., Todi, S.V., Scaglione, K.M., Xu, P., Williams, A.J., Cohen, R.E., Peng, J., and Paulson, H.L. (2008). The deubiquitinating enzyme ataxin-3, a polyglutamine disease protein, edits Lys63 linkages in mixed linkage ubiquitin chains. Journal of Biological Chemistry *283*, 26436–26443.

Wu, Y.-L., Chang, J.-C., Lin, W.-Y., Li, C.-C., Hsieh, M., Chen, H.-W., and Liu, K.-L. (2017). Treatment with Caffeic Acid and Resveratrol Alleviates Oxidative Stress Induced Neurotoxicity in Cell and *Drosophila* Models of Spinocerebellar Ataxia Type3. *Scientific Reports*, *7*, 11641.

Xue, Y., Wang, Q., Long, Q., Ng, B. L., Swerdlow, H., Burton, J., Skuce, C., Taylor, R., Abdellah, Z., and Zhao, Y. (2009). Human Y Chromosome Base-Substitution Mutation Rate Measured by Direct Sequencing in a Deep-Rooting Pedigree. Current Biology *19*, 1453–1457.

Yousuf, S., Atif, F., Ahmad, M., Hoda, N., Ishrat, T., Khan, B. and Islam, F. (2009). Resveratrol exerts its neuroprotective effect by modulating mitochondrial dysfunctions and associated cell death during cerebral ischemia. Brain Research *1250*, 242–253.

Zhang, S.C., Wernig, M., Duncan, I.D., Brüstle, O. and Thomson, J.A. (2001). In vitro differentiation of transplantable neural precursors from human embryonic stem cells. Nature Biotechnology *19***,** 1129-1133.

Zheng, H., Berman, N.E.J., and Klaassen C.D. (1995). Chemical modulation of metallothionein I and III mRNA in mouse brain. Neurochemistry International *27*(1), 43-58.

Zhong, X., and Pittman, R.N. (2006). Ataxin-3 binds VCP/p97 and regulates retrotranslocation of ERAD substrates. Human Molecular Genetics *15*, 2409–2420.

Zhou, L., Wang, H., Wang, P., Ren, H., Chen, D., Ying, Z., and Wang, G. (2013). Ataxin-3 protects cells against H2O2-induced oxidative stress by enhancing the interaction between Bcl-X(L) and Bax. Neuroscience *243*, 14-21.

Zhu, S., Li, W., Zhou, H., Wei, W., Ambasudhan, R., Lin, T., Kim, J., Zhang, K., and Ding, S. (2010). Reprogramming of human primary somatic cells by OCT4 and chemical compounds. Cell stem cell *7*, 651-655.

Zoghbi, H.Y., and Orr, H.T. (2000). Glutamine repeats and neurodegeneration. Annual Review of Neuroscience *23*, 217-247.

10 Danksagung

Zunächst möchte ich mich bei Prof. Dr. Oliver Brüstle für die Möglichkeit der Promotion an seinem Institut unter hervorragenden Forschungsbedingungen bedanken.

Prof. Dr. Philipp Koch danke ich für die Überlassung meines Themas und für die fachliche Beratung und Betreuung während meiner Zeit als Doktorandin.

Prof. Jörg Höhfeld, Prof. Michael Pankratz und Prof. Pavel Kroupa danke ich dafür, dass sie sich freundlicherweise bereiterklärt haben, mein Prüfungskomitee zu bilden.

Dr. Peter Breuer möchte ich für viele interessante fachliche Diskussionen, weise Ratschläge und stets aufheiternde Witze danken.

Ksenia Vinnikova, Daniel Poppe, Kevin Weynans und Ruven Wilkens danke ich dafür, dass Arbeitskollegen auch sehr gute und wichtige Freunde werden können, die sowohl das Arbeits- als auch das Privatleben extrem positiv bereichern können.

Meinen ehemaligen Arbeitskollegen Bettina Bohl, Ammar Jabali, Fabio Marsoner, Vira Iefremova, Karolina Kleinsimlinghaus, Kathrin Stüber und Jonas Doerr danke ich für ein witziges und positves Arbeitsklima, wodurch die Arbeit Spaß gemacht hat und dank einiger sehr witziger Annekdoten auch positiv in Erinnerung bleiben wird.

Meinem Mann Christian Gröger danke ich für unendlich viele Dinge!

Meinen Eltern Petra und Michael Jatho danke ich dafür, dass es mich gibt und dass sie zusammen mit meinen Schwiegereltern Margrit und Helmut Gröger immer für mich da sind.

11 Erklärung

Diese Dissertation wurde an dem Institut für Rekonstruktive Neurobiologie des Universitätsklinikums Bonn unter der Leitung von Herrn Prof. Dr. Philipp Koch angefertigt.

Hiermit versichere ich, dass die vorliegende Arbeit ohne unzulässige Hilfe Dritter und ohne die Benutzung anderer als angegebener Quellen angefertigt wurde. Die aus fremden Quellen direkt oder indirekt übernommenen Gedanken sind als solche kenntlich gemacht.
Die vorgelegte Arbeit ist außerdem nicht bereits anderweitig als Dissertation eingereicht worden und ich habe früher noch keinen Promotionsversuch unternommen.

Bonn, den

Jasmin Jatho-Gröger